A Study on Coupling between Slot and Wire Antennas

March 1998

Takehiro Horioka

Doctoral dissertation

A Study on Coupling between Slot and Wire Antennas

スロットとワイヤーアンテナ間の結合に関する研究

Takehiro Morioka

Doctoral Program in Engineering

University of Tsukuba

March 1998

CONTENTS

1. Introduction 1
   1.1 Historical background 1
   1.2 Composition of the dissertation 7
2. Mutual coupling between elements and the diffraction effect by the edge 9
   2.1 Background 9
   2.2 Boundary conditions 11
   2.3 Moment method 17
   2.4 Geometrical theory of diffraction 25
3. A slot antenna with a parasitic wire for dual band operation 31
   3.1 Background 31
   3.2 Antenna structures 35
   3.3 Numerical results 37
   3.4 Conclusions 56
4. Reduction of coupling between two wire antennas using a slot 57
   4.1 Background 57
   4.2 Formulation 59
   4.3 Antenna structures 64
   4.4 Numerical results on an infinite ground plane 67
   4.5 Numerical results on a finite ground plane 77
   4.6 Conclusions 85
5. Conclusions 86

Future study 91

References 93

Appendix A 97
Hybrid method of moment method and geometrical theory of diffraction

Acknowledgement 103

List of papers 104

CHAPTER 1

Introduction

1.1 Historical Background

Many kinds of electromagnetic phenomena occur around us. They are thunders, static electricity and so on. It was 600 years before Christ, that the human first recognized these electromagnetic phenomena. A Greek noted that when amber is rubbed with silk, it produces sparks and attracts particles of fluff and straw. About 1750, Franklin established the law of conservation of charges and named the two kinds of charges positive and negative. Later, Coulomb measured electric and magnetic forces with a delicate torsion balance that he invented. In 1820 Ampere invented the solenoidal coil for producing magnetic fields and theorized that the atoms in a magnet are magnetized by the tiny circulating electric currents. At the same time, Ohm published his famous relationship between current, voltage and resistance known as Ohm's law. In 1831, Faraday demonstrated that a changing magnetic field could produce electric current. Faraday's extensive experimental investigations enabled Maxwell to establish the interdependence of electricity and magnetism in a profound and elegant manner. Maxwell showed his equations and foretold the existence of electromagnetic waves in 1864, but many scientists of his time were skeptical of his theories. In 1886, Hertz generated and detected meter-wavelength radio waves with an end loaded dipole as transmitter and a resonant square loop antenna as receiver. With the spark transmitter and receiver, he demonstrated that the polarization, reflection, and refraction of radio waves were identical with light except for a difference in wavelength.

Marconi designed tuning circuits, a large antenna, and ground systems for longer wavelengths and was able to transmit signals over long distances. In 1901 he made a sensation by sending radio signals across the Atlantic Ocean. The utilization of electromagnetic waves has developed rapidly since then. Now, electromagnetic waves are used in many areas and we can not live a day comfortably without their use.

The application of electromagnetic waves is spreading over wide areas. Especially the radio communication has been rapidly developed. Now we can communicate with anyone being anywhere with portable telephones. The information over the sea can be seen on television. We use electromagnetic waves without paying any attention to them usually. Since Hertz and Marconi, antennas have become increasingly important to our society and now they are indispensable. We can see them everywhere at homes and workplaces, on cars and aircraft, while ships, satellites and spacecraft bristle with them. In order to use electromagnetic waves effectively in the devices, antennas are the very important parts as the interfaces between space and circuits. It depends mainly on the antenna characteristics whether the effective system for transmitting or receiving electromagnetic waves can be constructed or not. To achieve the effective system, we have to choose antennas that have suitable characteristics for the system, such as the directivity and input impedance. In the radio communications the operating wavelength used usually are from a few centimeters to a few meters. When an antenna is located in the neighborhood of a scatterer or an antenna, the antenna characteristics are different from the free space characteristics. For example, the return loss and the radiation pattern are different from those when they are measured in free space. This is because of couplings between

the elements. Generally the coupling makes antenna behavior more complex and the antenna characteristics hard to predict, but it can give new and better characteristics that a single element can not have if the coupling is used effectively. A well-known TV receiving antenna, a Yagi-Uda array antenna is the case where the coupling is used effectively. A Yagi-Uda array antenna consists of three parts functionally. They are directors, reflectors and one driven element. This antenna effectively uses adjusted couplings between these elements. A Yagi-Uda array antenna consists of only electric elements (wire). More attractive antenna characteristics are obtained from the combination of the electric (wire) and magnetic (slot) elements. Although the coupling can make antenna characteristics more attractive, it often causes system degradation problems. Array antenna elements are often located closely each other because of the space limitation. Radiation patterns of an array antenna are supposed to be the sum of the radiation patterns of each element located alone in free space. Actually it is not true because the coupling disturbs the original characteristics. The boundary conditions at the surface of the antenna are satisfied with the sum of electromagnetic fields radiated from each antenna element. Thus attentions should be paid to couplings between the elements when you design array antennas. Another example of the problem occurs in the base station of the mobile communication system. With the development of the wireless communications many antennas are needed for different purposes and it is often required to have antennas close together in a limited area. In this case, radiated power from an antenna is received by the other antennas around it and often makes system degradation problems such as cross-talk.

In this paper, couplings between a slot antenna and a parasitic wire, and

couplings between two wire antennas are considered and discussed through some examples. Slot antennas and wire antennas are the most basic antenna elements. Wire antennas have the radii relatively small compared with the wavelength. Well-known dipole, loop and helical antennas are the examples of the wire antenna. These wire antennas have simple shapes and are useful. Thus the application of wire antennas can be seen in many areas. The dipole antenna is the most famous wire antenna. It has the length of a half wavelength of the operating frequency. The length of the monopole antenna, which is usually used on the conducting plate, is adjusted to a quarter wavelength. A monopole antenna on an infinite conducting plate can be analyzed as a dipole antenna in free space by using image theory. Slot antennas are made on a conducting plate by cutting an opening whose widths are narrow in terms of the operating wavelength. Slot antennas made on the surface of a conducting body are called "flush mount antenna" and they are used on a rocket and an airplane. For these applications, to reduce the air resistance is the most important problem. Slot antennas do not jut out from the surface of the airplane body and can avoid the air resistance. Slot antennas are excited by a coaxial cable or a waveguide and electromagnetic energy is radiated through the opening. When a slot antenna is made on a ground plane, electromagnetic fields are radiated into both sides of the ground plane. Usually we do not need the backward radiation, so it is often used with the cavity backed to radiate into one side.

Many studies have been done with the combinations of the slot antenna and the wire antenna. When the monopole antenna is set vertically on the ground plane, the radiation pattern in the vertical plane does not have the directivity in the monopole direction. In 1975, Long reported that a combined

antenna with a monopole antenna and two slot antennas can provide an omnidirectional radiation pattern in the vertical plane[1]. To obtain such a characteristic, two slot antennas should be located in parallel, half wavelength apart and be excited in a phase. In this combination the monopole antenna, which is excited in a 90° shifted phase from the slots, is set in the mid point of the two centers of the slot. Clavin studied a combination of a slot antenna and two non-fed monopole elements and obtained antenna structure with equal E- and H-plane patterns[2]. In his report, parasitic monopoles are set besides the slot vertically. Strong coupling can be obtained in this configuration. He also studied the improved antenna with inverted L elements instead of the monopoles. The analytical paper of the coupling in these combinations proposed by Clavin has been published[3][4]. The combinations of a slot and a dipole antenna have been also developed for a different purpose. Adachi and Ito proposed a slot antenna with a parasitic dipole antenna to obtain circular polarization[5]. A dipole antenna is set over a slot antenna to be in parallel to the ground plane and detailed parameters, such as the dipole length, the distance from the slot and the rotation angle are provided in their paper. The studies on the combination of slot antennas and wire antennas are mainly concerned in radiation patterns such as pattern shaping. Interesting results shown above can be obtained by the combination of the slot and the wire.

The applications of electromagnetic waves make our lives convenient. On the other hand, a lot of devices radiate electromagnetic waves and they produce new problems with the increase of their applications. Because the radiated electromagnetic field from a device is not needed for the other devices of the different system, the electromagnetic environment around us

is getting worse and worse with the development of wireless communications. Thus the importance of the electromagnetic compatibility (EMC) is increasing nowadays. The problems of the electromagnetic disturbance began with the utility of radio waves for communications. The influence of the electromagnetic disturbance is increasing as the following reasons. The device driving voltage becomes lower to save energy and the devices are set close together with the reduction of the device size. The counter measure for electromagnetic interference (EMI) is required and should be done for each problem individually. Also these EMI problems can be considered as a coupling between antennas and electromagnetic fields in space.

There are two ways to approach the coupling between antenna elements. One is to enhance the effect of the coupling to obtain the characteristics that the system requires and the other is to reduce coupling between the elements to avoid interference. Although the first aim to improve antenna characteristics by using coupling effectively is studied in many papers and it is applied in many antennas as mentioned before. These studies do not show all the possible characteristics of the combination of the slot antenna and the wire antenna. Their purposes are mainly to shape radiation patterns or to obtain good circular polarization. The antennas required to achieve the effective system are supposed to be obtained with the combinations of the slot antenna and the wire antenna. The other aim to reduce coupling between antennas is a new application of the slot. An ordinary way to reduce coupling is to set a conducting plate or a loaded wire between the antennas. These ways complicate antenna structure. If the slot can reduce the coupling between two antennas, nothing jets out from the ground plane except the antennas. In this research these two ways to approach the coupling between

the slot antenna and the wire antenna are investigated and developed through concrete examples.

1.2 Composition of the dissertation

The purpose of this dissertation is to investigate the effect of the coupling between elements with two different problems. They are

1. The influence of the coupling is used effectively to make the antenna characteristics new and better.
2. Reduction of coupling is needed to avoid system degradation problems.

This dissertation consists of five parts. The introduction to these studies is stated in Chapter 1. In Chapter 2, some important theories are explained to change the actual problem into the calculation model. At the same time the boundary conditions at the surface of the slot and the wire are shown. Moment method (MM) and geometrical theory of diffraction (GTD) are presented in the same chapter. MM is a well-known numerical method for calculating electromagnetic field problems associated with obstacles of the small dimension with respect to the wavelength. In certain applications the combination of MM with asymptotic techniques such as GTD can yield solutions which neither method alone can solve problems effectively. Antennas for dual band operation are investigated in Chapter 3 as an example of the effective utilization of the coupling. A dual-band antenna is needed for the dual-mode cellular phone system. Since the operating frequencies of the system may be different, the phone and the antenna should be operated well at both frequency bands. Three types of antennas with the combination of a slot antenna and a parasitic wire are proposed. Detailed sizes of these antennas are shown in Section 3.2. Also the reduction

of the coupling between antennas is a very important technique to avoid electromagnetic disturbance, and in Chapter 4, a new method to reduce the coupling between two wire antennas using a slot is developed and a coupling coefficient is introduced to evaluate the coupling between two antennas. The hybrid method of MM and GTD is used to take diffracted fields by the edge into account to calculate coupling coefficients. Numerical and measured coupling coefficients are shown. By applying GTD, the effect of the ground plane can be included in calculating coupling coefficients and the optimum size of the ground plane that is needed to reduce the coupling is obtained. One of the most important characteristics calculated by GTD is a radiation pattern. Radiation characteristics with a finite ground plane are also simulated and shown with the measured data. The last chapter is for conclusions, where the results obtained through these studies are summarized.

CHAPTER 2

Mutual coupling between elements and diffraction effect by the edge

2.1 Background

Once we can obtain current distribution on antennas, the important characteristics of antenna such as radiation patterns and input impedance can be obtained. Thus it is very important to obtain current distribution accurately both in the experiment and calculation. We can obtain exact solutions only when the problems have a quite simple form as a dipole antenna. The studies of current distribution on the wire antenna have been done by Pocklington and Hallen. In 1938, Hallen derived the integral equation of the dipole antenna and obtained current distribution analytically[6]. These studies at that time were done under the limitation that the wire antenna should be straight. It is the special case that the problems that we want to analyze have such simple forms. To analyze real problems, we use numerical methods such as the moment method (MM) and the finite difference time domain (FD-TD) method. From 1960's the development of computers is remarkable. The speed of calculation has become faster and the memory size of the computer has become larger. Thus more arbitrary shapes of the antenna, such as loop and spiral antennas, could be analyzed. Mei and Harrington are the pioneers in analyzing these antennas, which have more generalized shapes. Mei achieved to derive the integral equation for a spiral antenna in 1965[7] and in 1967 Harrington proposed moment method in electromagnetics[8][9]. The achievement of arbitrary shaped antenna analyses prompted other researcher to study more

complex antenna structures. Many studies have been published since then. Now, with the development of electronic devices we can use higher frequencies. In such a high frequency range, the size of the scatterer becomes large in terms of the operating wavelength. Then we will have the other problems with these methods. For example, the size of the matrix becomes large and the larger size of memories is needed to compute.

Before 1873, Maxwell showed that the propagation of light could be viewed as an electromagnetic phenomenon. The relationship between ray optics and wave propagation is apparent from the work of Huygens in 1690 and Fresnel in 1818, but was not formally shown until the work of Luneberg in 1944 and Kline in 1951[10]. The method, geometrical optics is well known for high frequency analysis. This method has the advantage to understand phenomenon intuitively as the principle of the light path and not to be limited with the shape of the scatterer to analyze. The laws of geometrical optics are derived from the canonical problem of the plane wave reflection and refraction at an infinite planar dielectric interface. Geometrical optics is based upon an assumption that the wavelength is zero. So the wave characteristics such as diffraction can not be treated with this method. A diffracted ray is a ray that follows a path that cannot be explained as either reflection or refraction. In 1962, Keller added the components of diffraction to geometrical optics to improve the accuracy. The geometrical theory of diffraction (GTD), concerned by Keller in the 1950s and developed continuously since then, is established as a leading analytical technique in the prediction of high frequency diffraction phenomena[11][12][13]. Basically, GTD is an extension of geometrical optics by the inclusion of additional diffracted rays to describe the diffracted field. The concept of diffracted rays

was developed by Keller from the asymptotic evaluation of the known exact solution to scattering from simple shapes, referred to as the canonical problems for GTD. In the papers, diffraction coefficients derived from the canonical problem are multiplied with the incident ray at the point of diffraction to produce the initial value of the field on the diffracted rays. These coefficients are non-uniform in the sense that they are invalid in certain regions such as the so-called transition regions. Since early work appropriate integral functions for the transition regions have been developed to give uniform solutions for quite general problems in edge and convex surface diffraction. Rigorous mathematical foundations and the basic simplicity of the ray tracing techniques which permits GTD to treat quite complicated structures, are the main attractions of the method. The hybrid method of MM and GTD[14] is very useful to analyze antennas and structures around them.

2.2 Boundary conditions

If there are some regions that have different permittivity and permiability, the boundary conditions for electromagnetic waves at an interface between two regions are needed. To analyze problems for a slot and a wire antenna, we divide a space into two regions separated by an infinite ground plane and a slot as shown in fig.2.1a. The region above the ground plane is named region 1 and the other side of the ground plane is region 2. A wire antenna is located in region 1 and a slot antenna is made on the ground plane. In region 1, it is assumed that electromagnetic fields radiated from the slot antenna as $\overline{E}^1_{slot}, \overline{H}^1_{slot}$ and $\overline{E}^1_{wire}, \overline{H}^1_{wire}$ are the radiated fields from the wire antenna. Under the ground plane, $\overline{E}^2, \overline{H}^2$ are the electromagnetic

fields radiated from the slot. Thus the total electromagnetic fields in region 1 are expressed as follows.

$$\overline{E}^1_{Total} = \overline{E}^1_{slot} + \overline{E}^1_{wire} \qquad (2.1)$$

$$\overline{H}^1_{Total} = \overline{H}^1_{slot} + \overline{H}^1_{wire} \qquad (2.2)$$

The boundary conditions at the boundary of the slot and the ground plane are expressed as

$$\overline{n} \times \overline{H}^1_{Total} = \overline{J}_g \qquad \text{(on the ground plane)} \qquad (2.3)$$
$$\overline{E}^1_{Total} \times \overline{n} = 0$$

$$\overline{n} \times \left(\overline{H}^1_{Total} - \overline{H}^2\right) = \overline{J}_{slot} \qquad \text{(on the slot)} \qquad (2.4)$$
$$\overline{E}^1_{Total} \times \overline{n} = \overline{E}^2 \times \overline{n}$$

where $\overline{n}$ is the unit vector pointing out region 2 normal to the surface of the boundary. $\overline{J}_{slot}$ is the electric current flowing across the slot aperture.

By applying the equivalence principle to these boundaries, the ground plane can be removed and we can assume that the electric and the magnetic currents $\overline{J}_s = \overline{n} \times \overline{H}^1_{Total}$ and $\overline{M}_s = \overline{E}^1_{Total} \times \overline{n}$ flow on the slot surface and the electric current $\overline{J}_g = \overline{n} \times \overline{H}^1_{Total}$ flows on the ground plane surface to satisfy the electromagnetic field boundary conditions. These currents are the equivalent surface sources and the same fields can be obtained in region 1. In region 2, the electromagnetic fields do not exist. Then the whole boundary between region 1 and 2 can be covered with the electric conductor. Finally the problem can be separated into two regions. Region 1 has a wire antenna, two surface electric currents ($\overline{J}_g$ and $\overline{J}_s$) and a magnetic current sheet ($\overline{M}_s$) on the ground plane. Also region 2 has a magnetic current sheet $-\overline{M}_s$ under the ground plane as shown in fig.2.1b. To remove the ground plane the image theory is used to region 1. As the images of the surface electric

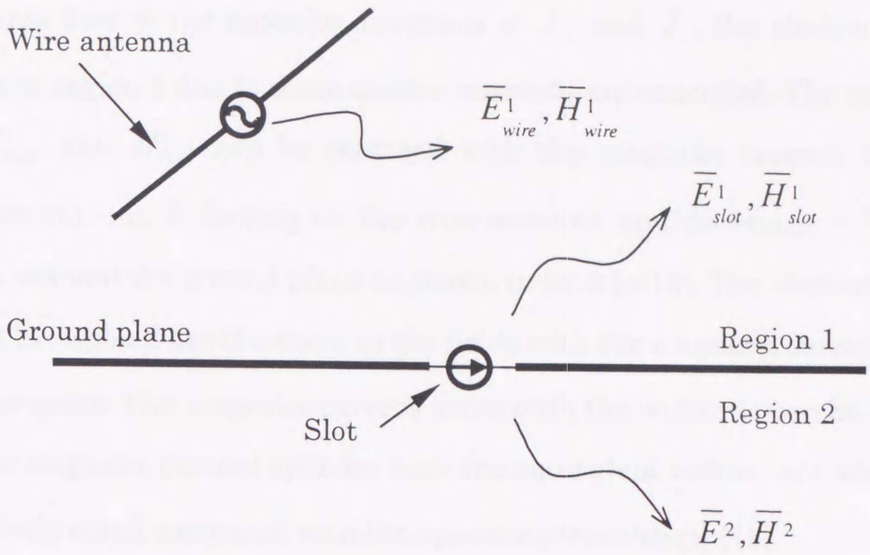

fig. 2.1a Analytical model.

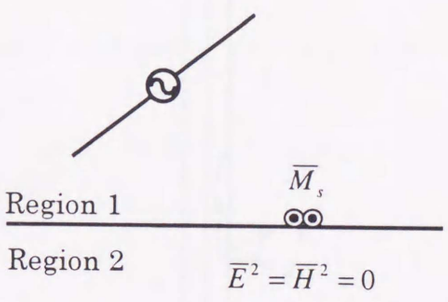

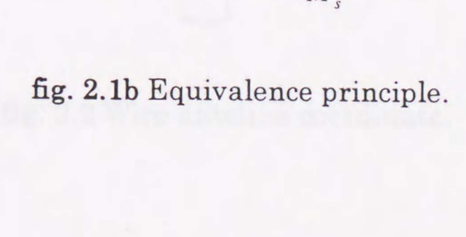

fig. 2.1b Equivalence principle.

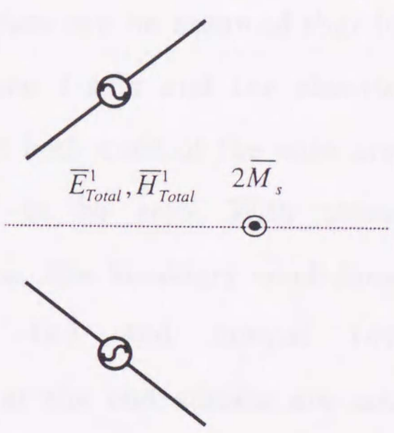

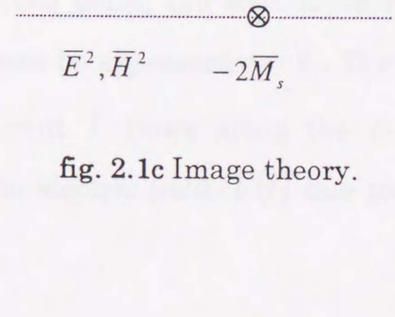

fig. 2.1c Image theory.

currents flow in the opposite directions of $\bar{J}_g$ and $\bar{J}_s$, the electromagnetic fields in region 1 due to these electric currents are cancelled. The same field as $\bar{E}^1_{Total}$ and $\bar{H}^1_{Total}$ can be obtained with the magnetic current $2\bar{M}_s$, the electric current $\bar{I}$ flowing on the wire antenna and its image $-\bar{I}$ in free space without the ground plane as shown in fig.2.1c[15]. The electromagnetic fields in region 2 are the same as the fields with the magnetic current $-2\bar{M}_s$ in free space. The magnetic current sheet with the width w can be replaced by the magnetic current cylinder with the equivalent radius $w/4$ when w is relatively small compared with the operating wavelength[16].

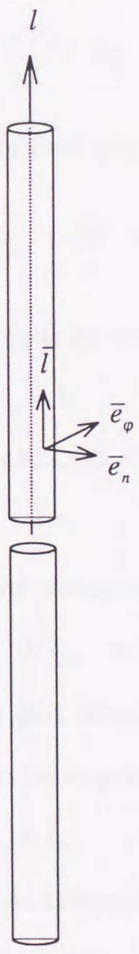

fig. 2.2 Wire antenna coordinate.

Consider a thin wire antenna made of a perfect conductor in free space as shown in fig. 2.2. The electric current on the surface can be assumed that it flows on the l-axis and the electric currents at both ends of the wire are considered to be zero. With these assumptions, the boundary conditions tangential (φ) and normal (n) directions at the end surface are not needed. Only the boundary condition in the l direction is required.

When the wire antenna is fed at the gap of the feed point, the electric field in the gap can be expressed as $\bar{E}_i$. The electric current $\bar{I}$ flows along the l-axis and the electric field $\bar{E}(\bar{I})$ due to

$\bar{I}$ exists outside the feed gap. As the electric field can not penetrate into the conductor, tangential component of $\bar{E}(\bar{I})$ becomes zero at the surface of the wire as $\bar{E}(\bar{I})\times\bar{n}=0$. At the feed point, the electric fields outside and inside the boundary surface should be continuous. So the following relationships can be obtained.

$$\bar{E}_i\times\bar{e}_n=\bar{E}(\bar{I})\times\bar{e}_n=E_l\bar{e}_\varphi+E_\varphi\bar{l}=E_l\bar{e}_\varphi \qquad (2.5)$$

As the radius of the wire is small, the electric field component in φ direction E_φ can be assumed to be zero. With the assumption that the feed point gap d is very small compared with the operating wavelength, the electric field $\bar{E}_i$ equals to $\frac{-V_0}{d}\bar{l}$ by using the feed voltage V_0. To generate the electric field within the feed gap, impressed electric field $E_{imp}\bar{l}$ is needed and E_{imp} is expressed as $E_{imp}=\frac{V_0}{d}$. From these relationships, the electric field boundary condition on the wire antenna is obtained as

$$\bar{E}(\bar{I})\times\bar{e}_n+E_{imp}\bar{e}_\varphi=0 \qquad (2.6)$$

where the impressed electric field strength E_{imp} is zero except at the feed point[17].

For the slot antenna, the magnetic field in region 1 and region 2 are expressed as $\bar{H}^1_{Total}$ and $\bar{H}^2$, respectively. The equivalence principle is applied to the slot aperture and the boundary condition on the slot antenna in region 1 can be expressed as

$$\bar{n}\times(\bar{H}^1_{Total}-\bar{H}^2)=\bar{I}_0 \qquad (2.7).$$

$\bar{I}_0$ is the electric current flowing across the slot aperture and is zero except at the feed point or at the loaded point.

By using the Dirac's delta function δ, the boundary conditions on the

wire antenna and the slot antenna are expressed as

$$\overline{E}^{1}_{Total} \times \overline{n} = -\overline{e}_{\varphi} V_0 \delta(l) \qquad \text{(wire antenna)} \quad (2.8)$$

$$\overline{n} \times \left(\overline{H}^{1}_{Total} - \overline{H}^{2}\right) = \overline{e}_{\varphi} I_0 \delta(\rho - \rho_0) \qquad \text{(slot antenna)} \quad (2.9)$$

where $\overline{n}$ and $\overline{e}_{\varphi}$ are the unit vectors normal and tangential (perpendicular to $\overline{l}$ or $\overline{\rho}$) to the surface of the wire antenna and the slot antenna, respectively. l and ρ are the coordinates along the wire antenna and the slot antenna. It is assumed that the feed point of the wire antenna is located at $l = 0$ and ρ_0 is the feed point or the loaded point in the slot. V_0 and I_0 are the feed voltage on the wire and the electric current at the feed point or at the loaded point in the slot, respectively.

By using vector potentials and $\overline{H}^{1}_{slot} = -\overline{H}^{2}$ [18], the boundary conditions (2.8)-(2.9) are expressed as

$$\left(-j\omega\overline{A} + \frac{1}{j\omega\mu_0\varepsilon_0} \nabla\nabla\cdot\overline{A} - \frac{1}{\varepsilon_0}\nabla\times\overline{F} \right) \times \overline{n} = -\overline{e}_{\varphi} V_0 \delta_0(l) \qquad (2.10)$$

$$\overline{n} \times \left[\frac{1}{\mu_0}\nabla\times\overline{A} - 2j\left\{ \omega\overline{F} + \frac{j}{\omega\mu_0\varepsilon_0}\nabla\left(\nabla\cdot\overline{F}\right) \right\} \right] = \overline{e}_{\varphi} I_0 \delta(\rho - \rho_0) \qquad (2.11)$$

where $\omega = 2\pi f$ and f is the operating frequency. $\overline{A}$ and $\overline{F}$ are the magnetic and the electric vector potential due to the electric and the magnetic current, respectively. The vector potentials $\overline{A}$ and $\overline{F}$ are written as

$$\overline{A}(\overline{r}) = \frac{\mu_0}{4\pi}\int_l \overline{I}(\overline{r}') \frac{e^{-jk|\overline{r}-\overline{r}'|}}{|\overline{r}-\overline{r}'|} dl' \qquad (2.12)$$

$$\overline{F}(\overline{r}) = \frac{\varepsilon_0}{4\pi}\int_\rho 2\overline{M}(\overline{\rho}') \frac{e^{-jk|\overline{r}-\overline{r}'|}}{|\overline{r}-\overline{r}'|} d\rho' \qquad (2.13)$$

where $\overline{r}'$ and $\overline{\rho}'$ are the position vectors from the origin to a certain point on the wire antenna and the slot antenna, respectively.

2.3 Moment method

The moment method (MM) is a method to solve integral equations, which are written in the functional equation changed into matrix form. The unknown electric current $\bar{I}$ distribution on the antenna is expressed with the series of a set of known functions as

$$\bar{I} = \sum_n I_n \bar{J}_n(\bar{r}') \qquad (2.14)$$

where I_n is the unknown coefficient and $\bar{J}_n$ is the nth subsectional

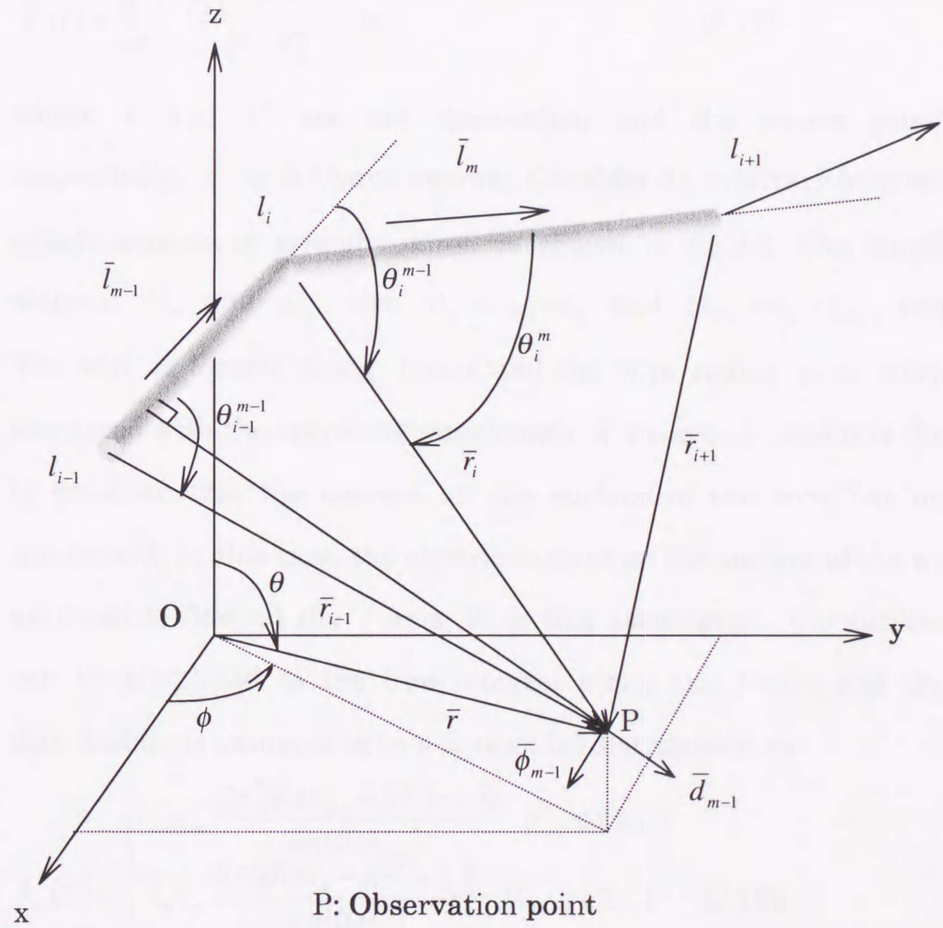

fig. 2.3 Wire element coordinate.

expansion function defined at the position $\bar{r}'$ on the antenna. When the electric current $\bar{J}_n(\bar{r}')$ is flowing in free space, the electric and the magnetic fields due to the current can be shown as below by using the magnetic vector potential $\bar{A}_n(\bar{r})$.

$$^{J}\bar{E}_n(\bar{r}) = -j\omega\bar{A}_n(\bar{r}) + \frac{1}{j\omega\varepsilon_0\mu_0}\nabla\left(\nabla\cdot\bar{A}_n(\bar{r})\right) \qquad (2.15)$$

$$^{J}\bar{H}_n(\bar{r}) = \frac{1}{\mu_0}\nabla\times\bar{A}_n(\bar{r}) \qquad (2.16)$$

$$\bar{A}_n(\bar{r}) = \frac{\mu_0}{4\pi}\int_V \frac{\bar{J}_n(\bar{r}')e^{-j\beta|\bar{r}-\bar{r}'|}}{|\bar{r}-\bar{r}'|}dv \qquad (2.17)$$

where $\bar{r}$ and $\bar{r}'$ are the observation and the source point vectors, respectively. β is the wave number. Consider an arbitrary bent wire dipole, which consists of straight wires as shown in fig.2.3. The lengths of the element Δl_m and Δl_{m-1} are $\Delta l_m = l_{m+1} - l_m$ and $\Delta l_{m-1} = l_m - l_{m-1}$, respectively. The wire is located along l-axis and the wire radius a is much smaller compared with the operating wavelength λ as $a << \lambda$. And it is thin enough to consider that the current on the surface of the wire has only the l component. In this case, the electric current on the surface of the wire can be assumed to flow on the l-axis. With this assumption, the surface integral can be simplified to the line integral along the l-axis and the current distribution is assumed to be a sinusoidal distribution as

$$\bar{J}_m(\bar{r}') = \begin{cases} \bar{l}_{m-1} I_m \dfrac{\sin\{\beta(\Delta l_{m-1} + l(\bar{r}') - l_i)\}}{\sin(\beta\Delta l_{m-1})} & (l_{i-1} \le l \le l_i) \\ \bar{l}_m I_m \dfrac{\sin\{\beta(\Delta l_m - l(\bar{r}') + l_i)\}}{\sin(\beta\Delta l_m)} & (l_{l+1} \ge l \ge l_i) \\ 0 & \text{elsewhere} \end{cases} \qquad (2.18).$$

The electric field due to half of this electric current $\bar{J}_m$ from l_{i-1} to l_i can be

written with the magnetic vector potential which has only $\bar{l}_{m-1}$ component as

$$E^{//}_{m-1}(\bar{r}) = -j\omega A_{m-1} + \frac{1}{j\omega\varepsilon_0\mu_0}\frac{\partial^2 A_{m-1}}{\partial l^2} \qquad (2.19)$$

$$E^{\perp}_{m-1}(\bar{r}) = \frac{1}{j\omega\varepsilon_0\mu_0}\frac{\partial^2 A_{m-1}}{\partial d\partial l} \qquad (2.20)$$

where d is the distance from the center of the wire to the observation point P. From fig.2.3 $d_{m-1} = r_i \sin\theta_i^{m-1}$. The symbol // indicates the component parallel to the vector $\bar{l}_{m-1}$ and $\perp$ indicates the components in the $\bar{d}_{m-1}$ direction. The l component of the vector potential A_{m-1} is expressed as the integral of the electric current J_m as

$$A_{m-1} = \frac{\mu_0}{4\pi}\int_{l_{i-1}}^{l_i} J_m(\bar{r}')\frac{e^{-j\beta|\bar{r}-\bar{r}'|}}{|\bar{r}-\bar{r}'|}dl' \qquad (2.21).$$

With this vector potential, the electric field in (2.19) can be rewritten as

$$E^{//}_{m-1} = -\frac{1}{4\pi\varepsilon_0\omega}\int_{l_{i-1}}^{l_i}\left[\frac{\partial^2}{\partial l^2}\frac{e^{-j\beta|\bar{r}-\bar{r}'|}}{|\bar{r}-\bar{r}'|} + \beta^2\frac{e^{-j\beta|\bar{r}-\bar{r}'|}}{|\bar{r}-\bar{r}'|}\right]J_m(\bar{r}')dl' \qquad (2.22).$$

Finally the electric field components parallel and tangential to the vector $\bar{l}_{m-1}$ are expressed as

$$E^{//}_{m-1} = \frac{j30.I_m}{\sin(\beta\Delta l_{m-1})}\left[\frac{\cos(\beta\Delta l_{m-1})}{r_i}e^{-j\beta r_i} - \frac{e^{-j\beta r_{i-1}}}{r_{i-1}}\right] \qquad (2.23)$$

$$E^{\perp}_{m-1} = \frac{-30.I_m}{r_i\sin\theta_i^{m-1}}\left[\left\{1 + j\cos\theta_i^{m-1}\cot(\beta\Delta l_{m-1})\right\}e^{-j\beta r_i} - j\frac{\cos\theta_{i-1}^{m-1}}{\sin(\beta\Delta l_{m-1})}e^{-j\beta r_{i-1}}\right] \qquad (2.24).$$

The magnetic field due to the electric current is expressed in the cylindrical coordinates with the vector potential as

$$\bar{H}_{m-1}^{\phi'} = \frac{1}{\mu_0}\nabla \times A_{m-1}\bar{l}_{m-1} = -\frac{1}{\mu_0}\frac{\partial A_{m-1}}{\partial d}$$

$$= \frac{-I_m}{j4\pi r_i \sin\theta_i^{m-1}\sin(\beta\Delta l_{m-1})} \cdot \qquad (2.25).$$

$$\left[e^{-j\beta r_{i-1}} - e^{-j\beta r_i}\left\{\cos(\beta\Delta l_{m-1}) - j\cos\theta_i^{m-1}\sin(\beta\Delta l_{m-1})\right\}\right]$$

The total electromagnetic fields ${}^J\bar{E}_m(P)$, ${}^J\bar{H}_m(P)$ at the observation point P due to the electric current $\bar{J}_m(\bar{r}')$ flowing on the two segments of the wire are expressed as

$${}^J\bar{E}_m(P) = \bar{l}_{m-1}E_{m-1}^{//} + \bar{d}_{m-1}E_{m-1}^{\perp} + \bar{l}_m E_m^{//} + \bar{d}_m E_m^{\perp} \qquad (2.26)$$

$${}^J\bar{H}_m(P) = \bar{\phi}'_{m-1}\bar{H}_{m-1}^{\phi'} + \bar{\phi}'_m\bar{H}_m^{\phi'} \qquad (2.27)$$

where $\bar{d}_{m-1}$ is the unit tangential vector to the plane which includes points l_{m-1}, l_m and P. Also $\bar{d}_m$ represents the unit tangential vector to the plane consisting of three points l_m, l_{m+1} and P. The vectors $\bar{\phi}'_{m-1}$ and $\bar{\phi}'_m$ are defined as follows.

$$\bar{\phi}'_{m-1} = \bar{l}_{m-1} \times \bar{d}_{m-1} \qquad (2.28)$$

$$\bar{\phi}'_m = \bar{l}_m \times \bar{d}_m \qquad (2.29)$$

The total electromagnetic field radiated from the electric current on the antenna can be expressed as

$${}^J\bar{E}(P) = \sum_m {}^J\bar{E}_m(P) \qquad (2.30)$$

$${}^J\bar{H}(P) = \sum_m {}^J\bar{H}_m(P) \qquad (2.31)$$

When the magnetic current distributes in free space the electromagnetic fields due to the magnetic current can be written by using the electric vector potential $\bar{F}_{m-1}(\bar{r})$ as

$$\bar{H}_{m-1}(\bar{r}) = -j\omega\bar{F}_{m-1}(\bar{r}) + \frac{1}{j\omega\varepsilon_0\mu_0}\nabla\left(\nabla \cdot \bar{F}_{m-1}(\bar{r})\right) \qquad (2.32)$$

$$\overline{E}_{m-1}(\overline{r}) = -\frac{1}{\varepsilon_0}\nabla \times \overline{F}_{m-1}(\overline{r}) \qquad (2.33)$$

where

$$\overline{F}_{m-1}(\overline{r}) = \frac{\varepsilon_0}{4\pi}\int_V \overline{M}_{m-1}(\overline{r}')\frac{e^{-j\beta|\overline{r}-\overline{r}'|}}{|\overline{r}-\overline{r}'|}d\rho' \qquad (2.34).$$

The magnetic current is defined as $\overline{M} = \sum K_m \overline{M}_m$ by using same sinusoidal expansion functions as (2.18). Then the total electromagnetic fields due to the magnetic current are written as follows.

$${}^{M}\overline{E}(P) = \sum_m {}^{M}\overline{E}_m(P) = \sum_m \left(\overline{\phi}'_{m-1}\,{}^{M}E^{\phi'}_{m-1} + \overline{\phi}'_m\,{}^{M}E^{\phi'}_m\right) \qquad (2.35)$$

$${}^{M}\overline{H}(P) = \sum_m {}^{M}\overline{H}_m(P) = \sum_m \left(\overline{\rho}_{m-1}\,{}^{M}E^{//}_{m-1} + \overline{d}_{m-1}\,{}^{M}E^{\perp}_{m-1} + \overline{\rho}_m\,{}^{M}E^{//}_m + \overline{d}_m\,{}^{M}E^{\perp}_m\right) \qquad (2.36)$$

where ρ is the coordinate along the magnetic current.

The electromagnetic fields radiated from the electric and the magnetic currents are the sum of these electromagnetic fields as

$$\overline{E} = {}^{J}\overline{E}(P) + {}^{M}\overline{E}(P) \qquad (2.37)$$

$$\overline{H} = {}^{J}\overline{H}(P) + {}^{M}\overline{H}(P) \qquad (2.38).$$

The elements, ${}^{M}E^{\phi'}_{m-1}$, ${}^{M}E^{\phi'}_{m}$, ${}^{M}H^{//}_{m-1}$, ${}^{M}H^{//}_{m}$, ${}^{M}H^{\perp}_{m-1}$, ${}^{M}H^{\perp}_{m}$, ${}^{J}E^{//}_{m-1}$, ${}^{J}E^{//}_{m}$, ${}^{J}E^{\perp}_{m-1}$, ${}^{J}E^{\perp}_{m}$, ${}^{J}H^{\phi'}_{m-1}$ and ${}^{J}H^{\phi'}_{m}$ are shown as follows[19].

$${}^{M}E^{\phi'}_{m-1} = \frac{K_m}{j4\pi r_i \sin\theta_i^{m-1}\sin(\beta\Delta\rho_{m-1})} \cdot \left[e^{-j\beta r_{i-1}} - e^{-j\beta r_i}\left\{\cos(\beta\Delta\rho_{m-1}) - j\cos\theta_i^{m-1}\sin(\beta\Delta\rho_{m-1})\right\}\right] \qquad (2.39)$$

$${}^{M}E^{\phi'}_{m} = \frac{K_m}{j4\pi r_i \sin\theta_i^{m}\sin(\beta\Delta\rho_{m})}\left[e^{-j\beta r_{i+1}} - e^{-j\beta r_i}\left\{\cos(\beta\Delta\rho_{m}) - j\cos\theta_i^{m}\sin(\beta\Delta\rho_{m})\right\}\right] \qquad (2.40)$$

$$^{M}H^{//}_{m-1} = \frac{j30K_m}{Z_0^2 \sin(\beta\Delta\rho_{m-1})}\left[\frac{\cos(\beta\Delta\rho_{m-1})}{r_i}e^{-j\beta r_i} - \frac{e^{-j\beta r_{i-1}}}{r_{i-1}}\right] \qquad (2.41)$$

$$^{M}H^{//}_{m} = \frac{j30K_m}{Z_0^2 \sin(\beta\Delta\rho_{m})}\left[\frac{\cos(\beta\Delta\rho_{m})}{r_i}e^{-j\beta r_i} - \frac{e^{-j\beta r_{i+1}}}{r_{i+1}}\right] \qquad (2.42)$$

$$^{M}H^{\perp}_{m-1} = \frac{-30K_m}{Z_0^2 r_i \sin\theta_i^{m-1}}\left[\left\{1 + j\cos\theta_i^{m-1}\cot(\beta\Delta\rho_{m-1})\right\}e^{-j\beta r_i} - j\frac{\cos\theta_{i-1}^{m-1}}{\sin(\beta\rho_{m-1})}e^{-j\beta r_{i-1}}\right] \qquad (2.43)$$

$$^{M}H^{\perp}_{m} = \frac{-30K_m}{Z_0^2 r_i \sin\theta_i^{m}}\left[\left\{1 - j\cos\theta_i^{m}\cot(\beta\Delta\rho_{m})\right\}e^{-j\beta r_i} + j\frac{\cos\theta_{i+1}^{m}}{\sin(\beta\rho_{m})}e^{-j\beta r_{i+1}}\right] \qquad (2.44)$$

$$^{J}E^{//}_{m-1} = \frac{j30I_m}{\sin(\beta\Delta l_{m-1})}\left[\frac{\cos(\beta\Delta l_{m-1})}{r_i}e^{-j\beta r_i} - \frac{e^{-j\beta r_{i-1}}}{r_{i-1}}\right] \qquad (2.45)$$

$$^{J}E^{//}_{m} = \frac{j30I_m}{\sin(\beta\Delta l_{m})}\left[\frac{\cos(\beta\Delta l_{m})}{r_i}e^{-j\beta r_i} - \frac{e^{-j\beta r_{i+1}}}{r_{i+1}}\right] \qquad (2.46)$$

$$^{J}E^{\perp}_{m-1} = \frac{-30I_m}{r_i \sin\theta_i^{m-1}}\left[\left\{1 + j\cos\theta_i^{m-1}\cot(\beta\Delta l_{m-1})\right\}e^{-j\beta r_i} - j\frac{\cos\theta_{i-1}^{m-1}}{\sin(\beta\Delta l_{m-1})}e^{-j\beta r_{i-1}}\right] \qquad (2.47)$$

$$^{J}E^{\perp}_{m} = \frac{-30I_m}{r_i \sin\theta_i^{m}}\left[\left\{1 - j\cos\theta_i^{m}\cot(\beta\Delta l_{m})\right\}e^{-j\beta r_i} + j\frac{\cos\theta_{i+1}^{m}}{\sin(\beta\Delta l_{m})}e^{-j\beta r_{i+1}}\right] \qquad (2.48)$$

$$^{J}H^{\phi'}_{m-1} = \frac{-I_m}{j4\pi r_i \sin\theta_i^{m-1}\sin(\beta\Delta l_{m-1})}\cdot \left[e^{-j\beta r_{i-1}} - e^{-j\beta r_i}\left\{\cos(\beta\Delta l_{m-1}) - j\cos\theta_i^{m-1}\sin(\beta\Delta l_{m-1})\right\}\right] \qquad (2.49)$$

$$^{J}H^{\phi'}_{m} = \frac{-I_m}{j4\pi r_i \sin\theta_i^{m}\sin(\beta\Delta l_{m})}\left[e^{-j\beta r_{i+1}} - e^{-j\beta r_i}\left\{\cos(\beta\Delta l_{m}) - j\cos\theta_i^{m}\sin(\beta\Delta l_{m})\right\}\right] \qquad (2.50)$$

where θ_{i-1}^{m-1} is the angle between two vectors $\bar{l}_{m-1}$ and $\bar{r}_{i-1}$, and θ_i^{m-1} is the angle between $\bar{l}_{m-1}$ and $\bar{r}_i$ as shown in fig.2.3. Z_0 is the characteristic impedance of free space. The total electric and magnetic fields shown in (2.37) and (2.38) should satisfy the boundary conditions on the surface of the electric and the magnetic conductors and they can be expressed as

$$\overline{E} \times \overline{e}_n = -\overline{e}_\varphi V_0 \delta(l_0) \qquad (2.51)$$

$$\overline{e}_n \times \overline{H} = \overline{e}_\varphi I_0 \delta(\rho_0) \qquad (2.52)$$

where $\overline{e}_n$ and $\overline{e}_\varphi$ are the normal and tangential unit vectors to the surface of the electric and magnetic conductors as shown in fig.2.2.

The residual R is defined to be the sum of the tangential components at the surface.

$$R_W(l) = E_l + V_0 \delta(l_0) \qquad \text{(on the wire surface)} \quad (2.53)$$

$$R_S(\rho) = H_\rho - I_0 \delta(\rho_0) \qquad \text{(on the slot surface)} \quad (2.54)$$

In the method of weighted residuals the I_m's are found such that the residual is forced to zero in an average sense. Then the weight functions, which are already known are multiplied to R and integrated as

$$\int_l W_m R dl' \qquad (2.55)$$

Here Galerkin's method[20] is used, with which the same functions as in (2.18) are used as the weight function W_m. Finally (2.53) is rewritten as

$$\int_{\Delta l_m} W_m(l) E_l dl' + \int_{\Delta l_m} W_m V_0 \delta(l_0) dl' = 0 \qquad (2.56).$$

This is a simultaneous equation about unknown coefficients I_n and (2.56) can be expressed in matrix form as

$$Z_{mn} I_n + C_{mn} V_n = V_m \qquad (2.57).$$

Similarly from the residual (2.54) on the surface of the magnetic current the following relationship is obtained.

$$C_{mn} I_n + Y_{mn} V_n = I_m \qquad (2.58)$$

The boundary conditions at each point of the slot and wire antennas are finally expressed in matrix form as

$$\begin{bmatrix} Y_S & C_{SW} \\ C_{WS} & Z_W \end{bmatrix} \begin{bmatrix} V_S \\ I_W \end{bmatrix} = \begin{bmatrix} I_S \\ V_W \end{bmatrix} \qquad (2.59)$$

where Y_S, Z_W, C_{SW} and C_{WS} are the self-admittance of the slot, self-

impedance of the wire and mutual couplings between the slot and wire, respectively. Once the elements of the matrix can be obtained, we can obtain the electric and magnetic currents immediately. The matrix elements are shown below[19].

$$Y_{mn} = \frac{1}{K_m K_n}\int_{\rho_{i-1}}^{\rho_i}\left({}^{M}H^{//}_{m-1}+{}^{M}H^{//}_{m}+{}^{M}H^{\perp}_{m-1}+{}^{M}H^{\perp}_{m}\right)K_n\frac{\sin\{\beta(\Delta\rho_{n-1}+\rho(\bar{r}')-\rho_i)\}}{\sin(\beta\Delta\rho_{n-1})}d\rho'_n$$

$$+\frac{1}{K_m K_n}\int_{\rho_i}^{\rho_{i+1}}\left({}^{M}H^{//}_{m-1}+{}^{M}H^{//}_{m}+{}^{M}H^{\perp}_{m-1}+{}^{M}H^{\perp}_{m}\right)K_n\frac{\sin\{\beta(\Delta\rho_{n}-\rho(\bar{r}')+\rho_i)\}}{\sin(\beta\Delta\rho_{n})}d\rho'_n \qquad (2.60)$$

$$Z_{mn} = \frac{1}{I_m I_n}\int_{l_{i-1}}^{l_i}\left({}^{J}E^{//}_{m-1}+{}^{J}E^{//}_{m}+{}^{J}E^{\perp}_{m-1}+{}^{J}E^{\perp}_{m}\right)I_n\frac{\sin\{\beta(\Delta l_{n-1}+l(\bar{r}')-l_i)\}}{\sin(\beta\Delta l_{n-1})}dl'_n$$

$$+\frac{1}{I_m I_n}\int_{l_i}^{l_{i+1}}\left({}^{J}E^{//}_{m-1}+{}^{J}E^{//}_{m}+{}^{J}E^{\perp}_{m-1}+{}^{J}E^{\perp}_{m}\right)I_n\frac{\sin\{\beta(\Delta l_{n}-l(\bar{r}')+l_i)\}}{\sin(\beta\Delta l_{n})}dl'_n \qquad (2.61)$$

$$C_{mn} = \frac{1}{I_m K_n}\int_{l_{i-1}}^{l_i}\left({}^{J}H^{\phi'}_{m-1}+{}^{J}H^{\phi'}_{m}\right)K_n\frac{\sin\{\beta(\Delta l_{n-1}+l(\bar{r}')-l_i)\}}{\sin(\beta\Delta l_{n-1})}dl'_n$$

$$+\frac{1}{I_m K_n}\int_{l_i}^{l_{i+1}}\left({}^{J}H^{\phi'}_{m-1}+{}^{J}H^{\phi'}_{m}\right)K_n\frac{\sin\{\beta(\Delta l_{n}-l(\bar{r}')+l_i)\}}{\sin(\beta\Delta l_{n})}dl'_n \qquad (2.62)$$

$$C_{mn} = -C_{nm} \qquad (2.63)$$

2.3 Geometrical theory of diffraction

When the characteristics of the wire antennas on or near a conducting body are analyzed by the moment method. A wire grid model[21] or a surface patch model[22] is used to represent the conducting surface. The problem is significantly limited by the size of the computer memory when these methods are applied to such a problem. Thus the moment method is applied to the problems when the conducting bodies are not very large in terms of the operating wavelength. When the frequency is sufficiently high where the wave characteristics need not be considered, geometrical optics (GO) is a very useful and easily understood method[23]. GO was developed by simply considering the transport of the energy from one point to another without any reference to whether the transport mechanism is particle or wave in nature. Also physical optics (PO) is used to calculate the scattered fields[24]. The concept of PO can be considered more general than GO since the equations obtained from the boundary conditions at the illuminated surface of the conductor for the scattered field often reduce the high frequency limit for the equations of GO. Both theories are often applied to the calculation of the back scattered field from a scatterer, but the field in the forward scattering direction can not be obtained, in particular the shadow region. The current obtained by PO alone is incapable of correctly predicting a non-zero field in the shadow region because PO postulates a current only on the illuminated side and no current on the shadowed side. Although these two methods are very useful, they are inadequate to describe the behavior of the electromagnetic fields perfectly in many situations and it is necessary to include another field called a diffracted field. When the diffracted field is added to the GO field many practical radiation and scattering problems are

permitted to solve in a straightforward manner. The diffracted field makes a non-zero field in the shadow region and modifies the GO field in the illuminated region. Since diffraction is a local phenomenon at high frequencies, only the local conditions near the diffraction point are important. The diffracted ray amplitude can be determined from the appropriate boundary value problem. Such a problem is called a canonical problem and diffraction by the wedge is the most important canonical problem. Wedge diffraction in the extension of GO is proposed by Keller in 1953 and his theory is known as the geometrical theory of diffraction (GTD)[11][12][13]. The postulates of GTD are

1. The diffracted field propagates along the ray path including points on the boundary surface. These ray paths obey Fermat's principle.
2. Diffraction is a local phenomenon at high frequencies. It depends on the nature of the boundary surface and the incident field in the neighborhood of the diffraction point.
3. A diffracted wave propagates along its ray path so that power is conserved in a ray tube and that phase delay equals the wave number times the distance along the ray path from the diffraction point to the observation point.

As shown in fig.2.4 the obliquely incident and the obliquely diffracted rays at the diffraction point Q are described conveniently with the spherical coordinate system centered at Q. Let the position of the source of the incident ray be defined in such spherical coordinate system as (s',γ',ϕ'), and the observation point (s,γ,ϕ). The diffraction point Q is a unique point on

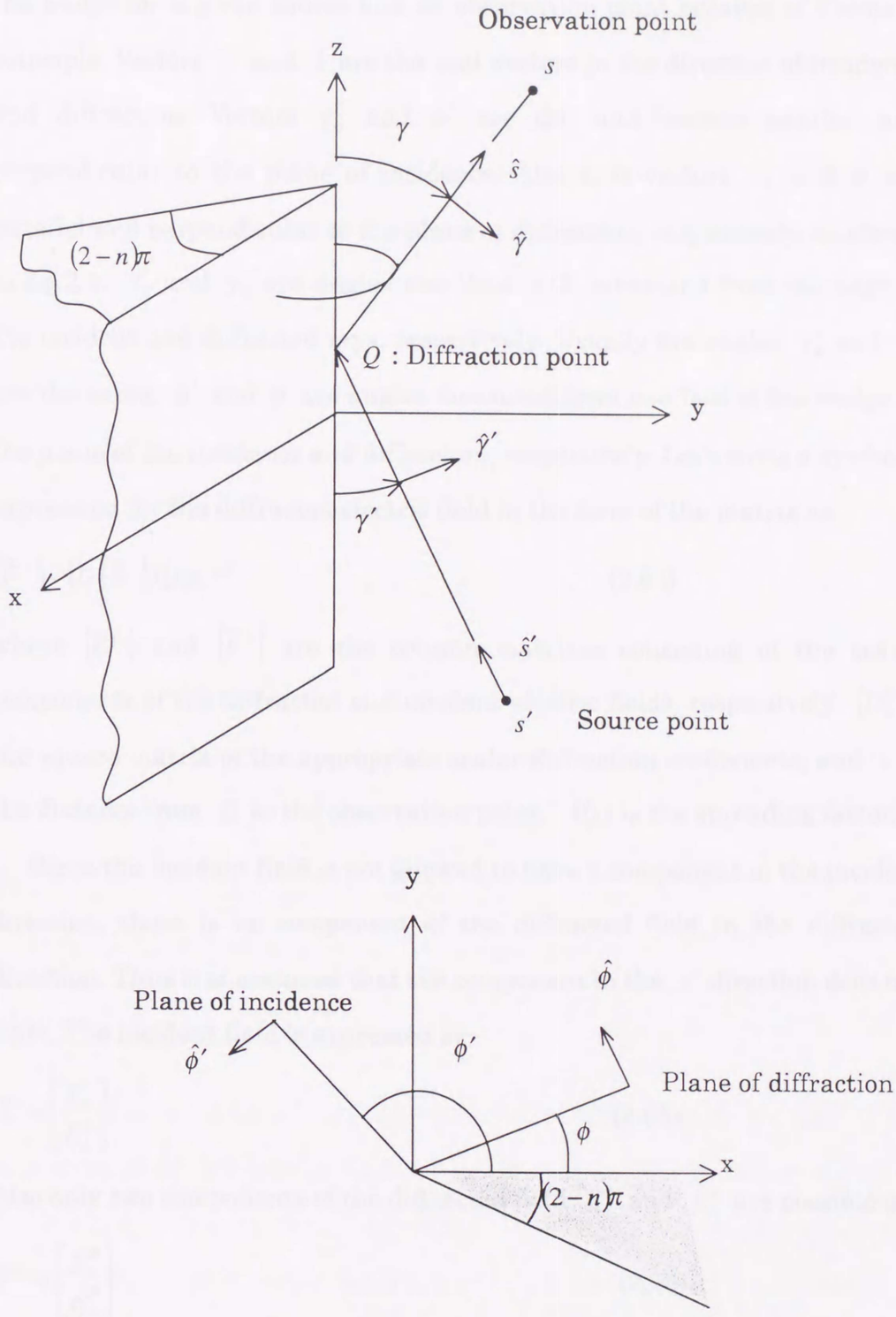

fig. 2.4 Ray fixed coordinate system.

the wedge for a given source and an observation point because of Fermat's principle. Vectors $\hat{s}'$ and $\hat{s}$ are the unit vectors in the direction of incidence and diffraction. Vectors $\hat{\gamma}_0'$ and $\hat{\phi}'$ are the unit vectors parallel and perpendicular to the plane of incidence. Also unit vectors $\hat{\gamma}_0$ and $\hat{\phi}$ are parallel and perpendicular to the plane of diffraction, respectively, as shown in fig.2.4. γ_0' and γ_0 are angles less than $\pi/2$. measured from the edge to the incident and diffracted rays, respectively. Usually the angles γ_0' and γ_0 are the same. ϕ' and ϕ are angles measured from one face of the wedge to the plane of the incidence and diffraction, respectively. Let's write a symbolic expression for the diffracted electric field in the form of the matrix as

$$\left[\overline{E}^d\right] = [D]\left[\overline{E}^i\right] A(s) e^{-j\beta s} \qquad (2.64)$$

where $\left[\overline{E}^d\right]$ and $\left[\overline{E}^i\right]$ are the column matrixes consisting of the scalar components of the diffracted and incident electric fields, respectively. $[D]$ is the square matrix of the appropriate scalar diffraction coefficients, and s is the distance from Q to the observation point. $A(s)$ is the spreading factor.

Since the incident field is not allowed to have a component in the incident direction, there is no component of the diffracted field in the diffracted direction. Thus it is assumed that the component in the s' direction does not exist. The incident field is expressed as

$$\overline{E}^i = \begin{bmatrix} E_{//}^i \\ E_{\perp}^i \end{bmatrix} \qquad (2.65).$$

Also only two components of the diffracted field $E_{//}^d$ and $E_{\perp}^d$ are possible as

$$\overline{E}^d = \begin{bmatrix} E_{//}^d \\ E_{\perp}^d \end{bmatrix} \qquad (2.66).$$

Incident electric fields in (2.65) can be expressed by using electric fields $E^{//}$

and $E^{\perp}$ shown in (2.19) and (2.20) as

$$E^{i}_{//} = E^{//}\bar{l}\cdot\hat{\gamma}' + E^{\perp}\bar{e}_{\varphi}\cdot\hat{\gamma}' \qquad (2.67)$$

$$E^{i}_{\perp} = E^{//}\bar{l}\cdot\hat{\phi}' + E^{\perp}\bar{e}_{\varphi}\cdot\hat{\phi}' \qquad (2.68)$$

where $\bar{l}$ and $\bar{e}_{\varphi}$ are the tangential unit vectors shown in fig.2.2. Clearly $[D]$ is a two by two matrix. Thus the relationship (2.64) is expressed as follows.

$$\begin{bmatrix} E^{d}_{//} \\ E^{d}_{\perp} \end{bmatrix} = \begin{bmatrix} -D_{//} & 0 \\ 0 & -D_{\perp} \end{bmatrix} \begin{bmatrix} E^{i}_{//} \\ E^{i}_{\perp} \end{bmatrix} A(s)e^{-j\beta s} \qquad (2.69)$$

The diffraction coefficients $D_{//}$ and $D_{\perp}$ are expressed as follows[25].

$$D_{\substack{//\\ \perp}}(L,\phi,\phi') = \frac{-e^{-j\pi/4}}{2n\sqrt{2\pi\beta}\sin\gamma_0'} \times \left[\cot\left(\frac{\pi+(\phi-\phi')}{2n}\right) F\left[\beta L a^{+}(\phi-\phi')\right] \right.$$

$$+\cot\left(\frac{\pi-(\phi-\phi')}{2n}\right) F\left[\beta L a^{-}(\phi-\phi')\right]$$

$$\mp\left\{ \cot\left(\frac{\pi+(\phi+\phi')}{2n}\right) F\left[\beta L a^{+}(\phi+\phi')\right] \right.$$

$$\left.\left. +\cot\left(\frac{\pi-(\phi+\phi')}{2n}\right) F\left[\beta L a^{-}(\phi+\phi')\right] \right\} \right] \qquad (2.70)$$

where $(2-n)\pi$ is the interior angle of the wedge. If $\beta L a^{\pm}(\phi\pm\phi')$ in the function F is represented by X, F is expressed as

$$F(X) = 2j\left|\sqrt{X}\right| e^{jX} \int_{\sqrt{X}}^{\infty} e^{-j\tau^2} d\tau \qquad (2.71).$$

This is a Fresnel integral [26] appeared in the diffraction coefficient. $F(X)$ can be regarded as a correction factor to be used in the transition regions of the shadow and reflection boundaries. The argument of the transition function, which is $X = \beta L a^{\pm}(\phi\pm\phi')$, may be calculated for a known value of βL when $a^{\pm}$ as a function of $(\phi\pm\phi')$ is known. The function $a^{\pm}(\phi\pm\phi')$ is expressed as

$$a^{\pm}(\phi \pm \phi') = 2\cos^2\left[\frac{2n\pi N^{\pm} - (\phi \pm \phi')}{2}\right] \qquad (2.72).$$

in which $N^{\pm}$ are the integrals which satisfy most nearly the four conditions as

$$2\pi n N^{+} - (\phi \pm \phi') = \pi \text{ and } 2\pi n N^{-} - (\phi \pm \phi') = -\pi \qquad (2.73).$$

The distance parameter L depends on the type of the incident wave and the incident angle γ_0, as well as the distances s and s'. And it is given as

$$L = \frac{s's\sin^2\gamma_0}{s+s'} \quad \text{(for spherical wave incidence)} \qquad (2.74).$$

The spatial attenuation factor $A(s)$ is defined as follows.

$$A(s) = \left[\frac{s'}{s(s'+s)}\right]^{\frac{1}{2}} \quad \text{(for spherical wave incidence)} \ (2.75).$$

CHAPTER 3

A slot antenna with a parasitic wire for dual band operation

3.1 Background

Two frequency bands are provided for wireless communication in Japan. An idea of a dual mode cellular phone system can be applied to the effective use of the frequency band. Although the increase of the users of the portable telephone is remarkable, frequency band for wireless communication is limited. A lot of endeavors have been made to use the limited frequency band effectively. For example, in the cellular phone system the same frequency is reused in the different cells that are separate from each other. Lately, to deal with the increase of the users, the idea of a dual mode cellular phone capable of operating in two different cellular systems has been introduced. And it is also important to save the cost of making two different frequency antenna systems. Thus the dual frequency antennas for base stations can save the cost. Figure 3.1 shows two types of dual frequency antenna that have been already studied. A parasitic dipole element is located closely to a driven dipole antenna as shown in fig. 3.1a. A cylindrical dipole used as a driven element is a very wide frequency band antenna. We can obtain a relative bandwidth (VSWR$\leqq$1.5) of about 20%. When the distance between these dipoles is designed to be within 0.1 operating wavelength, another resonant frequency can be obtained proportionally to the length of the parasitic dipole[27]. The current distribution on the driven dipole is influenced by the parasitic element strongly at the second resonant frequency. It is supposed that in free space two sinusoidal current distributions are induced on the

driven element when its length is about one wavelength. So the amplitude of the current at the feed point nearly equals to zero. When the parasitic element is close to the driven element, the current distribution is changed to the one that has a sinusoidal current distribution and the maximum current locates near the feed point[28]. Another dual frequency antenna is shown in

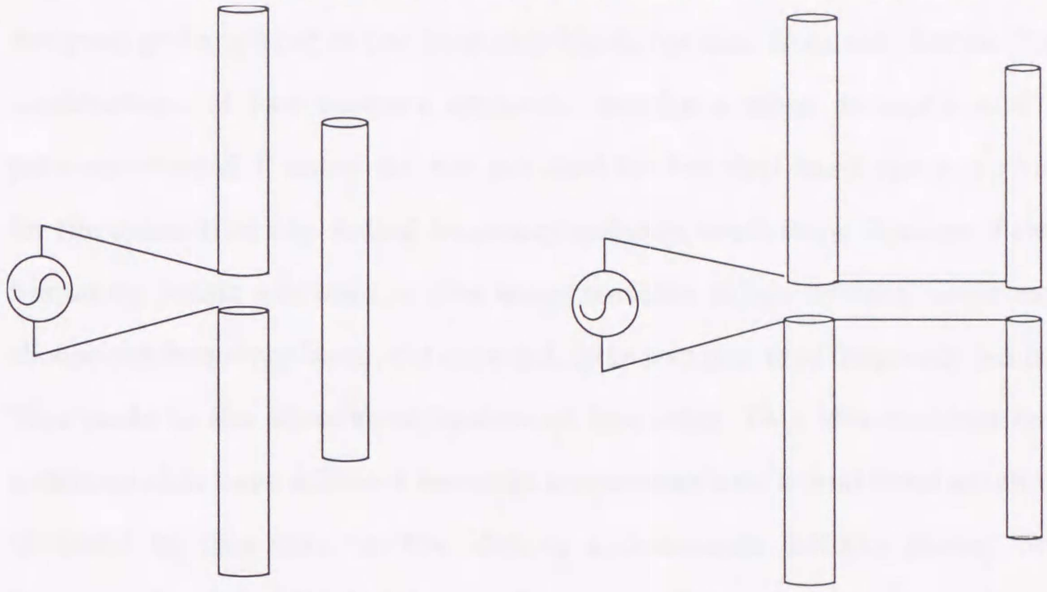

antenna a. antenna b.

fig. 3.1 Dual frequency antennas.

fig. 3.1b. This antenna consists of two driven dipoles and they are connected in series to the feed line. Not only the distance between two dipole antennas but also two resonant frequencies can be chosen freely with this antenna[29]. These dual band antennas are considered their applications for the base stations. On the other hand, the antennas for a portable phone are studied in many papers. For example, the characteristics of the whip antenna on a

portable phone have been analyzed using the wire grid model [30]. From the design point of view the antenna size must become comparable to the body of the portable phone if the body becomes excessively small. So a top-loaded whip antenna with a small cylinder is proposed to shorten antenna length[31]. These antennas and antennas on the portable phone body are designed and analyzed at one frequency band, not dual frequency bands. The combinations of two antenna elements, usually a whip monopole and a planner inverted F antennas, are not used for the dual band operation but for the space diversity. A dual frequency antenna is effective. Because if two frequency bands are used in the same portable phone system, users can choose one frequency band, not crowded, from two provided frequency bands. This leads to the effective utilization of frequency. This idea requires two antennas that have different resonant frequencies and a dual band antenna is useful in this case. In the idea of a dual-mode cellular phone, two frequency bands are fairly far apart from each other and the antenna should be operated well at both frequency bands. Usually two antennas, each of which has a feed point, are used when two different frequency bands are used. On the other hand, when two antennas are located closely each other, antenna characteristics, such as input impedance and radiation pattern, are different from the free space characteristics. Although two antennas must be used fairly apart to avoid these system distraction problems, the size of the portable phone is getting smaller and smaller with the development of small electronic devices. A dual band antenna is useful to save space for the installation of an antenna in a limited area. A dual band antenna that the signals are transmitted or received by two different antennas was reported with the experimental data[32]. This antenna consists of two planar inverted

F antennas that have different resonant frequencies about 10% apart from each other and each antenna has a feed point. This antenna is not designed for dual band operation. Also a dual band antenna combining a helical antenna and a monopole antenna has been reported[33]. This antenna has two frequency bands, which are fairly apart from each other.

In this chapter, three types of dual frequency antenna with the combination of a slot antenna and a parasitic wire element are proposed[34][35]. These antennas are designed for the dual band operation by using the coupling between a slot antenna and a parasitic wire. These antenna elements have strong coupling in the configurations proposed in this chapter and the coupling effects can make these antennas resonate at two frequency bands. It is well known that an antenna with the combination of a slot antenna and parasitic wires can be used for pattern shaping[1]-[5]. In literature [5], an antenna with the combination of a slot antenna with two parasitic wires is proposed and the strong coupling between the slot antenna and two wires is obtained in their configuration. Induced electric currents on the wire reradiate electromagnetic fields. Then the total field above the ground plane is the sum of the direct field radiated from the slot and the reradiated fields from the wires. If coupling is used effectively, it can give new and better characteristics which a single element can not have. A well-known TV receiving antenna, a Yagi-Uda array antenna is the case where the coupling is used effectively. A Yagi-Uda array antenna consists of three parts functionally. They are directors, reflectors and a driven element and this antenna effectively uses adjusted couplings between these elements. A Yagi-Uda array antenna consists of only wires instead of slots. More attractive antenna characteristics are obtained from the combination of

wires and slots.

Some design procedures of a dual frequency antenna are shown. The length of the parasitic wire determines the lower resonant frequency and the slot length determines the higher resonant frequency. The bandwidth at a low frequency band depends on the height of the wire and the parasitic wire has the optimum height to maximize the bandwidth. Radiation patterns depend on the electric and magnetic current distributions. At a lower frequency band, the parasitic wire becomes resonant and the radiation pattern is due to the shape of the wire element. On the other hand, a slot antenna resonates at a higher frequency band, so the radiation pattern at higher frequency depends on the slot configuration.

3.2 Antenna structures

Three types of antenna combining a slot antenna and a parasitic wire are shown in fig.3.2. A slot antenna is made on an infinite ground plane and the region under the ground plane is assumed an infinite half space. In the region over the ground plane, a parasitic wire element is set beside or over the slot and one or two ends of the parasitic wire are connected to the ground plane. The slot length is adjusted to about a half wavelength at a higher frequency. For dual band operation, the total length of the parasitic wire is adjusted to a quarter wavelength for antenna a. and one wavelength for antenna b. and c. at a lower frequency, respectively. In this paper the slot length is fixed to 100mm for antenna a. and b., and 115mm for antenna c. The slot is fed by a coaxial cable and the feed point is located near point A to adjust the input impedance. The parasitic wire has parallel and vertical

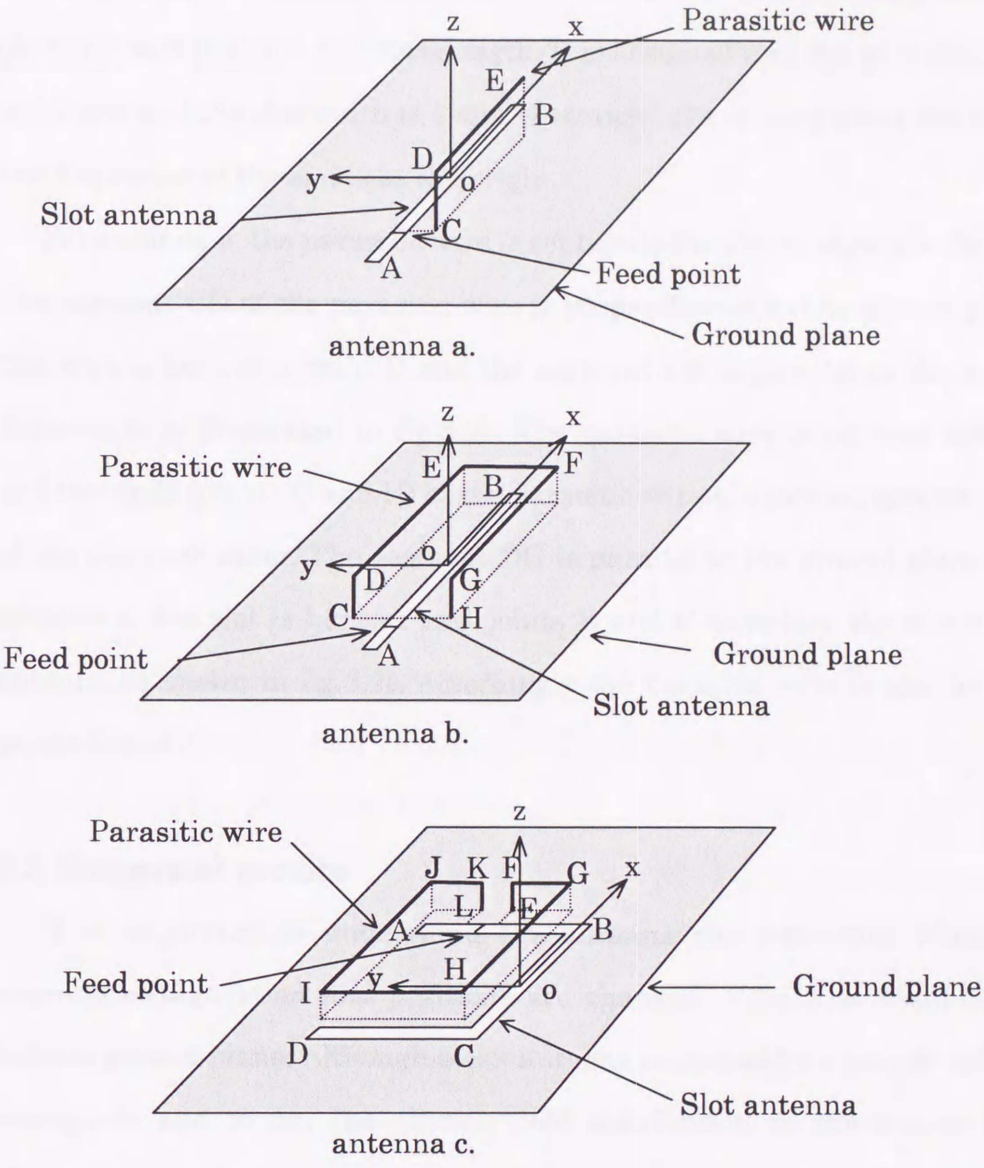

fig. 3.2 Antenna structures.

segments to the ground plane. The vertical wire is necessary to get a strong coupling between a slot and a wire. Electromagnetic coupling can induce electric current on the wire without a feed point on it, so only one feed point is needed in the slot. The slot antenna is made on the surface and it has a low profile. In these configurations, the low profile characteristic still remains

although the parasitic wire is set over or beside the slot. The height of the parasitic wire is about 1/30 wavelength. It is assumed that the wire diameter is 1.2 mm and the slot width is 1 mm. A straight slot is lying along the x-axis and the center of the slot is at the origin.

For antenna a. the parasitic wire is set beside the slot as shown in fig.3.2a. The segment CD of the parasitic wire is perpendicular to the ground plane. The wire is bent at a point D and the segment DE is parallel to the x-axis. Antenna b. is illustrated in fig.3.2b. The parasitic wire is set over the slot and two ends (points C and H) of the parasitic wire are located opposite side of the slot each other. The segment DG is parallel to the ground plane. For antenna c. the slot is bent at two points B and C to reduce the size of the antenna as shown in fig.3.2c. Accordingly the parasitic wire is also bent at points G and J.

3.3 Numerical results

It is important to understand the antenna characteristics when the antenna configuration and positions are changed. Here it is assumed an infinite ground plane. Although a slot antenna is excited by a coaxial cable, a waveguide and so on, the electric field distribution in the slot is little changed with the feeding method. Generally the electric field (magnetic current) in the slot distributes sinusoldally along the longer side and follows the Maxwell's distribution in the narrow side. For the Maxwell's distribution the amplitude of the electric field is the minimum in the center and increases as it gets close to the edge of the slot. It is assumed that the slot width is much smaller compared with the operating frequency and it is about 0.01 wavelength. Then the magnetic current distribution in the narrow direction

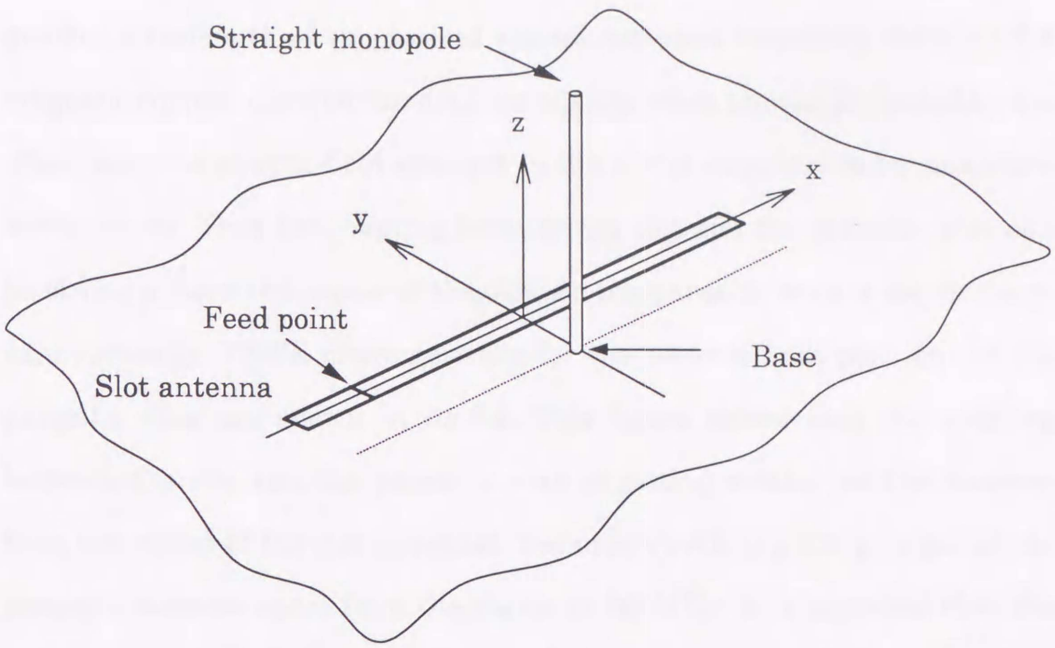

fig. 3.3 A slot antenna with a straight monopole.

can be considered as constant. Since the slot width is very narrow, a thin magnetic current wire is assumed just above the slot and the slot aperture is covered with the conductor by using the equivalence principle. Then image theory is used to remove the ground plane. Finally, the problem is changed to the magnetic and the electric current in free space. If the half wavelength slot antenna is fed at the center, the input impedance of the slot is large (about 600 Ω) and does not match the feed line. Thus usually an offset feed is applied to excite a slot. The slot antennas for antenna a. and b. are fed at a point in the slot, x=-33mm and for antenna c. the feed point is located at a point (x, y)=(18.5mm, 32mm). The combination of a straight slot antenna and a straight parasitic wire is the simplest combination, which is supposed to provide the basic characteristics. The length and width of the slot shown in fig.3.3 are 100mm and 2mm, respectively. The height and radius of a parasitic wire are 80mm and 0.6mm. The length of the wire is about a

quarter wavelength of the desired second resonant frequency. Because the magnetic current distribution does not change when the slot is excited by the offset feed, the electric field strength in the slot is supposed to be maximum at the center. Thus the coupling between the slot and the parasitic wire can be strong around the center of the slot. So the parasitic wire is set on the y-axis vertically. VSWR characteristics for the various base positions of the parasitic wire are shown in fig.3.4. This figure shows that the coupling between the slot and the parasitic wire is getting weaker as the distance from the center of the slot increases. Because VSWR is getting larger as the parasitic element apart from the x-axis at 860MHz, it is supposed that the influence of the parasitic wire becomes weaker. In the actual model, the distance between the center of the slot antenna and the parasitic wire can be as close as 1.6mm (the slot width and the wire radius are 2mm and 0.6mm, respectively). When the distance is 1.6mm, the strongest coupling is obtained in fig.3.4, but the minimum VSWR is about 9.6. As the difference of the VSWRs between the base positions of 1.6mm and 5mm is within 1, the distance between the slot and the base is fixed to 5mm. Then the base of the parasitic wire is moved with the distance 5mm and parallel to the slot (parallel to the x-axis). The minimum VSWR (6.8) is obtained when the base position is located near the feed point at (-25mm, -5mm) as shown in fig.3.5. In this paper a resonance frequency is defined as the frequency at the local minimum VSWR. By the effect of the coupling between the slot and the wire, the parasitic wire becomes resonant at 870MHz. Usually the slot does not resonate at that frequency, but the minimum VSWR is obtained due to coupling at 870MHz. These results suggest that the second resonant frequency can be obtained by the induced electric current on the parasitic

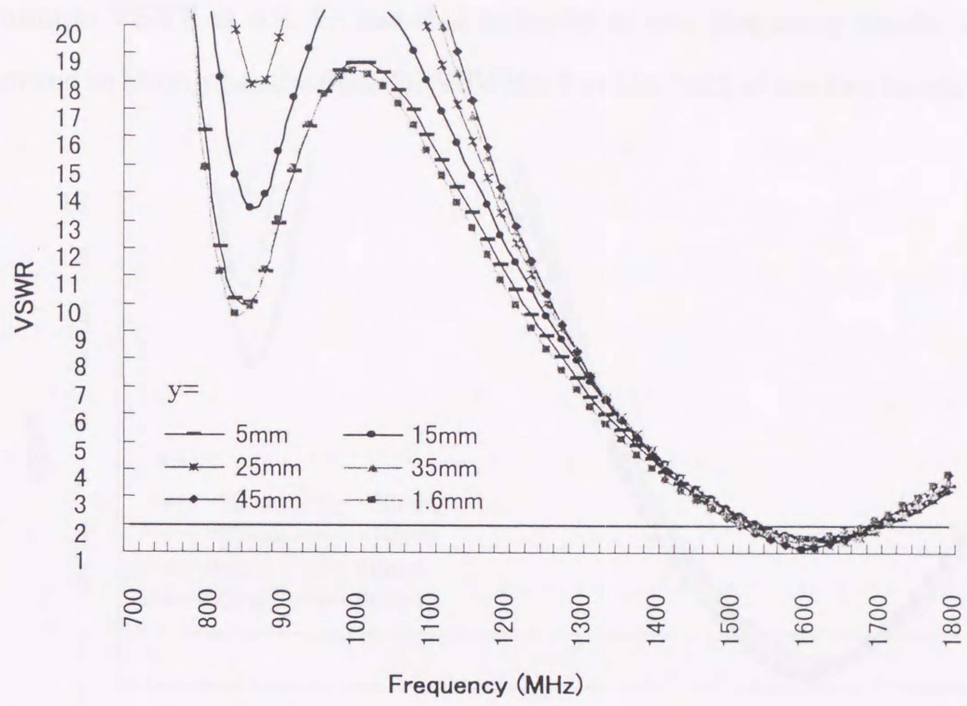

fig. 3.4 VSWR characteristics with respect to the base positions along the y-axis (x=0mm).

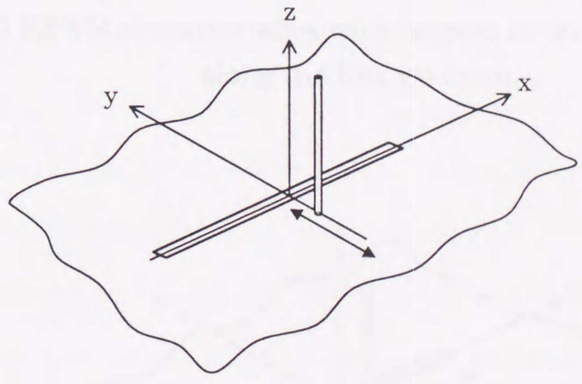

wire and the current makes the slot resonate at the second frequency. The input impedance of the antenna does not match the feed line when the minimum VSWR is 6.8. To use this antenna at two frequency bands, it is required to obtain bandwidths for VSWR≦2 at the both of the two bands.

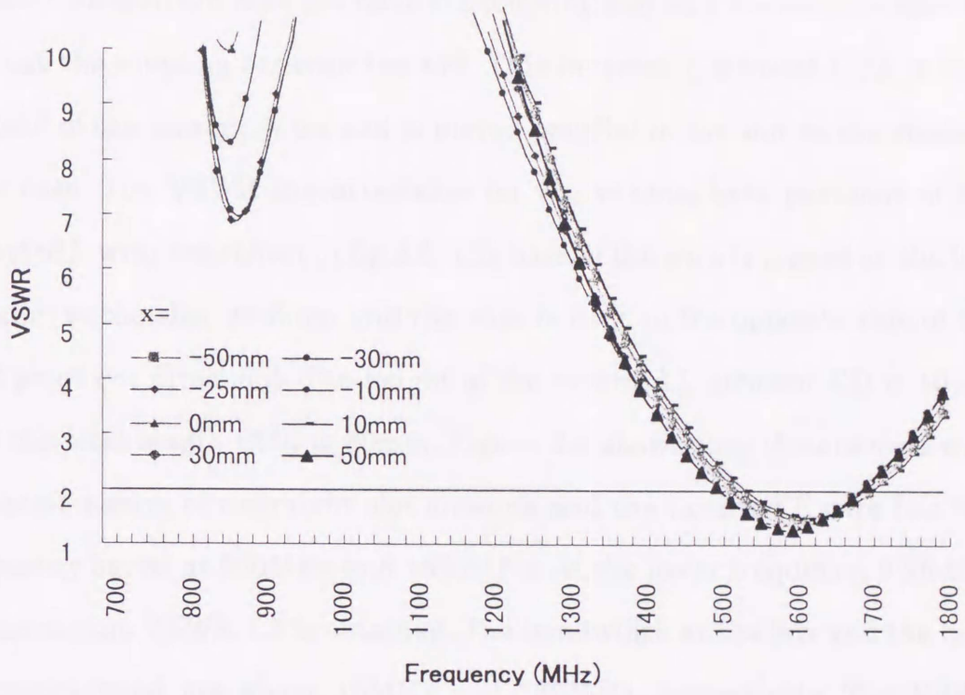

fig. 3.5 VSWR characteristics with respect to the base positions along the line y=-5mm.

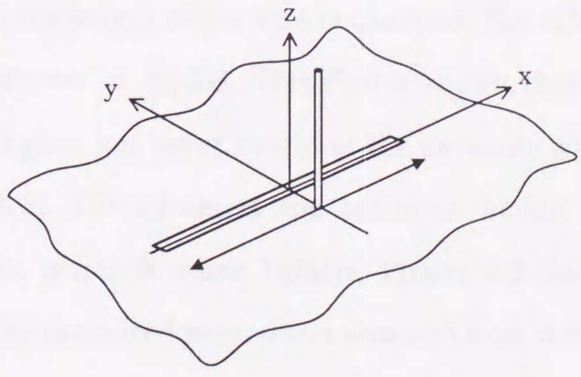

To bend a wire antenna is a very popular way to reduce the height of an antenna. This method is applied to the straight parasitic element as antenna a. shown in fig. 3.2a where the wire is bent at a point D to make segment DE parallel to both of the ground plane and the slot. In this configuration the parallel element DE does not have the coupling and only the vertical element CD has the coupling between the slot. This inverted L element CDE is used instead of the straight wire and is moved parallel to the slot as the straight wire case. The VSWR characteristics for the various base positions of the inverted L wire are shown in fig.3.6. The base of the wire is moved on the line parallel to the slot, y=-5mm and the wire is bent to the opposite side of the feed point (+x direction). The height of the inverted L element CD is 10mm and the total length CDE is 80mm. Figure 3.6 shows that the antenna with the combination of a straight slot antenna and the inverted L wire has two frequency bands at 920MHz and 1620MHz. At the lower frequency, 920MHz, the minimum VSWR 1.5 is obtained. The bandwidth at the low and the high frequency band are about 10MHz and 150MHz, respectively. The VSWR characteristics with respect to more detailed base positions are shown in fig. 3.7. The frequency at the minimum VSWR is shifted to a higher frequency as the base position is moved from the center to the feed point and the widest bandwidth is obtained at x=-8mm. Then the total length of the parasitic wire is fixed to 80mm and the height of the wire is changed. The calculated VSWR characteristics are shown in fig.3.8. This figure shows that the optimum height exists and a higher nor lower height of the parasitic wire reduces the bandwidth (VSWR$\leqq$2). CD=13mm is the optimum height to obtain the maximum bandwidth, which is about 12MHz. Figure 3.9 shows the VSWR characteristics with the optimized parameters obtained from these simulations.

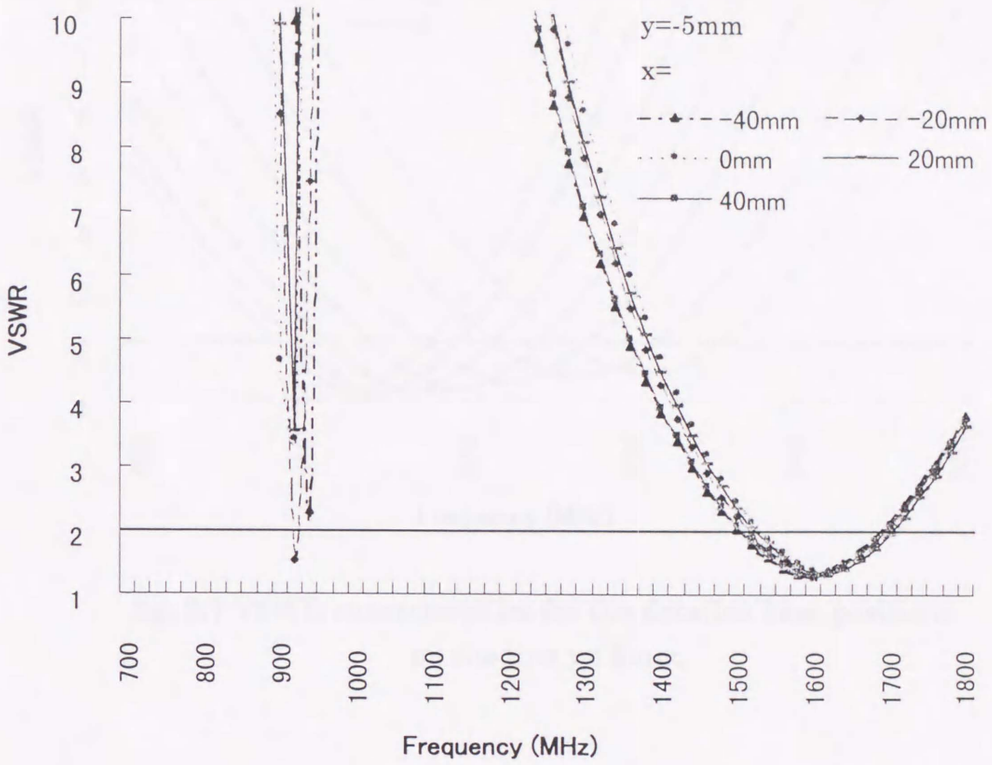

fig. 3.6 VSWR characteristics of the combination of a slot antenna with an inverted L wire with respect to the base positions.

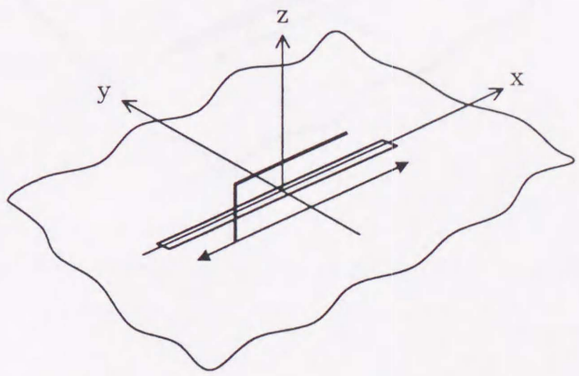

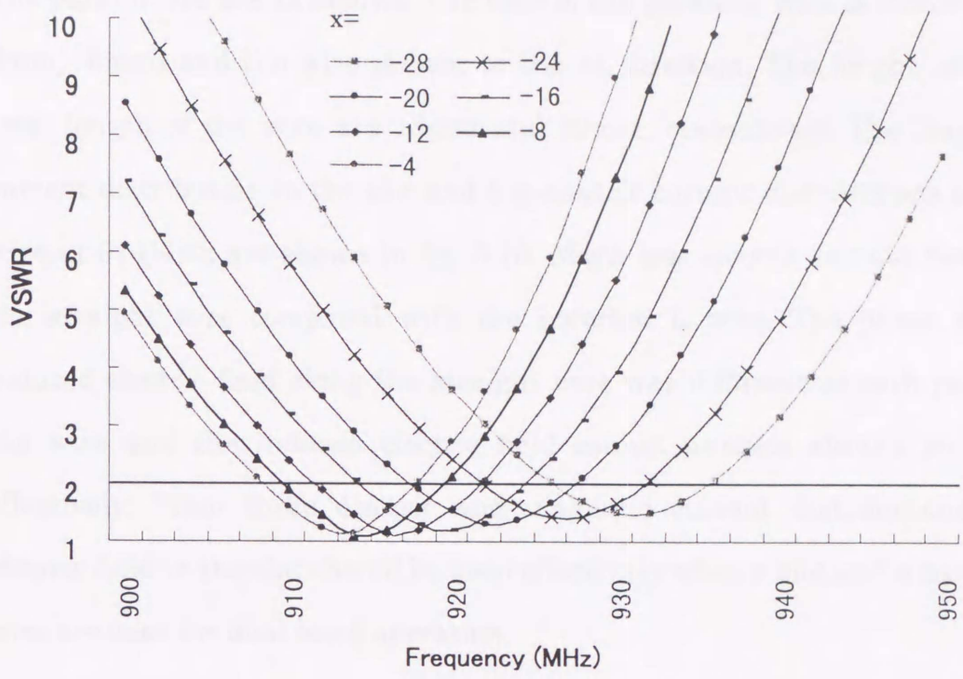

fig. 3.7 VSWR characteristics for the detailed base positions on the line y=-5mm.

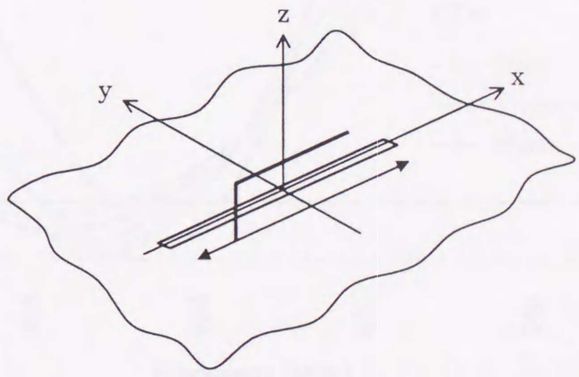

The parameters are as follows. The base of the parasitic wire is located at (-8mm, -5mm) and the wire is bent to the +x direction. The height and the total length of the wire are 13mm and 80mm, respectively. The magnetic current distribution in the slot and the electric current distributions on the wire at 914MHz are shown in fig. 3.10. Much less electric current flows on the straight wire compared with the inverted L wire. The phase of the induced electric field along the straight wire was different at each point of the wire and the induced electric field cannot produce electric currents effectively. From these electric and magnetic current distributions, the electric field in the slot should be used effectively when a slot and a parasitic wire are used for dual band operation.

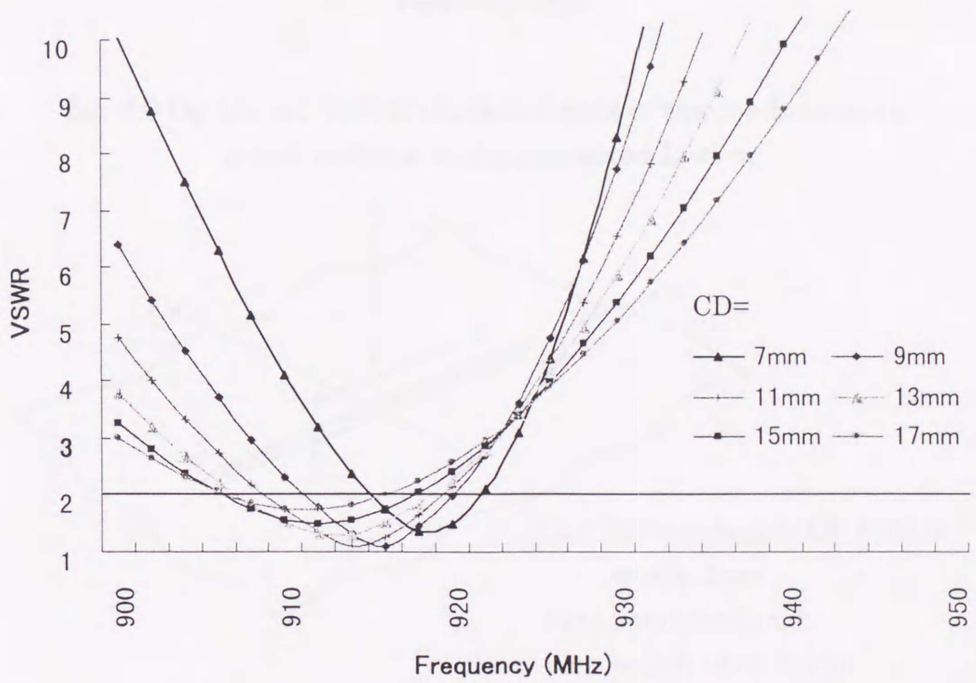

fig. 3.8 VSWR characteristics for various antenna heights.

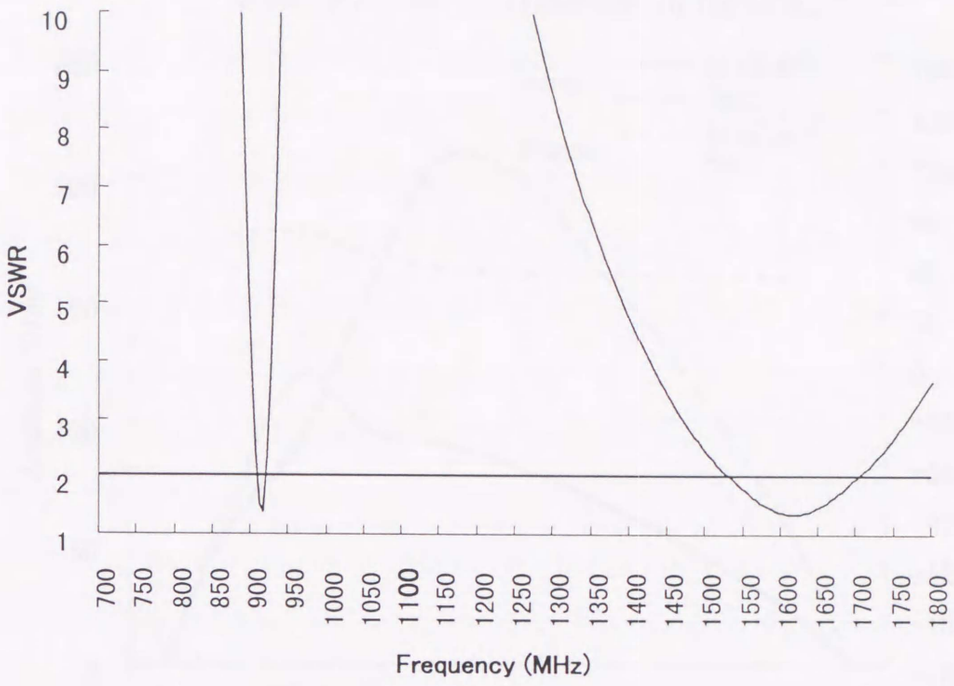

fig. 3.9 Optimized VSWR characteristics of the combination of a slot antenna and an inverted L wire.

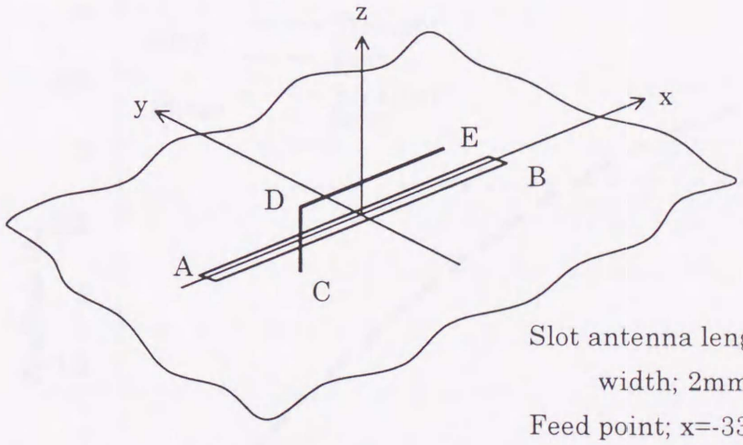

Slot antenna length AB; 100mm
width; 2mm
Feed point; x=-33mm
Wire length CDE; 80mm
height CD; 13mm
radius; 0.6mm
Base position; (x, y)=(-8mm, -5mm)

Magnetic current distributions in the slot.

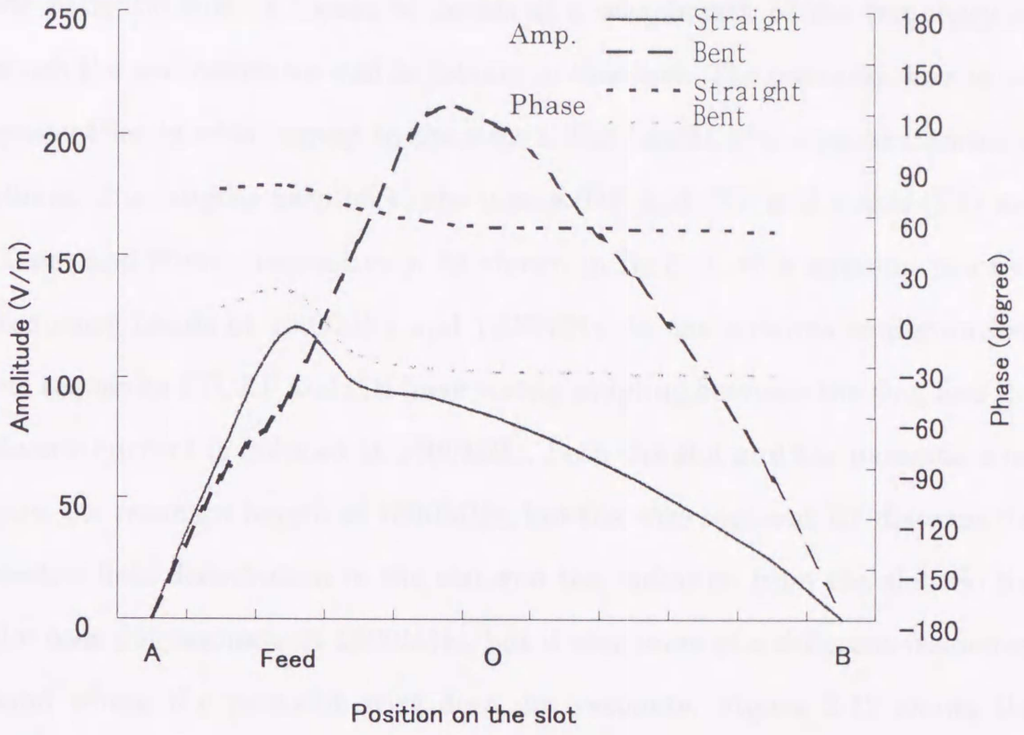

Electric current distributions on the wire.

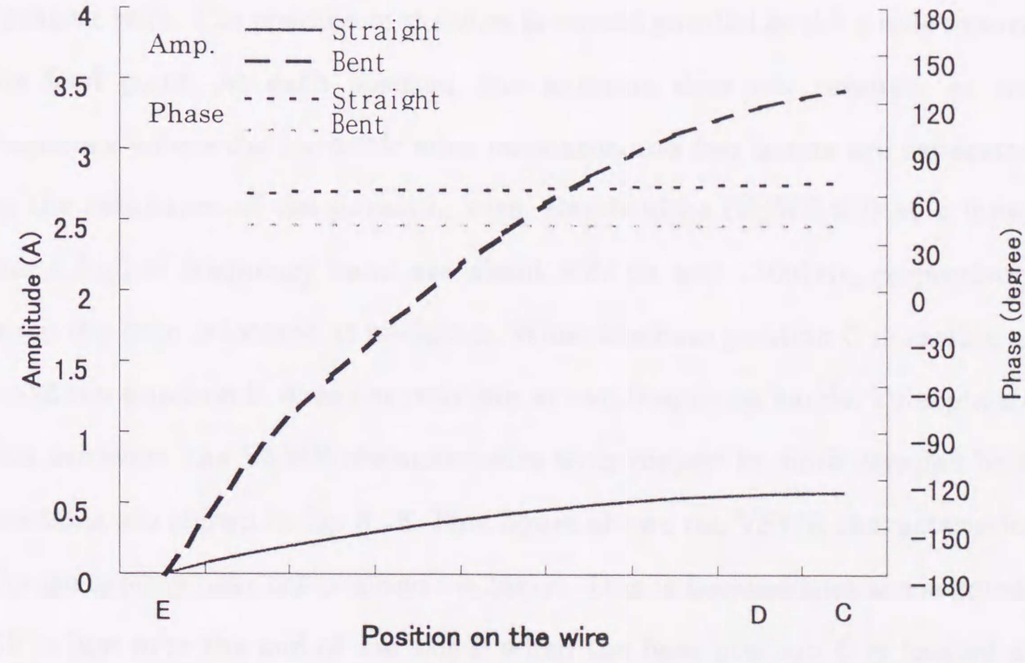

fig. 3.10 Electric and magnetic current distributions at 914MHz.

Antenna b., shown in fig.3.2b has two resonant frequencies. The length of the parasitic wire is chosen to be about a wavelength of the frequency at which the slot resonates and is 190mm in this case. The parasitic wire is set symmetrically with respect to the x-axis. The height of the parasitic wire is 10mm. The lengths parallel to the x-axis (DE and FG) and y-axis (EF) are 70mm and 30mm, respectively. As shown in fig.3.11, this antenna has two frequency bands at 1500MHz and 1800MHz. In the antenna configuration, the segments CD, EF and GH have strong coupling between the slot, and the electric current is induced at 1600MHz. Both the slot and the parasitic wire have the resonant length at 1600MHz, but the wire segment EF disturbs the electric field distribution in the slot and the radiation from the slot. So the slot does not resonate at 1600MHz, but it resonates at a different frequency band where the parasitic wire does not resonate. Figure 3.12 shows the VSWR characteristics of antenna b for the various base positions of the parasitic wire. The position of the wire is moved parallel to the x-axis toward the feed point. At each position, the antenna does not resonate at the frequency where the parasitic wire resonates and two bands are separated by the resonance of the parasitic wire. Bandwidths (VSWR$\leqq$2) at a lower and a higher frequency band are about 95MHz and 110MHz, respectively when the base is located at x=-50mm. When the base position C is located at x=-25mm antenna b. does not resonate at two frequency bands. To explicate this behavior, the VSWR characteristics with respect to more detailed base positions are shown in fig. 3.13. This figure shows the VSWR characteristics change rapidly near the position x=-25mm. This is because that the segment EF is just over the end of the slot B when the base position C is located at x=-20mm. The reason the characteristics change rapidly is explicated as

follows. It has been shown before that the effect of the inverted L wire is strongest when the base is at x=-20mm. Thus when the segment EF is not over the slot (x>-20mm) the effect of the vertical segments (CD and GH) is strong and the slot does not resonate at 1600MHz. On the other hand, when the segment EF is located over the slot (x<-20mm) EF disturbs the slot resonance.

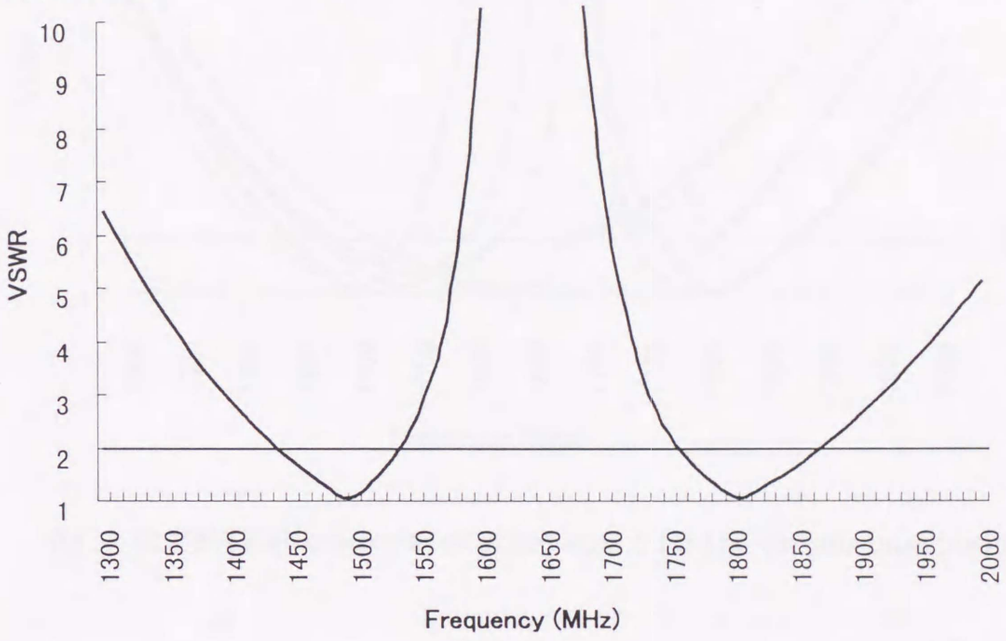

fig. 3.11 VSWR characteristics of antenna b.

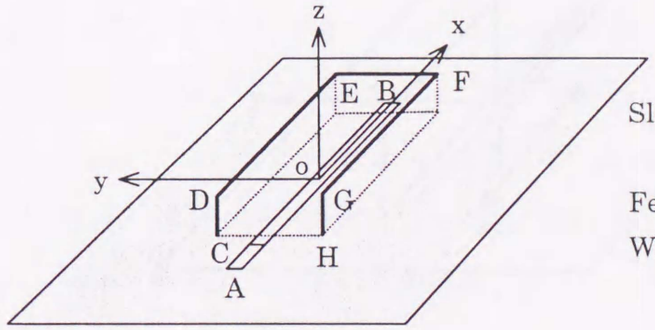

Slot length AB; 100mm
width; 2mm
Feed point; x=-33mm
Wire height CD and GH; 10mm
length DE and FG; 70mm
length EF; 30mm
radius; 0.6mm
Position C; (x, y)=(-50mm,15mm)

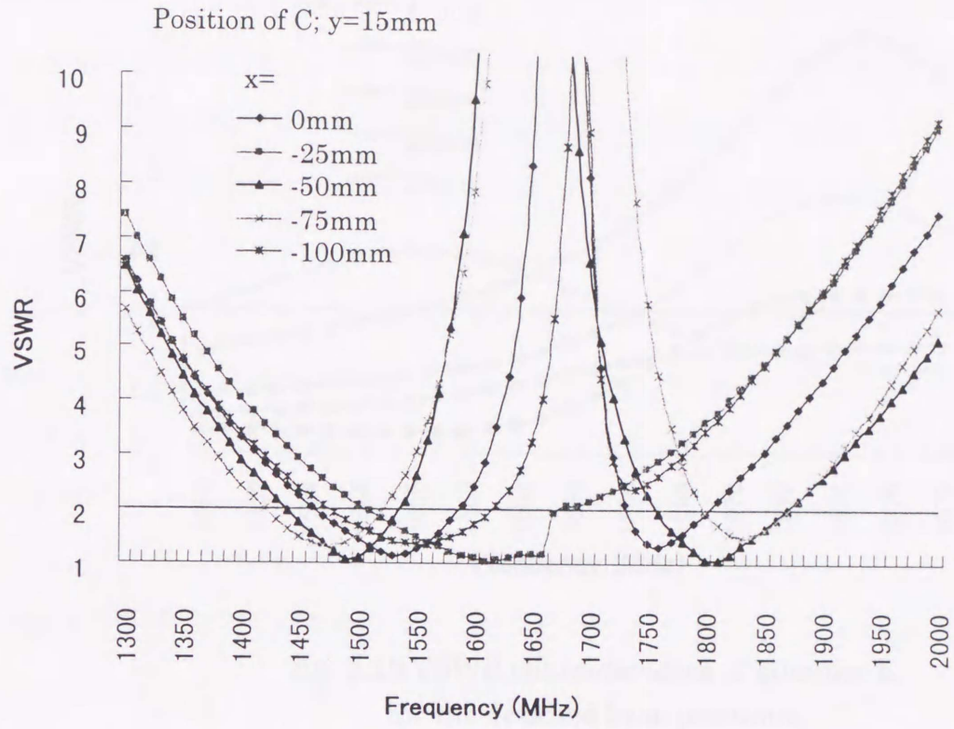

fig. 3.12 VSWR characteristics of antenna b for the various base positions.

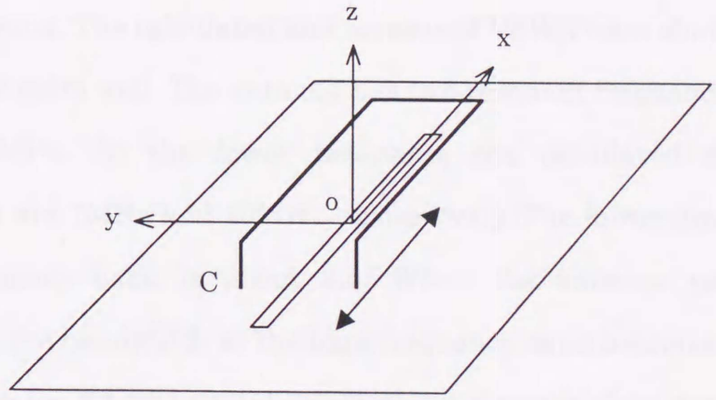

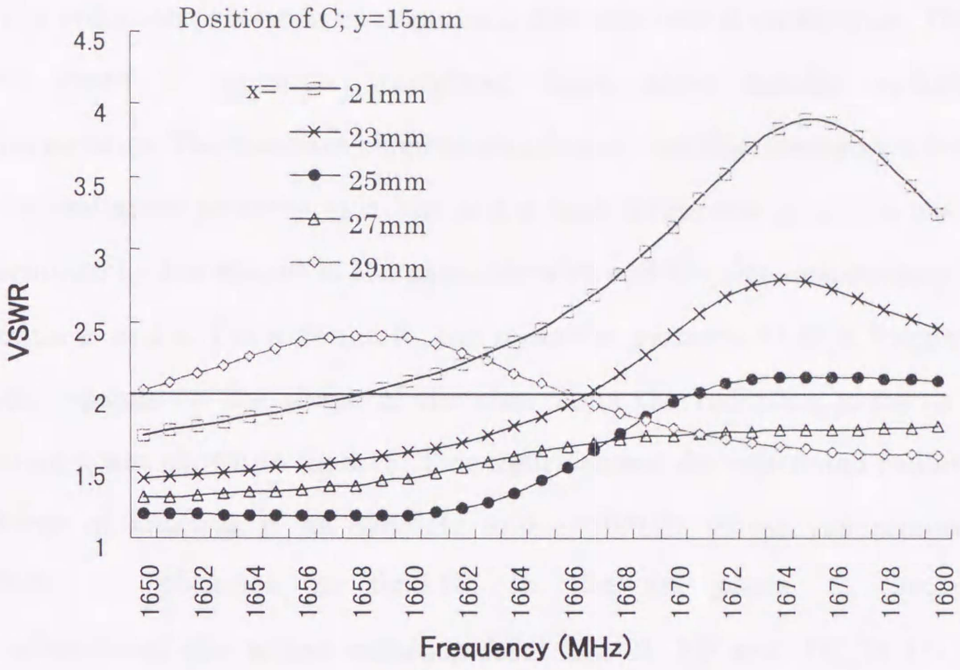

fig. 3.13 VSWR characteristics of antenna b.
for the detailed base positions.

Antennas used for mobile communication are required to be small. For antenna c. shown in fig.3.2c, the slot is bent at two points B and C, and the parasitic wire is also bent at points J and G near the ends to reduce the size of the antenna. The calculated and measured VSWR's are shown in fig. 3.14. They agree quite well. The antenna has two resonant frequencies at 825MHz and 1430MHz. At the lower resonance the calculated and measured bandwidth are 7MHz and 10MHz, respectively. The minimum VSWR at the high frequency band is about 3.5. When the antenna parameters are optimized, the bandwidth at the high frequency band becomes about 50MHz as shown in fig. 3.14. The total length and the height of the parasitic wire are adjusted to 188mm and 7mm, respectively. The bandwidth at the low frequency band is still narrow, but it may be increased by using a thicker parasitic wire.

The radiation pattern is an important characteristic of an antenna. These three types of antenna introduced here show similar radiation characteristics. The resonant element mainly radiates electromagnetic fields. So the radiation patterns at a low and a high frequency band are mainly determined by the shapes of the parasitic wire and the slot, respectively, for antenna a. and c. For antenna b., the radiation patterns at both frequency bands depends on the shape of the slot. Thus the radiation patterns for antenna c. are shown in fig.3.15. This figure shows the calculated radiation patterns of antenna c. at 825MHz and 1430MHz where the minimum VSWRs are obtained in fig.3.15. In the x-z plane E_θ becomes omnidirectional due to the radiation from LK, JI, EF and GH. In the y-z plane E_θ at 825MHz has a null in the $\theta = 0°$ direction. The reason is that the large electric currents flow from G to F and from J to K (their directions are opposite.), and their contribution to E_θ in the $\theta = 0°$ direction is canceled. At 1430MHz the radiation from the slot is dominant. Thus in the x-z plane E_ϕ is due to the radiation from the slot segment BC. In the y-z plane E_θ is the radiation from the slot segment BC and becomes omnidirectional.

Table 2.1 shows the gains (referred to an isotropic source) in each plane. The gains without a parasitic wire are also shown. A straight slot antenna without a parasitic wire and a bent slot antenna without a parasitic wire are resonant only at 1600MHz and 1345MHz, respectively. The gains of antennas a. and c. are close to the ones without a parasitic element at a higher frequency. This is because that the electric current that flows on the parasitic wire is little and it does not affect the radiation patterns at that frequency. At a lower frequency, it is supposed that the gains in each plane

depend upon the configuration of the parasitic wire for antenna a. and c. The slot antenna becomes resonant at a frequency where the parasitic wire does not resonate for antenna b., thus the gains are close to the ones without a parasitic wire at both of the higher and the lower frequencies.

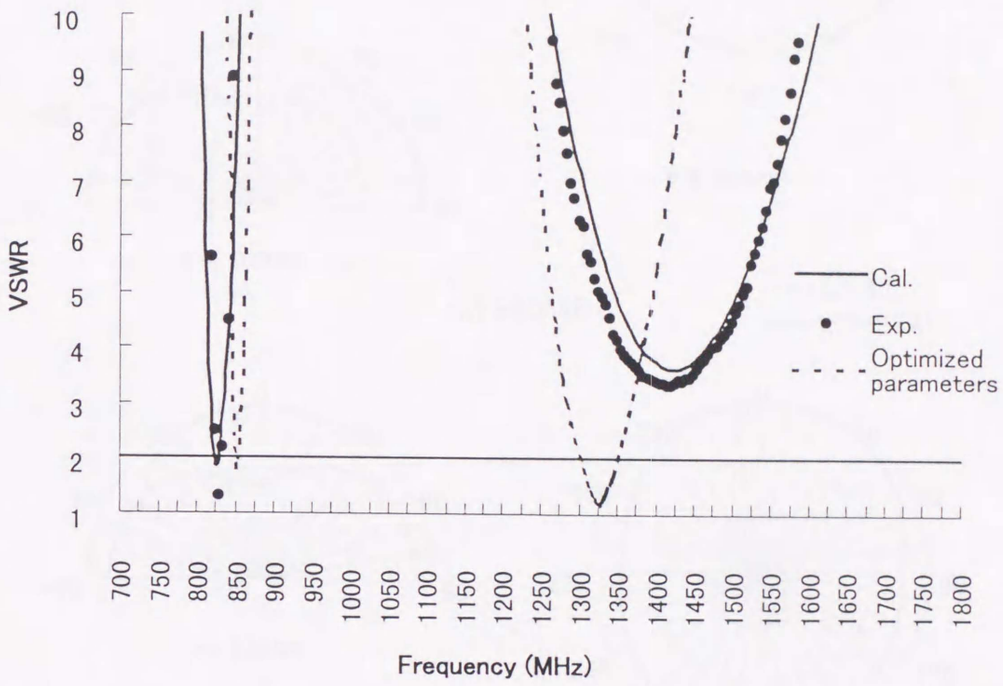

fig. 3.14 VSWR characteristics of antenna c.

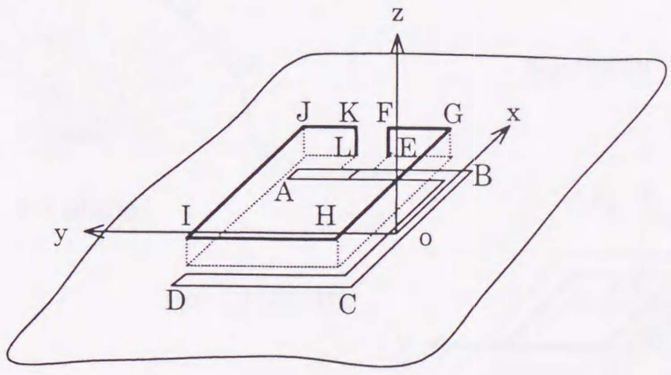

antenna c.

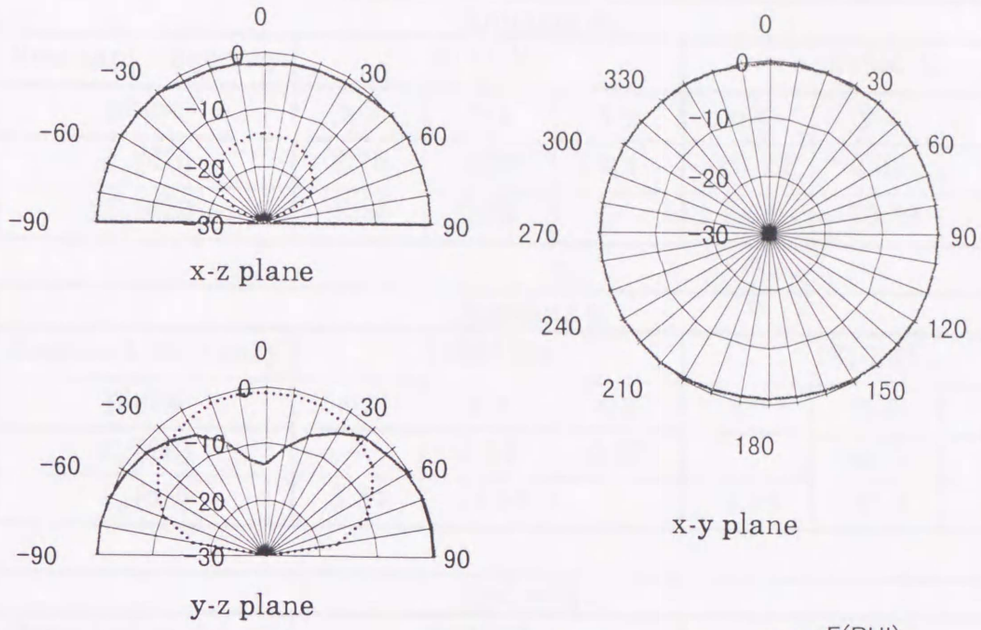

(a) 860MHz

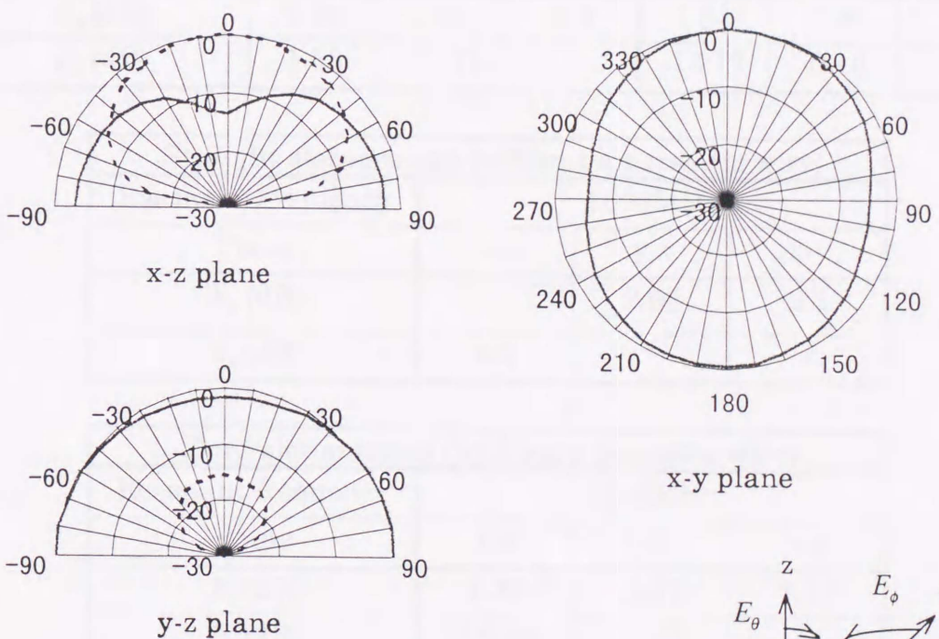

(a) 1310MHz

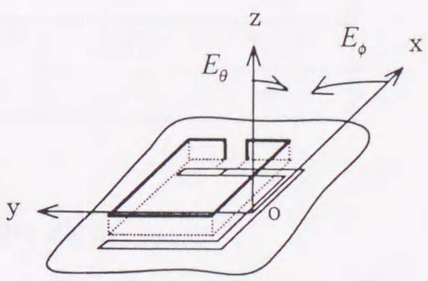

fig. 3.15 Radiation patterns for antenna c.

Antenna a.						
Resonant frequency	914MHz			1615MHz		
plane	x-z	y-z	x-y	x-z	y-z	x-y
E_θ (dB)	2.76	4.36	4.4	-10.79	2.02	2.0
E_ϕ (dB)	-6.25	0.39	-	2.08	-10.79	-

Antenna b.						
Resonant frequency	1490MHz			1810MHz		
plane	x-z	y-z	x-y	x-z	y-z	x-y
E_θ (dB)	-	3.34	0.23	-	4.75	4.75
E_ϕ (dB)	3.34	-23.53	-	-1.54	-31.9	-

Antenna c.						
Resonant frequency	860MHz			1310MHz		
Plane	x-z	y-z	x-y	x-z	y-z	x-y
E_θ (dB)	2.96	3.88	3.9	1.84	-2.92	1.87
E_ϕ (dB)	1.55	-11.11	-	-13.77	-0.16	-

Straight slot antenna (without a parasitic wire)			
Resonant frequency	1600MHz		
Plane	x-z	y-z	x-y
E_θ (dB)	-	2.05	2.1
E_ϕ (dB)	2.1	-	-

Bent slot antenna (without a parasitic wire)			
Resonant frequency	1345MHz		
Plane	x-z	y-z	x-y
E_θ (dB)	1.08	-3.12	1.12
E_ϕ (dB)	-19.19	1.08	-

table 2.1 Antenna gain.

3.4 Conclusions

A dual band antenna is useful to save space for the installation of antenna in a limited area. In this chapter, three types of dual band antenna are proposed as examples to effective utilization of the space. Although proposed antennas can operate at two frequency bands, they have only one feed point in the slot. These antennas have simple shapes and it is made easily in the experiment. First example, an antenna with the combination of a straight slot antenna and a parasitic inverted L wire is introduced to show the reason why these kinds of antennas resonate at two frequency bands. To explain the reason why this antenna has two frequency bands, the electric current distribution on the parasitic wire and the magnetic current distribution in the slot are shown. The electric current on the wire is induced by the coupling and the induced electric current makes the slot resonant at a low frequency band. The magnetic current should distribute in the slot to make the input impedance match the feed line, so the position and shape of the wire are important. Some design procedures of these types of dual frequency antennas with the combination of a slot antenna and a parasitic wire were obtained. They are (1).The length of the parasitic wire should be about a quarter or a half wavelength at a desired lower frequency and the slot antenna should be designed to be about a half wavelength at a higher frequency, respectively. (2). One end or two ends of the parasitic wire must be connected to the conducting plate and they should be located near the feed point on the slot. And a parasitic wire has the optimum height to increase the bandwidth at a lower frequency. The calculated VSWR's of the antenna c agree well with the measured data. We found that the slot radiation was strong at a higher frequency and the radiation from the parasitic wire was dominant at a lower frequency for antenna a. and c.

CHAPTER4
Reduction of coupling between two wire antennas using a slot

4.1 Background

In Chapter 3, an application of enhanced coupling is shown through three kinds of dual frequency antennas with the combination of a slot antenna and a parasitic wire. It is not true that the coupling always produces attractive characteristics, because the coupling disturbs the free space characteristics and makes antenna behavior more complicated. Thus coupling often causes system problems. The reduction of coupling is one of the important techniques and it is often required to avoid degradation of antenna characteristics. An example of the problem occurs in the base station for mobile communication. In the recent growth of radio communications, it is often required to have antennas operating at different frequencies close together because of the space limitations. This condition may make the antenna characteristics degrade. In this case radiated power from an antenna is received by the other antennas around it and makes system degradation problems such as cross-talk. The reduction of the coupling between two wire antennas operating at different frequencies has already been studied with respect to the load impedance of a receiving antenna[36]. Reducing the coupling by adjusting the load on the antenna is generally not practical, because the load impedance is usually fixed at the characteristic impedance of the transmission line connected to the antenna. In this paper, we etched an impedance-loaded slot into the ground plane between the two wire antennas to reduce the coupling between them and show the possibility

of the reduction of the coupling through three examples. Induced magnetic currents on the slot reradiate electromagnetic fields when the slot is illuminated by the incident electromagnetic fields. It is supposed that the reduction of the coupling can be obtained if reradiated fields from the slot can deny the direct fields from the transmitting antenna at the surface of the receiving antenna. Another thought may be possible. We can assume that in this configuration the slot acts as a space band-pass filter around a desired frequency where electromagnetic fields are transmitted under the ground plane through the slot. Thus the received power of the receiving antenna is reduced.

Two types of antenna over an infinite ground plane are considered. One type consists of two monopoles and a slot, and the other consists of two half-loops and a slot. One antenna is transmitting and the other is considered as a loaded receiving antenna or a scatterer. Here the moment method (MM) is used to analyze this problem. From the generalized matrix equations, the port relationships between the two wire antenna inputs and one load port of the slot are derived. Then the coupling coefficient is introduced to evaluate the coupling between the two wire antennas and is expressed by using the port parameters. With these port parameters, the electric current on the wires and the magnetic current on the slot are calculated by inverting a large matrix only once for various loads and a large amount of computation time is saved. The load impedance of the receiving antenna is fixed, and the location, length and load impedance of the slot are chosen appropriately to reduce the coupling coefficient. To resonate the slot (i.e. to increase the power transmitted through the slot), a capacitance is loaded in the center of the slot and the significant reduction of the coupling coefficient is obtained at 1.0GHz.

Then a simple load with two capacitors and an inductor is used to resonate the slot at both frequencies 1.0GHz and 1.5GHz, and the reduction of the coupling coefficients at the two frequencies is obtained. The problem is analyzed with an ideal model that has an infinite ground plane.

In the actual problem, the size of the ground plane is finite and the effect of the edges must be taken into account to calculate the coupling. To include the diffracted fields by the edges of the ground plane, the geometrical theory of diffraction (GTD) is applied to the problem. MM is used for the structures that are relatively small compared with the wavelength and GTD is applied to the problems when the conducting bodies are large in terms of the wavelength. With the hybrid method of MM and GTD it is possible to analyze more complex problems. By applying GTD to the problem, the effect of the ground plane can be included in the calculation of the coupling and the optimum size of the ground plane that is needed to reduce the coupling can be obtained. One of the most important characteristics calculated by GTD is a radiation pattern. A radiation pattern with a finite ground plane is different from the one with an infinite ground plane and radiation characteristics with a finite ground plane are also calculated.

4.2 Formulation[37][38]

The antenna structure on an infinite ground plane is shown in figs.4.1 and 4.2. A slot is placed between two wire antennas #1 and #2, designed to transmit signals at frequencies, f_1 and f_2, respectively. At frequency f_1, antenna #1 and #2 can be considered as a transmitting antenna and a loaded scatterer (a receiving antenna), respectively. Alternatively we consider the case where antenna #2 transmits at f_2 and antenna #1 is a loaded scatterer.

As the boundary conditions shown in Chapter 2, at the operating frequency f_1, it is assumed that electromagnetic fields $\overline{E}_T^{reg1}, \overline{H}_T^{reg1}$ above the ground plane are radiated from transmitting antenna #1. Electromagnetic fields $\overline{E}_R^{reg1}, \overline{H}_R^{reg1}$ are reradiated from the current induced on the receiving antenna #2. $\overline{E}_S^{reg1}, \overline{H}_S^{reg1}$ are the scattered fields by the slot. Under the ground plane, $\overline{E}^{reg2}, \overline{H}^{reg2}$ are the electromagnetic fields passed through the slot. The total electric field $\overline{E}_{Total}^{reg1}$ and magnetic field $\overline{H}_{Total}^{reg1}$ above the ground plane (region 1) are expressed as follows.

$$\overline{E}_{Total}^{reg1} = \overline{E}_T^{reg1} + \overline{E}_R^{reg1} + \overline{E}_S^{reg1} \tag{4.1}$$

$$\overline{H}_{Total}^{reg1} = \overline{H}_T^{reg1} + \overline{H}_R^{reg1} + \overline{H}_S^{reg1} \tag{4.2}$$

By applying the equivalence principle to the slot aperture, region 1 has two wire antennas (monopoles or half-loops) and a magnetic current sheet $\overline{M}$ on the ground plane. Region 2 has a magnetic current sheet $-\overline{M}$ under the ground plane. The same fields as $\overline{E}_{Total}^{reg1}, \overline{H}_{Total}^{reg1}$ can be obtained with the magnetic current $2\overline{M}$ and electric currents $\overline{I}^{\#1}, \overline{I}^{\#2}$ flowing on the wire antennas (dipoles or loops) in free space without the ground plane. The electromagnetic fields in region 2 are the same as the ones with the magnetic current $-2\overline{M}$ in free space. Finally the boundary conditions at the surface of the wire antennas and the slot are expressed with the vector equations as

$$\left\{ -j\omega_1 \left(\overline{A}^{\#1} + \overline{A}^{\#2}\right) + \frac{1}{j\omega_1 \mu_0 \varepsilon_0} \nabla\left(\nabla \cdot \left(\overline{A}^{\#1} + \overline{A}^{\#2}\right)\right) \right.$$

$$\left. -\frac{1}{\varepsilon_0} \nabla \times \overline{F} \right\} \times \overline{n} = -\overline{e}_\varphi V_0 \delta(l) \qquad \text{(transmitting antenna)} \tag{4.3}$$

$$\left\{ -j\omega_1 \left(\overline{A}^{\#1} + \overline{A}^{\#2}\right) + \frac{1}{j\omega_1 \mu_0 \varepsilon_0} \nabla\left(\nabla \cdot \left(\overline{A}^{\#1} + \overline{A}^{\#2}\right)\right) \right.$$

$$-\frac{1}{\varepsilon_0}\nabla\times\bar{F}\Big\}\times\bar{n}=-\bar{e}_\varphi Z_L I_L\delta(l) \quad \text{(receiving antenna)} \tag{4.4}$$

$$\bar{n}\times\left\{\frac{1}{\mu_0}\nabla\times\left(\bar{A}^{\#1}+\bar{A}^{\#2}\right)-2j\left(\omega_1\bar{F}+\frac{j}{\omega_1\mu_0\varepsilon_0}\nabla\left(\nabla\cdot\bar{F}\right)\right)\right\}$$

$$=\bar{e}_\varphi I_0\delta(\rho-\rho_0) \quad \text{(slot)} \tag{4.5}$$

where $\omega_1=2\pi f_1$. $\bar{A}^{\#1}$ and $\bar{A}^{\#2}$ are the magnetic vector potentials due to the electric currents on antenna #1 and #2. $\bar{F}$ is the electric vector potential due to the magnetic current. The vector potentials $\bar{A}^{\#1}, \bar{A}^{\#2}$ and $\bar{F}$ at an observation point $\bar{r}$ can be written as

$$\bar{A}^{\#1}(\bar{r})=\frac{\mu_0}{4\pi}\int_{l^{\#1}}\bar{I}^{\#1}(\bar{r}')\frac{e^{-jk|\bar{r}-\bar{r}'|}}{|\bar{r}-\bar{r}'|}dl' \tag{4.6}$$

$$\bar{A}^{\#2}(\bar{r})=\frac{\mu_0}{4\pi}\int_{l^{\#2}}\bar{I}^{\#2}(\bar{r}')\frac{e^{-jk|\bar{r}-\bar{r}'|}}{|\bar{r}-\bar{r}'|}dl' \tag{4.7}$$

$$\bar{F}(\bar{r})=\frac{\varepsilon_0}{4\pi}\int_{\rho}2\bar{M}(\bar{\rho}')\frac{e^{-jk|\bar{r}-\bar{r}'|}}{|\bar{r}-\bar{r}'|}d\rho' \tag{4.8}.$$

Here the electric currents $\bar{I}^{\#1}(l'), \bar{I}^{\#2}(l')$ and the magnetic current $\bar{M}(\rho')$ are expressed as follows.

$$\bar{I}^{\#1}(l')=\sum_{m=1}^{N_1}I_m^{\#1}\bar{J}_m(l'),\ \bar{I}^{\#2}(l')=\sum_{m=1}^{N_2}I_m^{\#2}\bar{J}_m(l'),\ \bar{M}(\rho')=\sum_{m=1}^{N_3}V_m\bar{M}_m(\rho') \tag{4.9}$$

where $\bar{J}_m(l')$ and $\bar{M}_m(\rho')$ are the mth subsectional expansion functions at the position l' and ρ'. $I_m^{\#1}, I_m^{\#2}$ and V_m are the unknown coefficients. N_1, N_2 and N_3 are the total number of the subsectional expansion functions defined on antennas #1, #2 and the slot, respectively. By using the moment method the boundary conditions (4.3)-(4.5) at each point of the wire antennas and the slot are expressed in the matrix form as

$$\begin{bmatrix} Y_{SS} & C_{SW}^{\#1} & C_{SW}^{\#2} \\ C_{WS}^{\#1} & Z_{WW}^{\#1\#1} & Z_{WW}^{\#1\#2} \\ C_{WS}^{\#2} & Z_{WW}^{\#2\#1} & Z_{WW}^{\#2\#2} \end{bmatrix} \begin{bmatrix} V_S \\ I_W^{\#1} \\ I_W^{\#2} \end{bmatrix} = \begin{bmatrix} I_S \\ V_W^{\#1} \\ V_W^{\#2} \end{bmatrix} \qquad (4.10)$$

where I_S, $V_W^{\#1}$ and $V_W^{\#2}$ are the electric current across the slot and the voltages on antennas #1 and #2. V_S, $I_W^{\#1}$ and $I_W^{\#2}$ are the voltage on the slot and the electric currents on the wire antennas. $C^{\#1}$ and $C^{\#2}$ represent the mutual coupling between the slot and antenna #1 or #2, respectively. Y_{SS}, $Z_{WW}^{\#1\#1}$ and $Z_{WW}^{\#2\#2}$ are the self admittance of the slot and self impedance of antennas #1 and #2. $Z_{WW}^{\#1\#2}$ and $Z_{WW}^{\#2\#1}$ are the mutual impedance between the two wire antennas. Obviously, the element of the matrix $C_{SW}^{\#1}$ equals $-C_{WS}^{\#1}$. Also the relationships $C_{SW}^{\#2} = -C_{WS}^{\#2}$ and $Z_{WW}^{\#1\#2} = -Z_{WW}^{\#2\#1}$ exist.

The load impedance Z_L is connected at $l = 0$ for the receiving antenna #2 and the electric current i_L flows at the port where the load Z_L is connected. Thus the relationship between i_L and the port voltage v_L becomes

$$v_L = -Z_L i_L \qquad (4.11)$$

If the admittance Y_S is loaded on the slot, the relationship between the voltage v_S and the electric current i_S at the load port is

$$i_S = -Y_S v_S \qquad (4.12)$$

where all the voltages and electric currents are expressed in RMS.

By inverting the matrix in (4.10), it can be rewritten as

$$\begin{bmatrix} V_S \\ I_W^{\#1} \\ I_W^{\#2} \end{bmatrix} = \begin{bmatrix} Y_{SS} & C_{SW}^{\#1} & C_{SW}^{\#2} \\ C_{WS}^{\#1} & Z_{WW}^{\#1\#1} & Z_{WW}^{\#1\#2} \\ C_{WS}^{\#2} & Z_{WW}^{\#2\#1} & Z_{WW}^{\#2\#2} \end{bmatrix}^{-1} \begin{bmatrix} I_S \\ V_W^{\#1} \\ V_W^{\#2} \end{bmatrix} = \begin{bmatrix} Z_{SS} & C_{SW}'^{\#1} & C_{SW}'^{\#2} \\ C_{WS}'^{\#1} & Y_{WW}^{\#1\#1} & Y_{WW}^{\#1\#2} \\ C_{WS}'^{\#2} & Y_{WW}^{\#2\#1} & Y_{WW}^{\#2\#2} \end{bmatrix} \begin{bmatrix} I_S \\ V_W^{\#1} \\ V_W^{\#2} \end{bmatrix} \qquad (4.13).$$

In this expression, all the elements of I_S, $V_W^{\#1}$ and $V_W^{\#2}$ are 0 except the two load ports and the feed port. By deleting the inverted matrix elements corresponding to zeros of $[I_s V_W^{\#1} V_W^{\#2}]^T$, the following 3×3 port relationship is

obtained.

$$\begin{bmatrix} v_S \\ i_F \\ i_L \end{bmatrix} = \begin{bmatrix} z_{SS} & c'_{SF} & c'_{SL} \\ c'_{FS} & y_{FF} & y_{FL} \\ c'_{LS} & y_{LF} & y_{LL} \end{bmatrix} \begin{bmatrix} i_S \\ v_F \\ v_L \end{bmatrix} \qquad (4.14)$$

where i_F is the electric current at the feed port. From (4.11), (4.12) and (4.14) the electric current i_L at the load port of the receiving antenna is expressed by using the known feed voltage v_F as

$$i_L = \frac{\left(z_{SS} + \frac{1}{Y_S}\right) y_{LF} - c'_{LS} c'_{SF}}{(1 + y_{LL} Z_L)\left(z_{SS} + \frac{1}{Y_S}\right) - c'_{LS} c'_{SL} Z_L} v_F \qquad (4.15)$$

Then the received power of the receiving antenna becomes

$$P_r = \mathrm{Re}(Z_L)|i_L|^2 \qquad (4.16)$$

The total power P_t transmitted into region 2 through the slot is calculated by integrating a Poynting vector in region 2. Then the coupling coefficient R_{re} is defined as the ratio of the received power P_r to the input power P_{in} and the transmission coefficient T is also defined as the ratio of the transmitted power P_t passing through the slot into region 2 to the input power[36].

$$R_{re} = \frac{P_r}{P_{in}} = \frac{\mathrm{Re}(Z_L)|i_L|^2}{\mathrm{Re}(v_F i_F^*)} \qquad (4.17)$$

$$T = \frac{P_t}{P_{in}} \qquad (4.18)$$

By eliminating v_S and i_L from (4.11), (4.12) and (4.14), the unknowns i_S and v_L are expressed in terms of v_F as

$$\begin{bmatrix} i_S \\ v_L \end{bmatrix} = -\begin{bmatrix} \frac{1}{Y_S} + z_{SS} & c'_{SL} \\ c'_{LS} & \frac{1}{Z_L} + y_{LL} \end{bmatrix}^{-1} \begin{bmatrix} c'_{SF} \\ y_{LS} \end{bmatrix} v_F \qquad (4.19)$$

where i_S and v_L are the non-zero elements of the column matrix on the right hand term in (4.13). Therefore if v_F, Z_L and Y_L are known, the unknown matrix $\left[V_s I_W^{\#1} I_W^{\#2}\right]^T$ can be calculated from (4.13). In this way a large $(N_1+N_2+N_3)\times(N_1+N_2+N_3)$ matrix in (4.13) is inverted only once to calculate the unknown coefficients in (4.9) for various load Z_L and Y_S. This is computationally much more efficient compared with the conventional method which inverts the large matrix for each Z_L and Y_S.

4.3 Antenna structures

Three antenna arrangements are considered. One of them is a combination of two monopole antennas transmitting signals at different frequencies and the others are the combinations of two half-loop antennas which are designed to operate at different frequencies. As shown in fig.4.1, two monopole antennas are separated by a distance $2L$. Antennas #1 and #2 are designed to operate at frequencies 1.5GHz and 1.0GHz, respectively. Two types A and B are considered. The antenna #1 is transmitting at 1.5GHz and the antenna #2 is a loaded scatterer (type A). Simultaneously antenna #2 is transmitting at 1.0GHz and antenna #1 is a loaded scatterer (type B). A slot whose width and length are w and $2l_3$, is made between antennas #1 and #2 as shown in fig.1. α is the angle measured from the x-axis to the slot axis ρ. $2l_3$ is about a half wavelength at 1.5GHz. The load is connected to the center of the slot. After the calculations with an infinite ground plane, types A and B on a finite square ground plane are also analyzed. With the finite

square ground plane, the origin of the coordinate is set on the center of the ground plane and edges are set parallel to the x- or y-axis. Two half-loop antennas #1 and #2 transmits signals at frequencies 1.5GHz and 1.0GHz, respectively. Two types of antenna arrangement are considered as shown in fig.4.2 (a) and fig.4.2 (b). Types of antenna #1 and #2 are shown in table4.1. The centers of the loop are on the x-axis in each antenna arrangement and it is assumed that the distance between two centers is $2L$. Antennas #1 and #2 are set parallel to the slot as shown in fig.4.2 (a) (types C and D). The port1 of antenna #1 and the port2 of antenna #2 are located side by side. In fig.4.2 (b) (types E and F), antenna #1 is parallel and antenna #2 is perpendicular to the y-axis. The port 2 of antenna #2 locates far side from the slot.

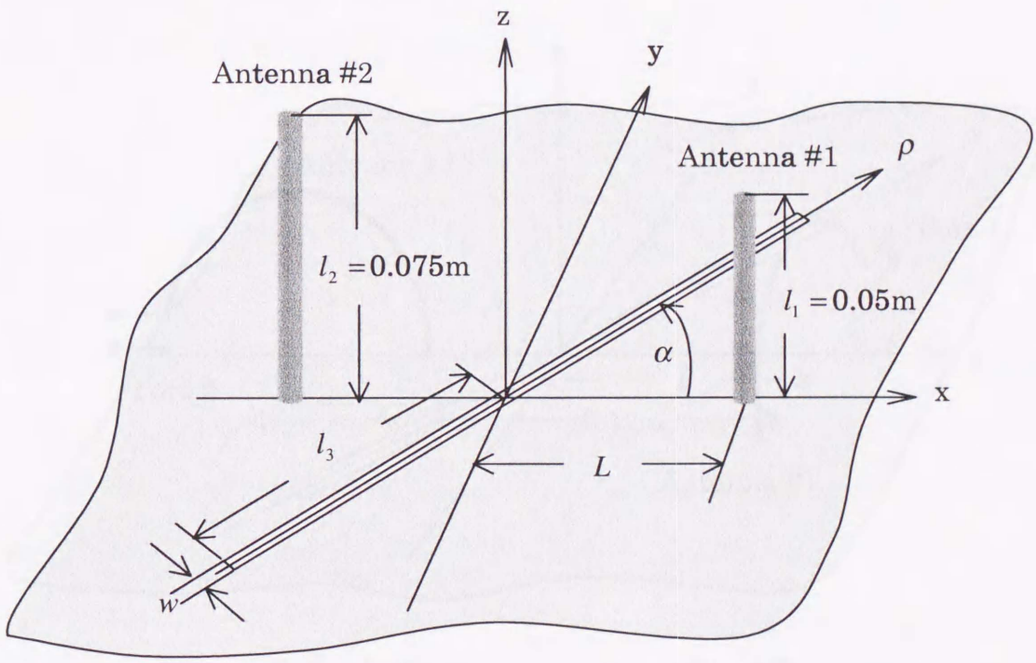

fig. 4.1 Two monopoles and a slot (types A and B).

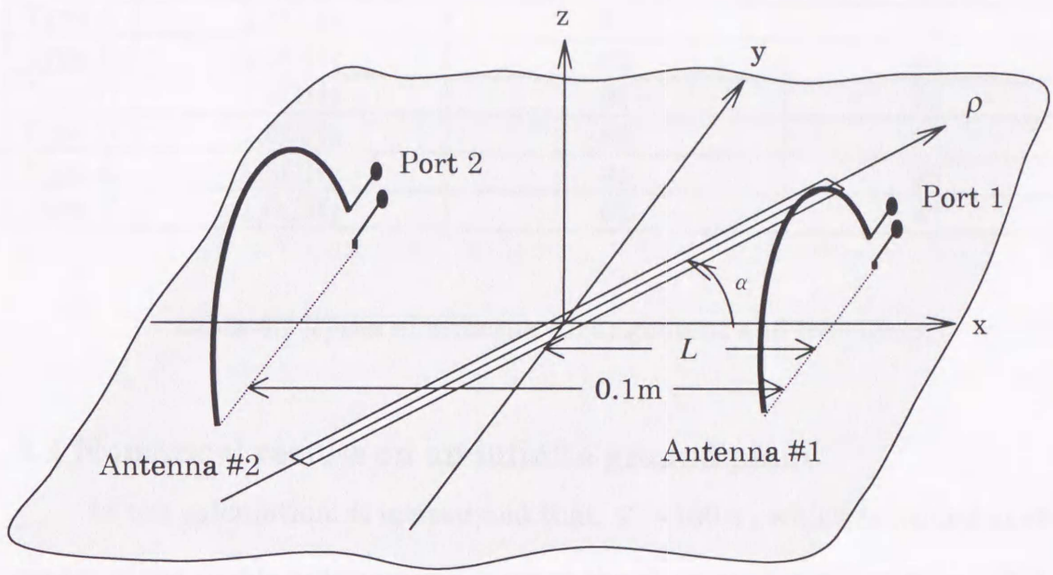

(a) Two half-loop antennas (types C and D).

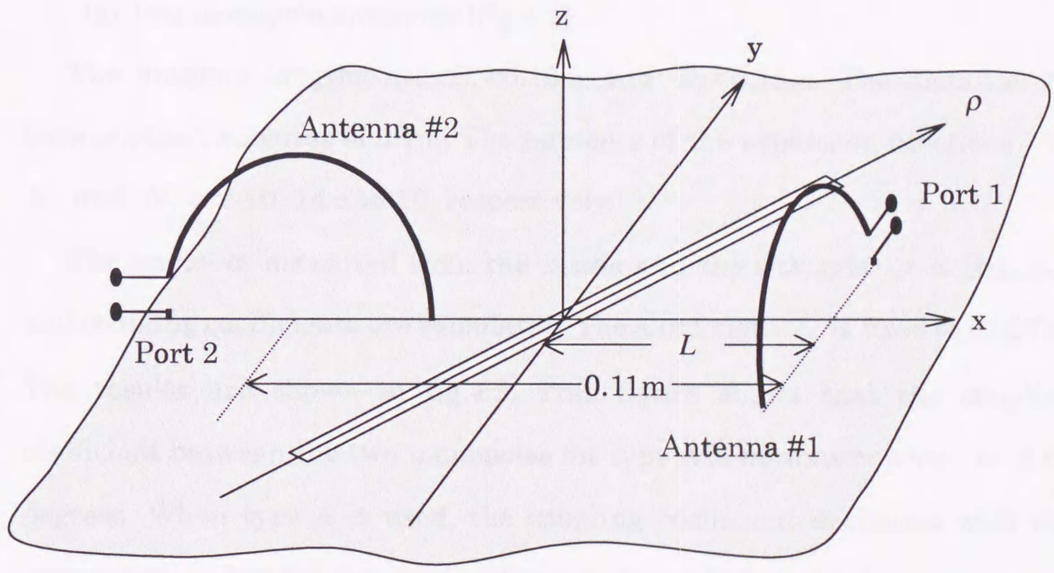

(a) Two half-loop antennas (types E and F).

fig. 4.2 Two half-loop antennas and a slot.

	Operating frequency	Transmitting antenna	Receiving antenna
Type A	1.5GHz	#1	#2
Type B	1.0GHz	#2	#1
Type C	1.5GHz	#1	#2
Type D	1.0GHz	#2	#1
Type E	1.5GHz	#1	#2
Type F	1.0GHz	#2	#1

table 4.1 Types of antenna arrangement and frequency.

4.4 Numerical results on an infinite ground plane

In the calculation, it is assumed that Z_L=100Ω, which is loaded at the center of the dipole antenna and is twice the characteristic impedance of the transmission line connected to the monopole antenna. The slot width is 1mm and the wire radius is 0.9mm.

(a) Two monopole antennas (fig.4.1)

The antenna lengths are $2l_1$=0.10m and $2l_2$=0.15m. The distance $2L$ between the two wires is 0.1m. The numbers of the expansion functions N_1, N_2 and N_3 are 10, 14 and 10, respectively.

The angle α measured from the x-axis and the slot axis ρ is changed and coupling coefficients are calculated. The slot length l_3 is fixed to 0.097m. The results are shown in fig.4.3. This figure shows that the coupling coefficient between the two monopoles for type A is minimum when α is 90 degrees. When type A is used, the coupling coefficient decreases with the increase of α, but the coupling coefficient of type B does not decrease as type A does. This is because the slot is not resonant at 1.0GHz and the electromagnetic fields passing through the slot into region 2 are small. Thus it is necessary to resonate the slot to reduce the coupling between antennas #1 and #2. Frequency characteristics of the transmission coefficients for

various slot lengths are shown in fig.4.4 where antenna #1 is fed and antenna #2 is a loaded scatterer. This figure shows that the transmission coefficient is maximum when the slot length is about a half wavelength of the operating frequency. Thus if the slot length is adjusted to a half wavelength of the operating frequency, the transmission coefficient is increased and the coupling coefficient is reduced. To reduce coupling of types A and B, it is needed that the angle α and the length of the slot $2l_3$ are 90 degrees and about a half wavelength of the operating frequency, respectively.

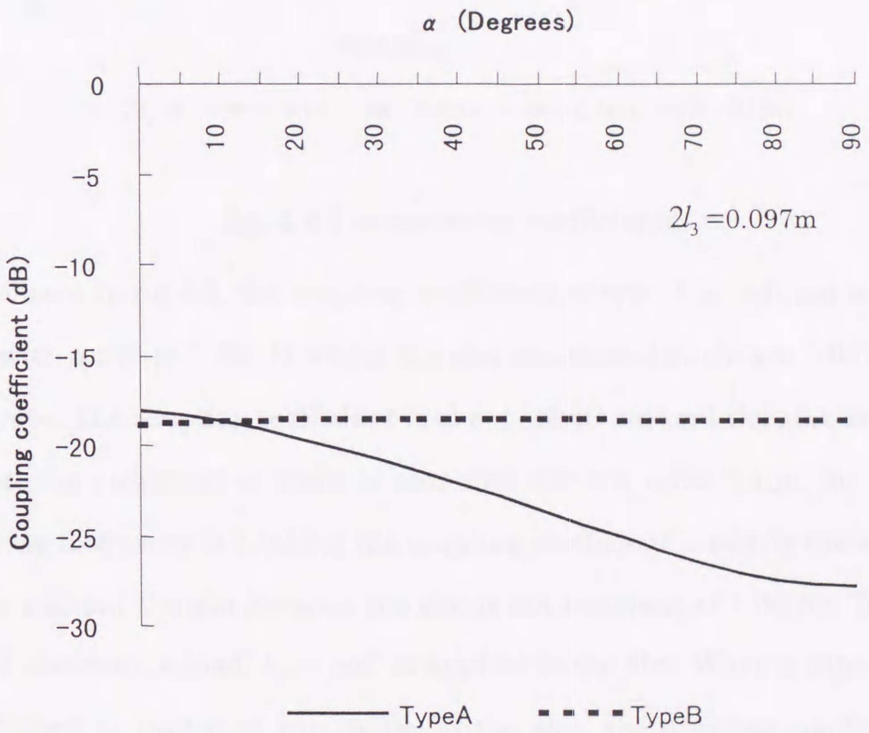

fig. 4.3 Coupling coefficients with respect to slot angles.

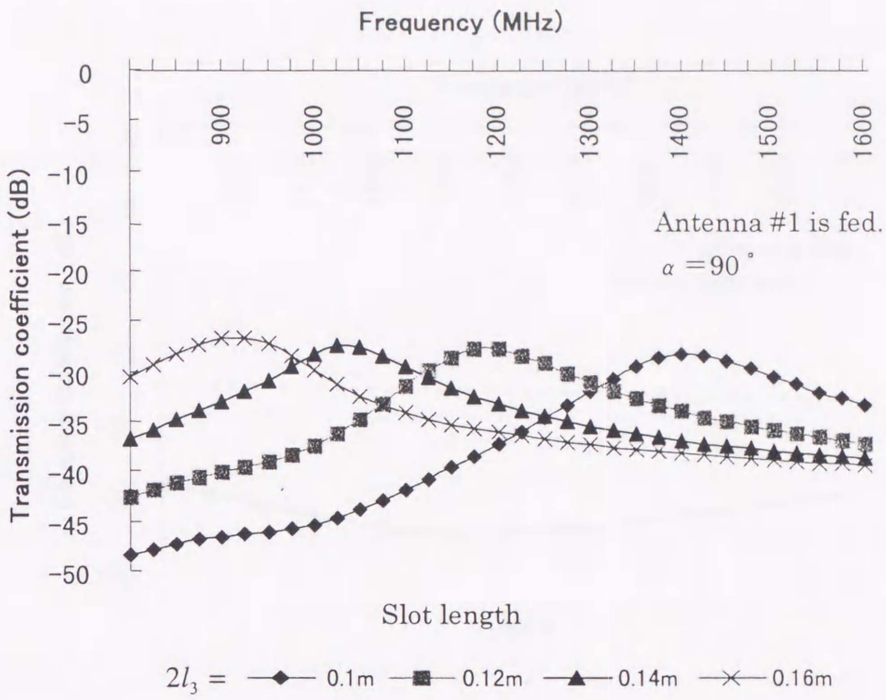

fig. 4.4 Transmission coefficients.

As shown in fig.4.5, the coupling coefficient of type A is reduced to under -28dB with a slot at 1.5GHz where the slot length and angle are 0.097m and 90 degrees. The coupling coefficient is about -18dB without the slot. By using the slot, the reduction of 10dB is obtained. On the other hand, for type B (operating frequency is 1.0GHz) the coupling coefficient is nearly the same as the one without the slot because the slot is not resonant at 1.0GHz. To make the slot resonant, a load $Y_S = j\omega C$ is applied to the slot. When a capacitance C of 0.58pF is loaded at the center of the slot, the coupling coefficient is reduced from -18dB to -28dB at 1.0GHz. Obviously the slot does not resonate at 1.5GHz when the capacitor is loaded at the slot. To resonate the slot at two frequency bands, a load with $Y_S = j\omega C$ and $Y_S = 0$ must be loaded at 1.0GHz and 1.5GHz, respectively. Then a simple circuit that consists of two capacitors and an inductor as shown in fig.4.6 is used and it is assumed that

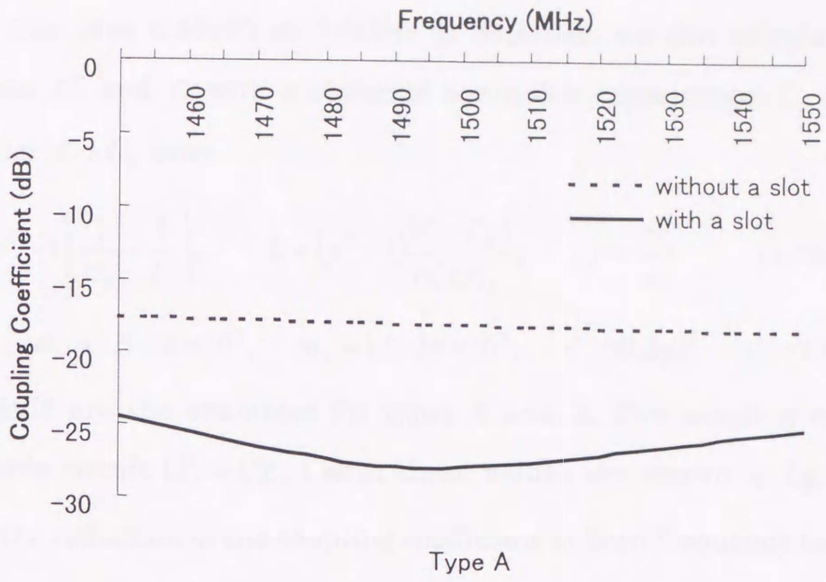

Type A

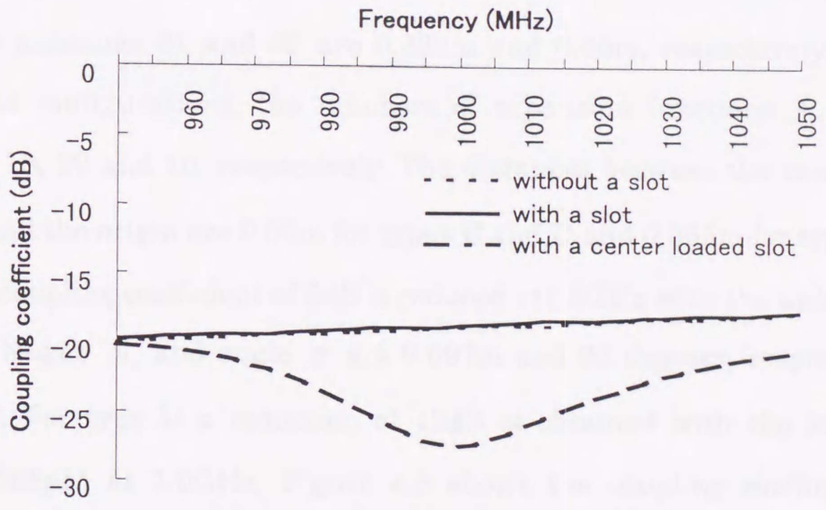

Type B

$\alpha = 90^\circ \quad 2l_3 = 0.097\text{m}$

fig. 4.5 Coupling coefficients for types A and B.

the input impedance of this circuit is Z_C. Once the optimized capacitance C (in this case 0.58pF) at 1.0GHz is obtained, we can calculate all the elements C' and L with a choice of a suitable capacitance C_0 under the condition $C > C_0$ from

$$\frac{1}{C'} = (p^2 - 1)\left(\frac{1}{C_0} - \frac{1}{C}\right), \qquad L = (p^2 - 1)\frac{(C - C_0)}{\omega_1^2 C C_0}, \qquad p = \frac{\omega_1}{\omega_2} \qquad (4.20)$$

where $\omega_1 = 1.5 \cdot 2\pi \times 10^9$, $\omega_2 = 1.0 \cdot 2\pi \times 10^9$. C_0=0.5pF, C'=2.9pF and L=3.88nH are the examples for types A and B. The coupling coefficients using this circuit ($Y_S = 1/Z_C$) with these values are shown in fig.4.7 which shows the reduction of the coupling coefficient at both frequency bands.

(b) Two half-loop antennas (fig.4.2)

Types of antenna #1 and antenna #2 are shown in table4.1 and the radii of loop antennas #1 and #2 are 0.032m and 0.05m, respectively. In these antenna configurations, the numbers of expansion functions N_1, N_2 and N_3 are 18, 20 and 10, respectively. The distances between the center of the loops and the origin are 0.05m for types C and D and 0.055m for types E and F. The coupling coefficient of 5dB is reduced at1.5GHz with the unloaded slot where length $2l_3$ and angle α are 0.097m and 90 degrees, respectively for type C. For type D a reduction of 42dB is obtained with the loaded slot (C = 0.568pF) at 1.0GHz. Figure 4.8 shows the coupling coefficient with respect to the capacitance loaded at the center of the slot. When the capacitance is 0.568pF, the minimum coupling coefficient of -65dB is obtained at 1.0GHz for type D. The coupling coefficients with the circuit in fig.4.6 are shown in fig.4.9 where C_0=0.5pF, C'=3.341pF and L=3.369nH are chosen. Figure 4.10 shows frequency characteristics of the coupling coefficient. For type E the reduction of 35dB is obtained when the unloaded

slot length and angle α are adjusted to 0.102m and 45 degrees, respectively at 1.5GHz. For type F the reduction of 22dB is obtained with the loaded slot (C = 0.50pF) at 1.0GHz. The capacitor is replaced by the same circuit loaded in the two examples shown before where C_0=0.45pF, C'=3.60pF and L=3.127nH are chosen. Then the coupling coefficients are reduced to under -57dB at 1.5GHz and -47dB at 1.0GHz.

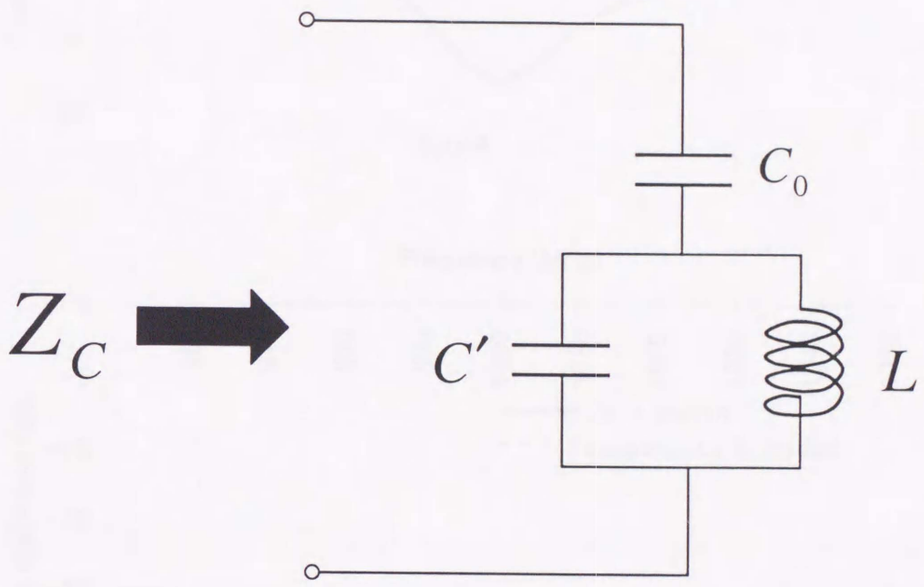

fig. 4.6 A circuit to resonate the slot.

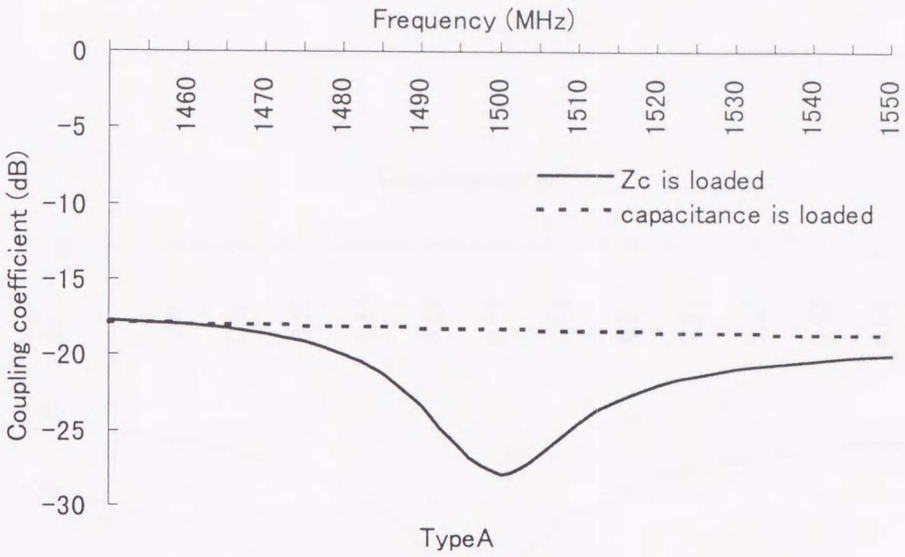

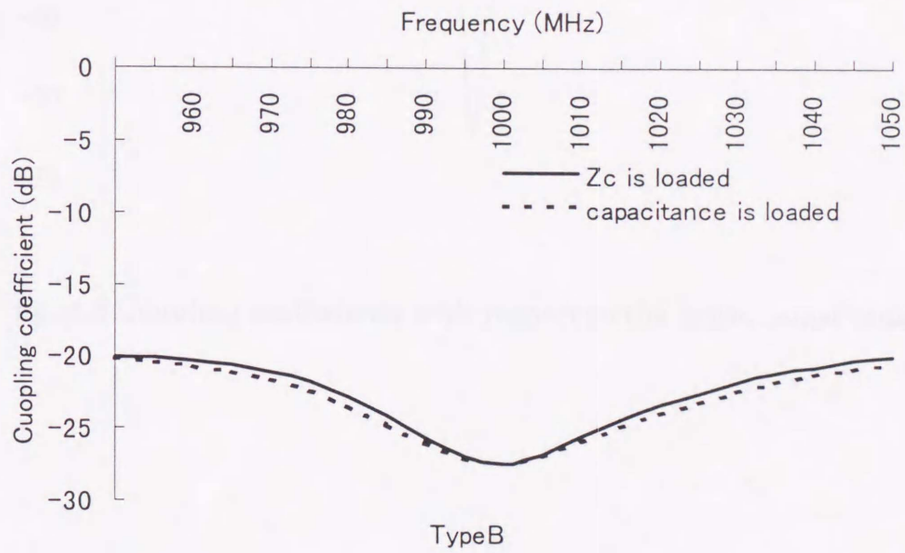

$\alpha = 90^\circ \quad 2l_3 = 0.097\text{m}$

fig. 4.7 Coupling coefficients with the circuit for types A and B.

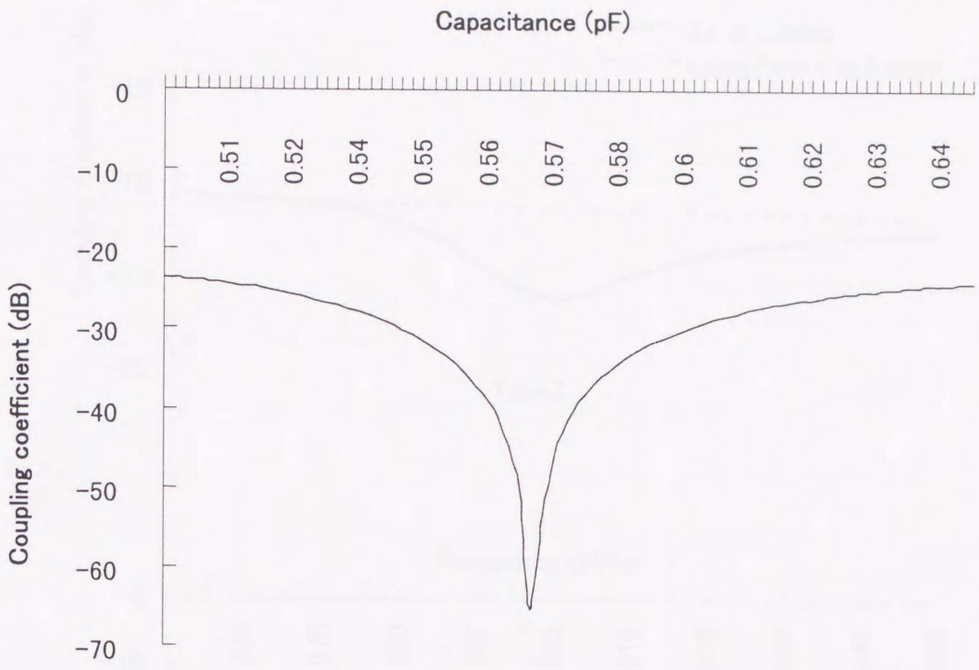

fig. 4.8 Coupling coefficients with respect to the capacitance value.

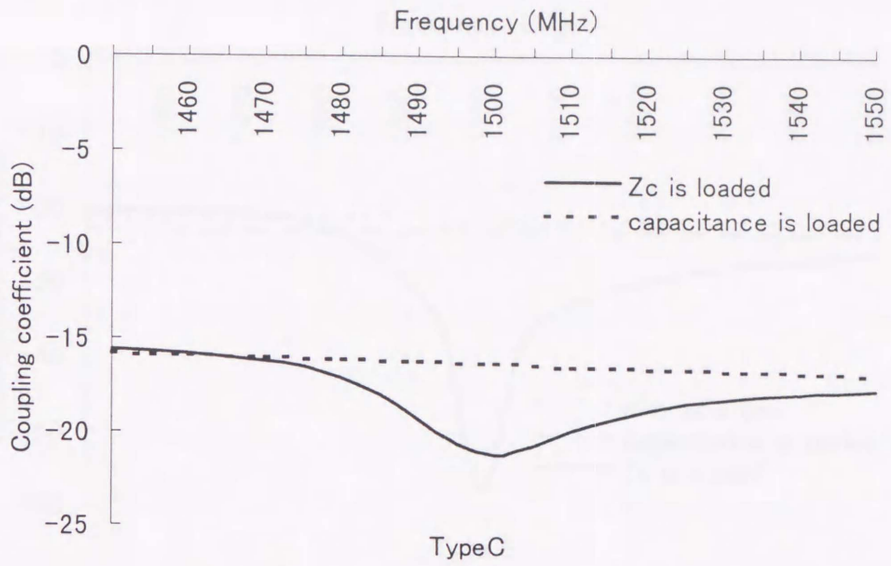

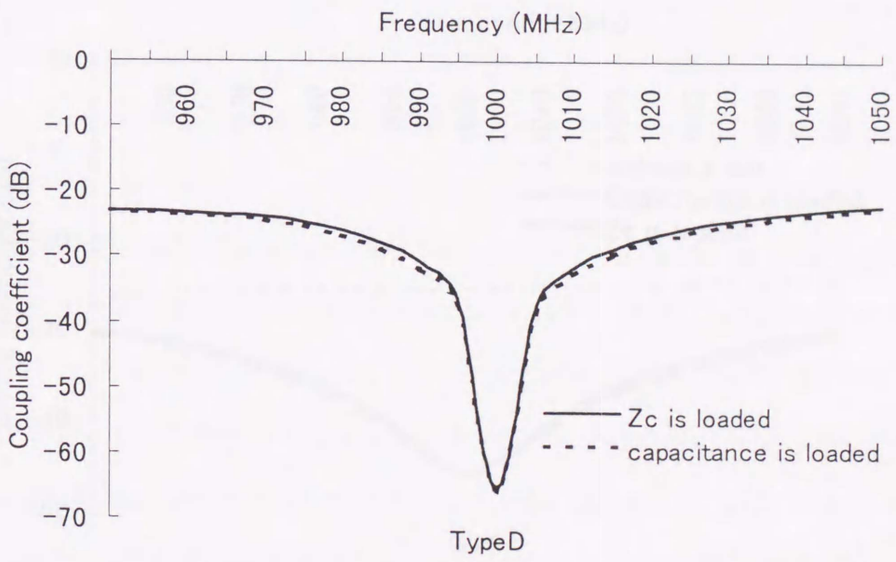

$\alpha = 90^\circ \quad 2l_3 = 0.097\text{m}$

fig. 4.9 Coupling coefficients with the circuit for types C and D.

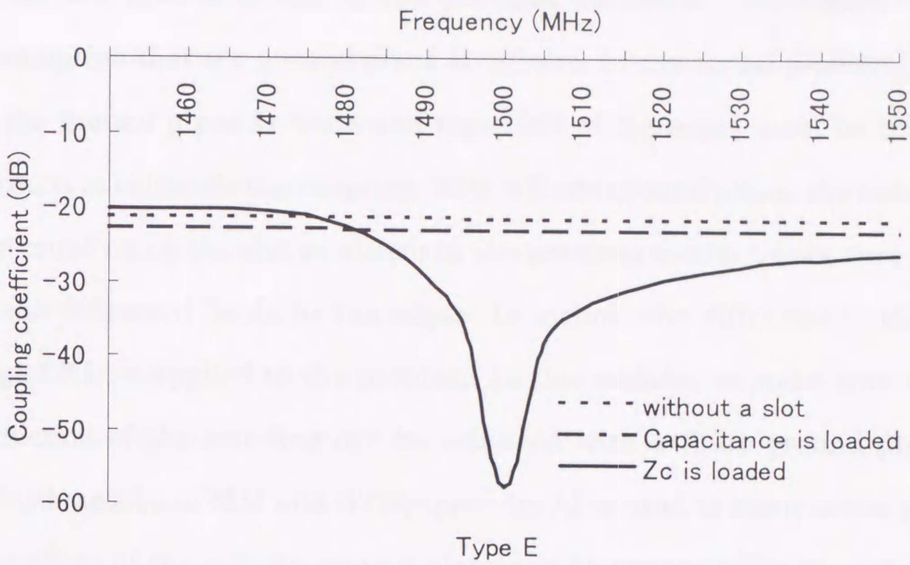

Type E

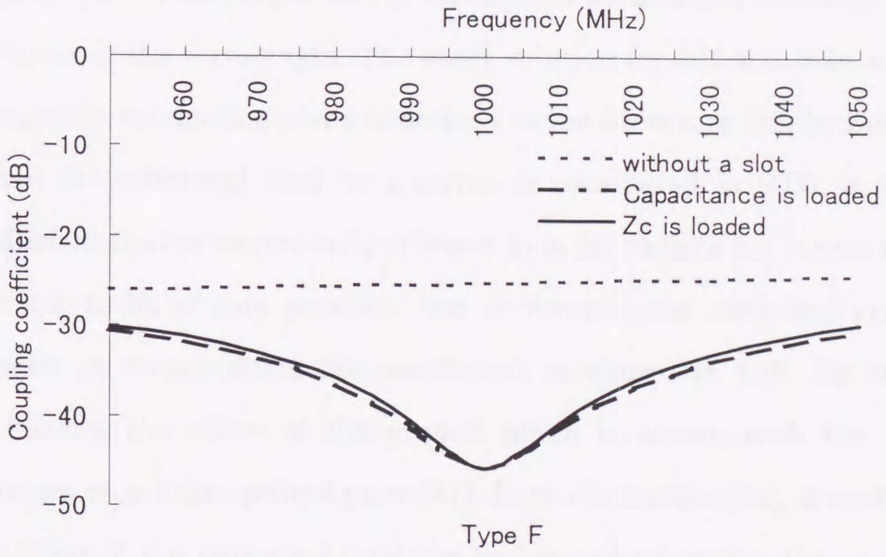

Type F

$\alpha = 45^\circ \quad 2l_3 = 0.102\text{m}$

fig. 4.10 Coupling coefficients for types E and F.

4.5 Numerical results on a finite ground plane

All the results shown in the previous section are calculated with the assumption that the ground plane is infinite. In the actual problem, the size of the ground plane is finite and the effect of the edges must be taken into account to calculate the coupling. With a finite ground plane, the reduction of the coupling by the slot as shown in the previous section is not sure because of the diffracted fields by the edges. To include the diffracted fields by the edge GTD is applied to the problem. In this section, to make sure that the reduction of the coupling can be achieved with a finite ground plane, the hybrid method of MM and GTD[Appendix A] is used to analyze the problem. The effect of the infinite ground plane can be expressed as the interactions between the antenna elements and the edges by using this method. GTD is a high frequency technique and is suitable for an analysis of a large scatterer in terms of the wavelength. The exact solution for diffraction by a corner of the perfect conducting plane is derived in the literature [39] by Satterwhite. When the diffracted field by a corner is considered in GTD, a diffraction coefficient that is numerically efficient in order to take the corner effect into account to be of any practical use in complicated modeling problems is needed. A corner diffraction coefficient is shown in [40]. By using this coefficient, the effect of the ground plane is shown with the monopole antenna on a finite ground plane[41]. In the literature [41], it is shown that the effect of the diffracted field can be ignored when the distance between monopole antenna and a corner is within 0.1 wavelength. Thus diffraction at the four corners of the ground plane can be ignored. To make a discussion simple it can be assumed that diffraction by the edges occurs once and two or more times of diffraction are negligible. The optimum size of the ground

plane is also shown and the measured coupling coefficients of types A and B are shown with calculated data.

As shown in fig.4.11 two monopoles and a slot are made on a finite square ground plane (the same as types A and B). The origin of the coordinate is located at the center of the ground plane and the four edges are parallel to the x- or y-axis. A side length of the square ground plane is assumed as W. Coupling coefficients with respect to the ground plane size are shown in fig.4.12. Coupling coefficients are changing with respect to W. At 1.0GHz the amplitude is within 4dB and when W becomes longer than 0.5m the difference of the coupling between an infinite and a finite ground plane is less than 1dB. Finally, the coupling coefficient with a finite ground plane converges to the one with an infinite ground plane. Although the slot is made on the finite ground plane the effect of the slot does not appear, because the slot is not resonant at 1.0GHz. This is the same as the infinite ground plane case. At 1.5GHz coupling coefficients without a slot are changing around the value with an infinite ground plane and its tendency is nearly the same as the one at 1.0GHz. This figure shows that the optimum size of the ground plane exists that is needed to reduce the coupling. When the size of the ground plane with a slot is about 400mm square, the maximum reduction of a coupling coefficient was obtained and it was about –31dB. When the 400mm square ground plane is used, the reduction of 13dB can be expected. If the size of the ground plane is optimized, more reduction of the coupling coefficient can be obtained compared with the one on an infinite ground plane. Figure 4.13 shows the measured and calculated coupling coefficients on a finite 600mm×600mm ground plane as examples where the effect of the edges is taken into account. Measured and calculated data are in good

agreement. As the slot does not resonate at 1.0GHz, reductions are not obtained with a slot. Because the slot is resonant at 1.5GHz, reductions of 12dB and 11.5dB are obtained by the experiment and calculation, respectively.

The radiation pattern is one of the most important antenna characteristics. Especially this method to reduce the coupling between wire antennas is considered for an application of wireless communication thus the radiation patterns of an antenna that is on a finite ground plane should be investigated for the base station antenna. Usually antennas used for wireless communication have an omnidirectional radiation pattern in the horizontal plane. If a transmitting antenna does not radiate electromagnetic fields in the direction of a receiving antenna to reduce the coupling, it is not good for wireless communication. Figures 4.14 and 4.15 show radiation patterns for type B and A, respectively, with a finite 600mm×600mm ground plane. Measured and calculated data are in good agreement. At 1.0GHz radiation patterns with and without a slot in the x-z plane are quite similar, because the slot does not resonate at that frequency. As the slot is lying along the y-axis, the slot does not affect radiation patterns at both of 1.0GHz and 1.5GHz. In the x-z plane at 1.5GHz, the slot resonates and radiates electromagnetic fields into both sides of the ground plane and the electric field strength under the ground plane (from 90 to 270 degrees) is not reduced under –10dB. The difference of the field strength between the one with and without a slot in the horizontal direction (90 degree and 270 degree) is within 2dB.

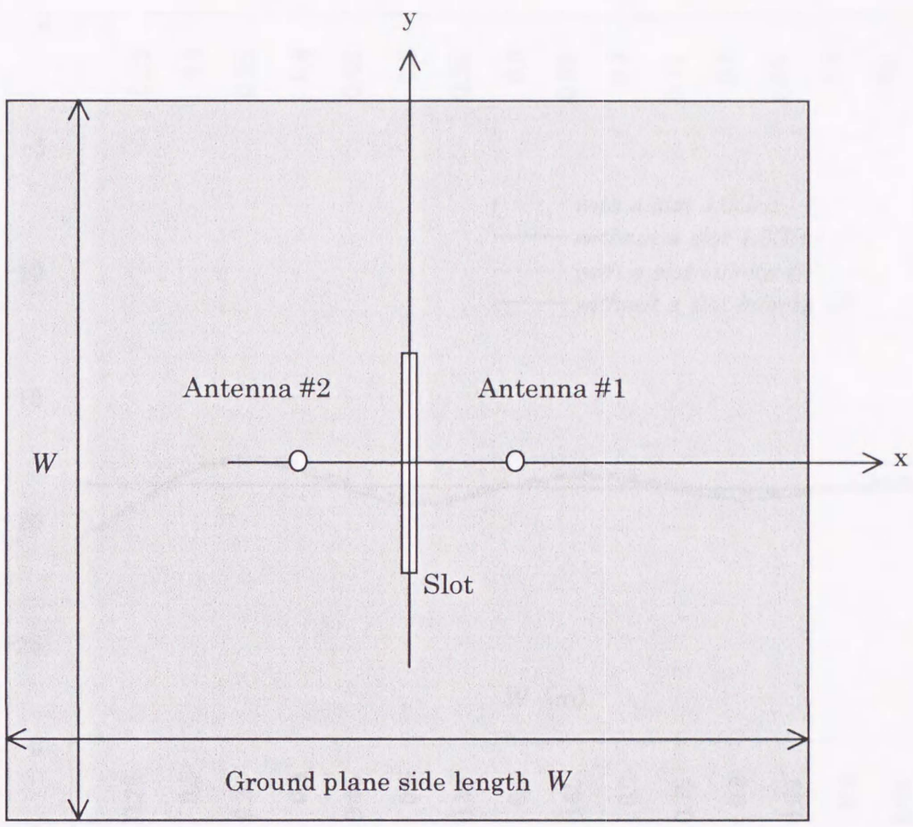

fig.4.11 Two monopoles on a finite square ground plane.

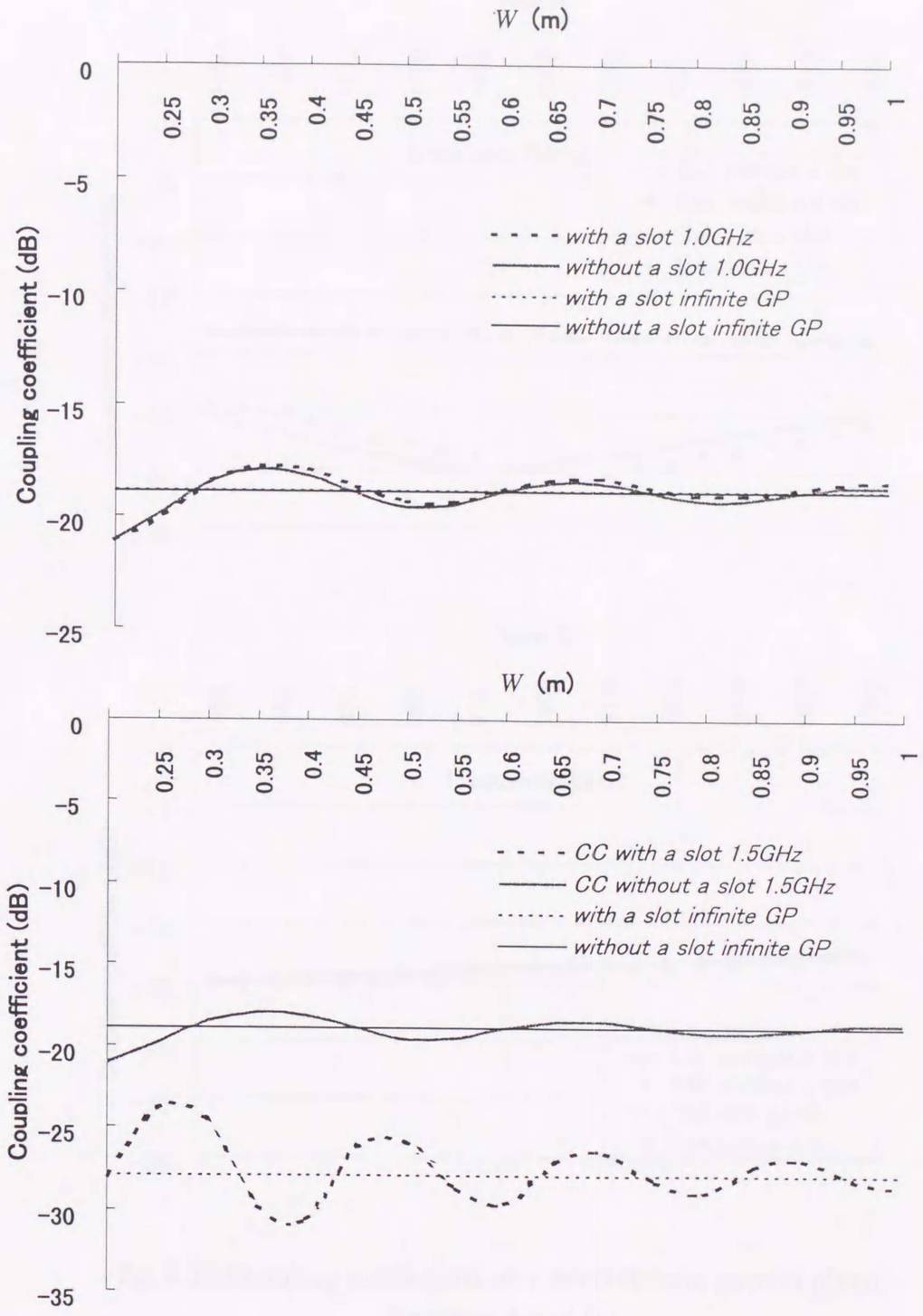

fig. 4.12 Coupling coefficients with respect to the ground plane size.

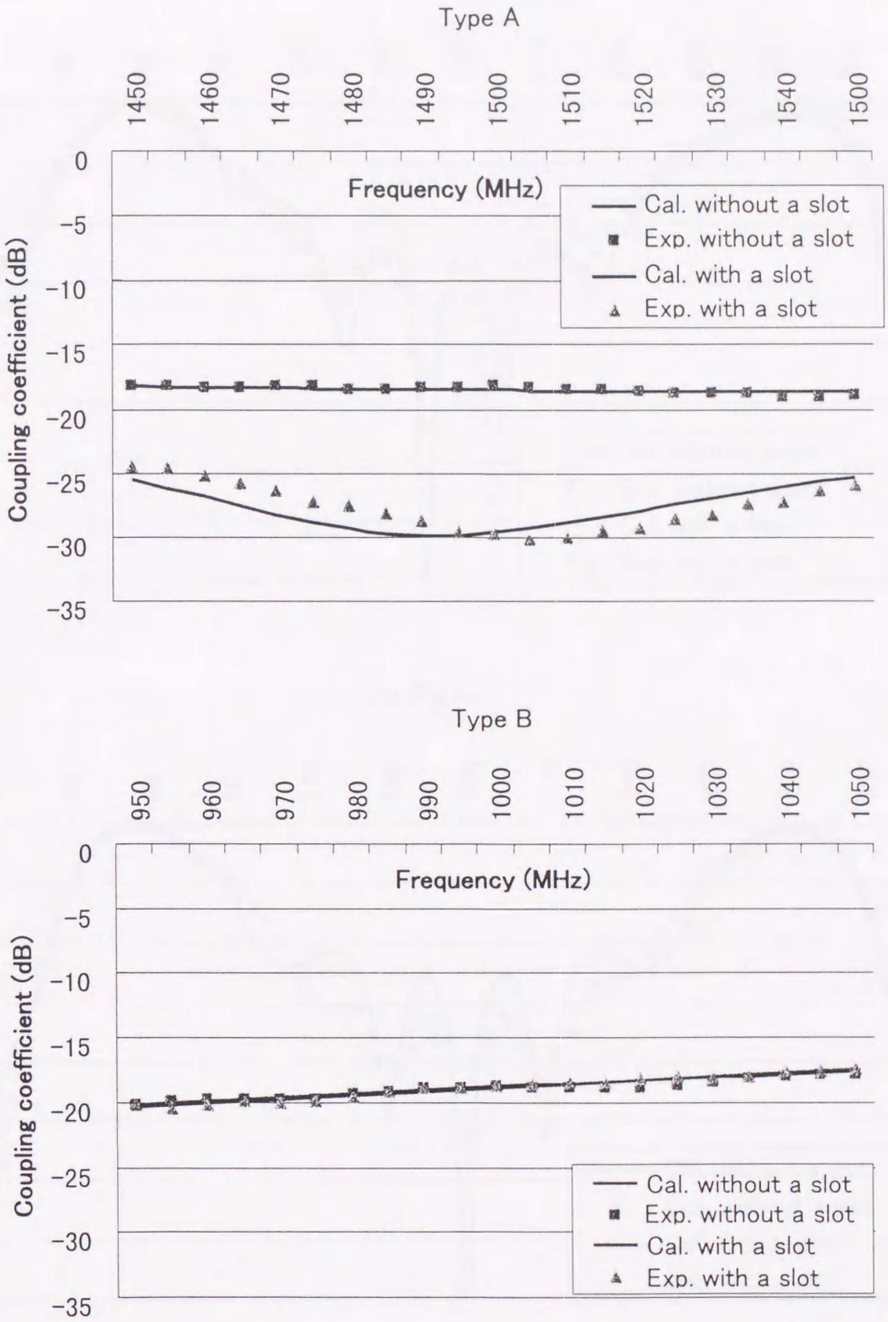

fig. 4.13 Coupling coefficients on a 600X600mm ground plane for types A and B.

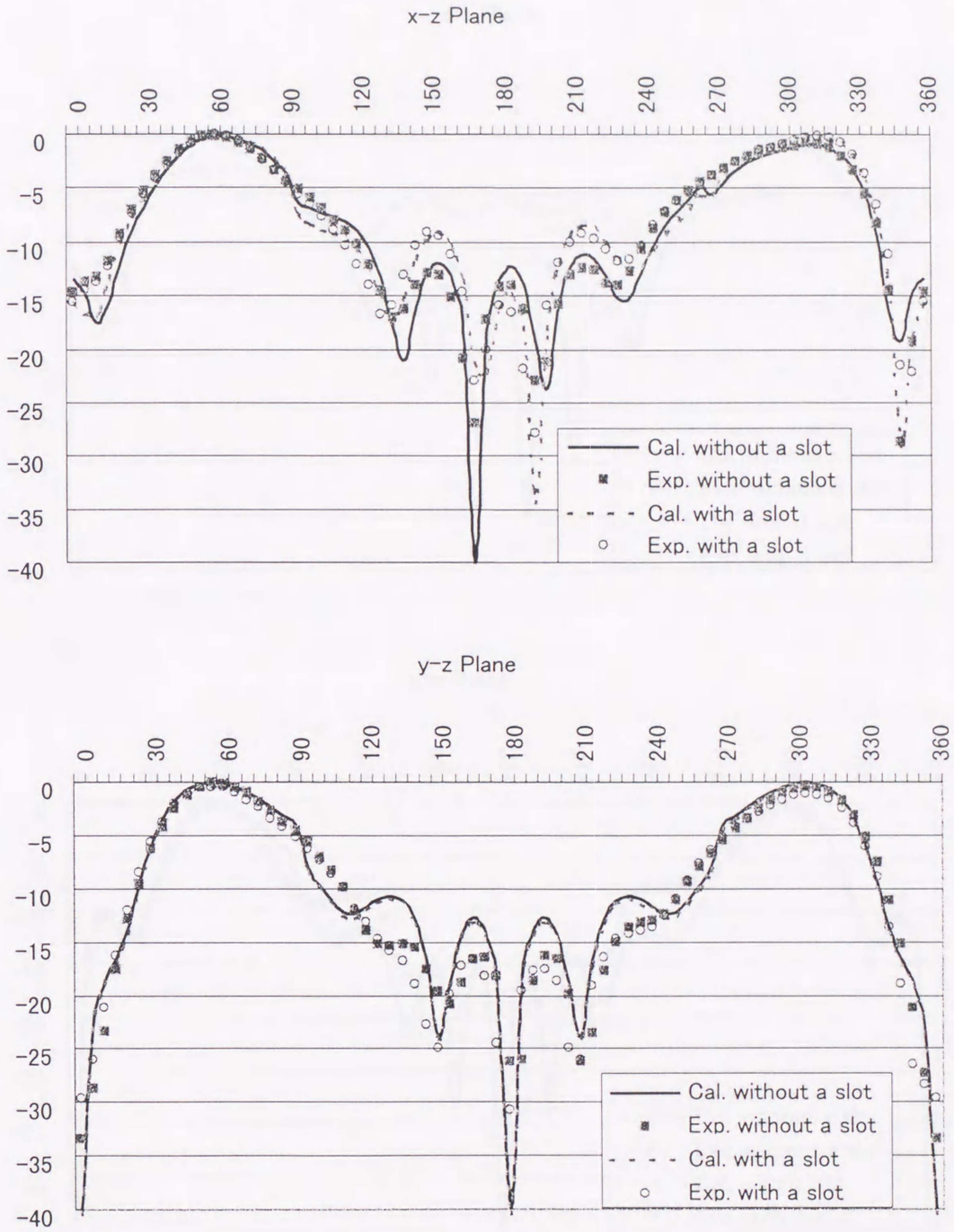

fig. 4.14 Radiation patterns of E (theta) at 1.0GHz.

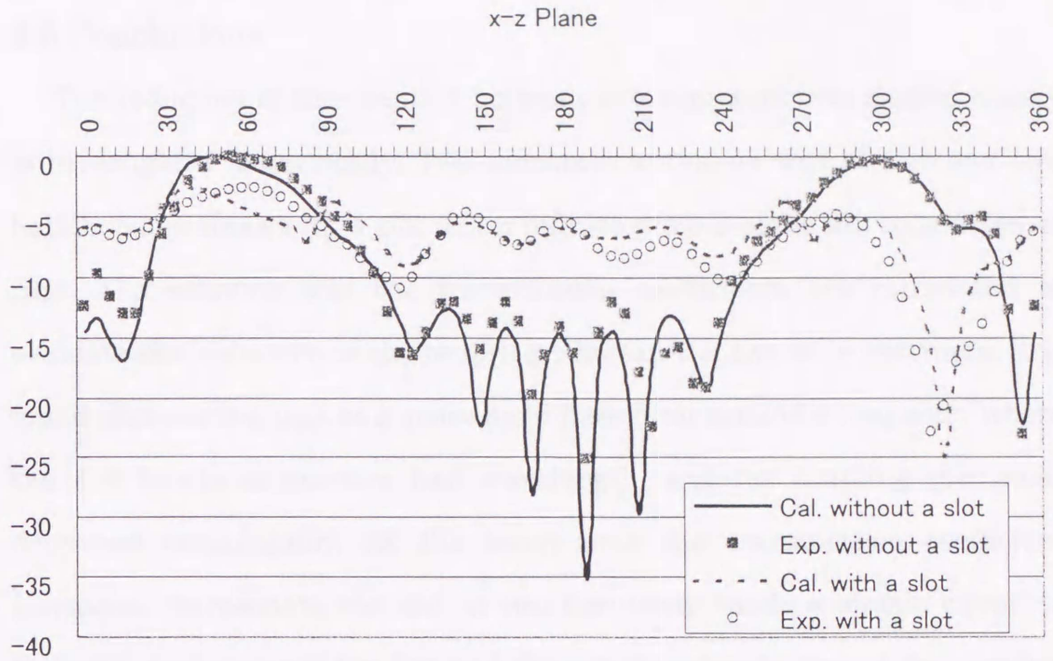

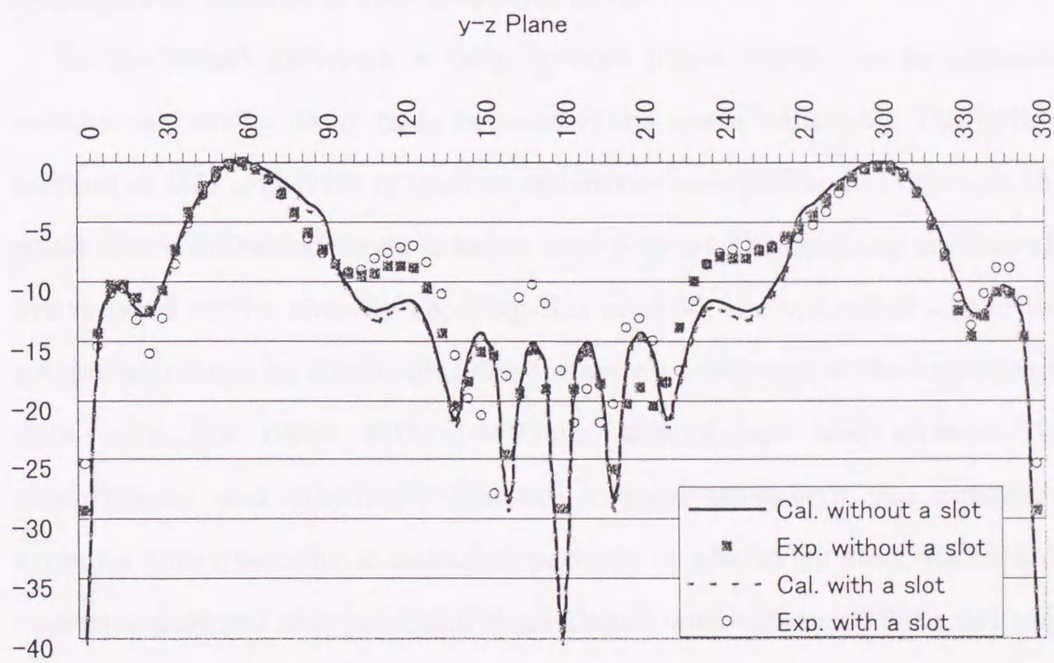

fig. 4.15 Radiation patterns of E (theta) at 1.5GHz.

4.6 Conclusions

The reduction of the coupling between two wire antennas located closely is investigated numerically. Two monopole antennas with a slot and two half-loop antennas with a slot on an infinite ground plane are considered at first. The coupling and the transmission coefficients are introduced to evaluate the reduction of the coupling between the two wire antennas. It is found that the slot acts as a space band-pass filter around a frequency where the slot length is about a half wavelength, and the coupling coefficient decreases considerably. At the same time the transmission coefficient increases. To resonate the slot at two frequency bands a simple circuit is loaded in the center of the slot and the significant reduction of the coupling coefficient is obtained at both frequency bands.

In the actual problems, a large ground plane which can be assumed infinite can not be often made because of the space limitation. The hybrid method of MM and GTD is used to calculate these problems. Although the effect of the diffracted fields is taken into account, the coupling coefficients are reduced with a slot. By applying this method, the optimized size of the ground plane can be obtained and the coupling coefficient of the experiment data with the finite 600mm×600mm ground are also shown. The experimental and calculated data are in good agreement. An important antenna characteristic, a radiation pattern, is also calculated. Calculated radiation patterns of types A and B are shown with measured data and they are in good agreement. At 1.0GHz the slot is not resonant and does not affect radiation patterns. At 1.5GHz the slot radiates electromagnetic fields into both sides of the ground plane and the field strength under the ground plane is nearly uniform.

Chapter 5

Conclusions

In this dissertation, coupling, which is very important to an antenna design was discussed through the two examples. One is the enhancement and the other is the reduction of the coupling between antenna elements. Although the coupling can make antenna characteristics more interesting, it often causes system degradation. Antenna elements are often located close together because of the space limitation. When array antennas are designed, the coupling between elements disturbs free space characteristics of each element, such as radiation patterns and input impedance, and makes array antenna characteristics hard to predict. When antennas are closely located, radiated power from one antenna is received by the other antennas around it and the unwanted received power makes system problems such as cross-talk and interference. In order to improve antenna characteristics and to avoid system problems on the antennas, the coupling between antenna elements should be carefully considered.

In Chapter 2, the equivalence principle was used and an analytical model was divided into two regions. Then image theory was applied to each region and they were changed into two free space analytical models. Then the boundary conditions at the surface of the electric and magnetic currents were considered. Also in the same chapter the moment method (MM) and the geometrical theory of diffraction (GTD) were explained. These techniques and the hybrid method of MM and GTD were applied to electromagnetic scattering problems.

The combination of the wire and the slot were used to consider couplings

between elements. New and better antenna characteristics were supposed to be obtained with the combinations of the wire and the slot, which have complementary characteristics each other. Three types of antenna with the combinations of a slot antenna and a parasitic wire were proposed for the examples of the coupling enhancement. Lately, to deal with the increase of the number of the portable phone, the idea of a dual-mode cellular phone capable of operating in two different cellular systems have been introduced. In this idea two frequency bands are fairly far apart from each other and antennas should operate at both frequency bands. Antennas proposed in Chapter 3 were designed for dual band operation. Although these antennas can operate at two frequency bands, they have only one feed point in the slot. A dual band antenna is also useful to save space for the installation of antenna in a limited area such as potable phones. The simplest combination may consist of a straight narrow slot antenna and a straight parasitic wire, which is set vertically to the ground plane. By using this antenna, the VSWR characteristics with respect to the distance between the center of the slot to the base of the wire were obtained. The bandwidth (VSWR$\leqq$2) could not be obtained with this combination at a low frequency band. Bending the wire element at a point is a technique often used to reduce antenna height. So the wire was bent at a point and the base position was changed. Then two bandwidths were obtained at 920MHz and 1600MHz. These results suggested us that the height and the base position of the parasitic wire are important. The segment parallel to the slot does not have the coupling from the slot. The phase of the induced electric field along the parasitic wire was different at each point along the wire and the electric current was cancelled. Thus the electric current on the straight wire did not flow compared with the

combination of the slot and bend wire. Another combination with a straight slot antenna and a parasitic wire bent at four points were introduced. In this configuration a segment of the wire is located over the slot and this segment has the strong coupling between the slot. When the lengths of the slot and the wire were adjusted to resonate at the same frequency, the segment across the slot disturbs the radiation from the slot. Thus the slot could not resonate at the designed frequency, but it resonated at different frequency bands where the parasitic wire did not resonate. To reduce the antenna size the slot antenna and the parasitic wire were bent at two and six points, respectively. Although the antenna was reduced to smaller size, the dual frequency characteristic remained.

Some design procedures of a dual frequency antenna with the combination of the slot antenna and the parasitic wire were obtained.

1. The length of the parasitic wire should be designed to be about a quarter or one wavelength at a desired lower frequency and the slot length should be designed to be about a half wavelength at a higher frequency.
2. One or two ends of the parasitic wire should be connected to the ground plane and they should be located near the feed point on the slot.
3. To increase the bandwidth at a lower frequency the parasitic wire has the optimum height and it is about 1/30 wavelength at a lower resonant frequency.

As seen on the examples shown in Chapter 3, attractive antenna characteristics such as dual band operation can be added to the antennas by using the coupling effectively.

Although the coupling can make antenna characteristics new and better,

interactions due to the coupling between antenna elements often cause the system degradation problems. Thus the other approach to the coupling between antennas is the reduction of the coupling to avoid problems. When the reduction between antenna elements is needed, usually a conducting plate is inserted between the elements. Ordinary ways to reduce the coupling complicate antenna structures and cause the distortion of radiation patterns. In Chapter 4, a method to reduce the coupling between two wire antennas by using a slot was investigated. Three antenna arrangements were considered. They were a combination of the two monopole antennas and two combinations of two half-loop antennas. Each antenna combination consisted of two wire antennas operating at different frequencies and the antennas were located in the neighborhood within a half wavelength of a higher frequency. To evaluate the reduction of the coupling between two antennas, the coupling coefficient was introduced and it was defined as the ratio of the received power of the receiving antenna to the input power at the feed port of the transmitting antenna. It was found that when the slot was illuminated by the radiated field from the transmitting antenna, the reradiated field from the slot canceled the direct field at the surface of the receiving antenna. Thus it is important to resonate the slot at two frequencies. As the slot was designed to be resonant at 1.5GHz, it did not resonate at 1.0GHz. A center loaded slot was introduced to make the slot resonate at both frequencies. To resonate the slot at 1.0GHz and 1.5GHz a simple circuit consisting of two capacitors and an inductor was loaded at the center of the slot. The relationships between the circuit elements were also shown to determine them. By using the circuit, the coupling coefficients were significantly reduced at both frequencies.

Actual problems are different from these calculation models, because the calculation models have an infinite ground plane. To make the calculation model more practical, the effect of the diffracted field should be taken into account. Thus the hybrid method of MM and GTD was applied to the problems. The optimized size of the ground plane was obtained from the calculated results. Measured coupling coefficients of the combination of the two monopole antennas were shown with the calculated data. Calculated and measured data were in good agreement with each other. It was shown that the reduction of the coupling coefficients with a finite ground plane could be also obtained by the proposed method, which made a slot between two antennas. An important antenna characteristic calculated by GTD is a radiation pattern. Radiation patterns at 1.0GHz and 1.5GHz with and without a slot were also shown with the calculated radiation patterns and they agreed well.

Future study

In every situation, to consider coupling is one of the most important approaches to analyze the antenna problems correctly. Couplings exist between antennas, between space and antennas and between electromagnetic fields and transmission lines.

Enhancement of coupling is an important technique to make antenna characteristics attractive. A lot of new application of the electromagnetic wave will be considered in the future. The different antenna characteristics are required for each application that uses electromagnetic waves. The required antenna characteristics will be obtained with the combination of the electric and the magnetic elements. For example, a feeding method without a contact is an application of the effective utilization of coupling. A contact wear problem can be avoided as the feed point does not have a contact. This method improves the dependability of the feed system.

With the development of the electronic devices, a voltage to drive devices is dropping to a lower voltage. Also the distance between devices becomes smaller as the device size reduces. Thus the devices become susceptible to the electromagnetic interference (EMI). Although electromagnetic compatibility (EMC) becomes an important problem increasingly, EMC problems are less interested in for the study. It is because that the EMC problems occur in many situations and the counterplans must be considered for each problem. These problems can be considered as the coupling between electromagnetic waves in space and the devices in a wide sense. Electromagnetic fields should be measured accurately to take a first step for the EMC problems. To measure the electromagnetic fields accurately, the

measurement system must be considered and modeled correctly in the computer simulation. In experiment, there are many error factors and we must take them away from the measurements. By doing so the measurement system is evaluated accurately. Finally, we can achieve the aim that the data calculated in the computer simulation and the one measured by the experiment are close each other in higher order.

References

[1] S. A. Long, "A combination of linear and slot antennas for quasi-isotropic coverage," IEEE Trans. Antennas and Propagat., AP-23, pp. 572-576, July 1975.

[2] A. B. Papierz, S. M. Sanzgiri, and S. R. Laxpati, "Analysis of antenna structure with equal E- and H- patterns," Proc. Inst. Elec. Eng., 124, pp. 25-30, Jan. 1977.

[3] A. Clavin, D. A. Huebner and F. J. Kilburg, "An improved element for use in array antennas," IEEE Trans. Antennas and Propagat., AP-22, pp. 521-526, July 1974.

[4] M. Kominami, and K. Rokushima, "Analysis of an Antenna composed of arbitrarily located slots and wires," IEEE Trans. Antennas and Propagat., AP-32, pp. 154-158, Feb. 1984.

[5] K. Itoh and T. Matsumoto, "Theoretical analysis of mutual coupling between slot and unipole antennas," Trans. IEICE Japan, 61-B, pp. 391-397, May 1978.

[6] E. Hallen, "Theoretical investigation into the transmitting and receiving qualities of antennae," Nova Acta Soc. Sci. Upsal., pp. 1-4, 1938.

[7] K. K. Mei, "On the integral equations of thin wire antennas," IEEE Trans. Antennas and Propagat., AP-13, pp. 374-378, May 1965.

[8] R. F. Harrington, "Matrix methods for field problems," Proc. IEEE, 55, 2, pp. 136-149, Feb. 1967.

[9] R. F. Harrington, "Field Computation by Moment Methods," IEEE, New York, 1993.

[10] J. B. Keller, "One hundred years of diffraction theory," IEEE Trans. Antennas and Propagat., AP-33, pp. 123-126, Feb. 1985.

[11] J. B. Keller, "Geometrical theory of diffraction," J. Opt. Soc. Am., vol. 52,

pp. 116- 130, 1962.

[12] G. L. James, "Geometrical theory of diffraction for electromagnetic waves," Peter Peregrinus Ltd., England, 1986.

[13] V. A. Borovikov and B. Y. Kinber, "Geometrical theory of diffraction," IEE, England, 1994.

[14] G. A. Thiele and T. H. Newhouse, "A hybrid technique for combining moment methods with the geometrical theory of diffraction," IEEE Trans. Antennas and Propagat., AP-23, pp. 62-69, 1975.

[15] R. F. Harrington, "Time-harmonic electromagnetic fields," McGraw-Hill, New York, pp. 106-110, 1961.

[16] R. W. P. King and C. W. Harrison, Jr., "Antennas and Waves," MIT Press, Cambridge, Massachusetts, 1969.

[17] K. Fujimoto, A. Henderson, K. Hirasawa and J. R. James, "Small antennas," Research Studies Press Ltd., England, 1987.

[18] H. Morishita, K. Hirasawa, and K. Fujimoto, "Analysis of a cavity-backed annular slot antenna with one point shorted," IEEE Trans. Antennas and Propagat., AP-39, pp. 1472-1477, Oct. 1991.

[19] H. Morishita, K. Fujimoto and K. Hirasawa, "Analysis of Rectangular Microstrip antenna having the same width as the ground plane," IEICE Trans. Japan, vol. J71-B, pp. 1274-1280, Nov. 1988.

[20] W. L. Stutzman and G. A. Thiele, "Antenna theory and design," John Wiley and Sons., pp. 306-347, 1976.

[21] Y. T. Lin and J. H. Richmond, "EM modeling of aircraft at low frequencies," IEEE Trans. Antennas and Propagat., AP-23, pp. 53-56, Jan. 1975.

[22] E. H. Newman, "Electromagnetic modeling of composite wire and surface geometries," IEEE Trans. Antennas and Propagat., AP-29, pp. 488-495,

May 1981.

[23] W. L. Stutzman and G. A. Thiele, "Antenna theory and design," John Wiley and Sons., pp. 447-454, 1976.

[24] R. F. Harrington, "Time-harmonic electromagnetic fields," McGraw-Hill, New York, pp. 127-128, 1961.

[25] W. L. Stutzman and G. A. Thiele, "Antenna theory and design," John Wiley and Sons., pp. 473-477, 1976.

[26] G. L. James, "Geometrical theory of diffraction for electromagnetic waves," Peter Peregrinus Ltd., England, pp. 19-22, 1986.

[27] H. E. King and J. L. Wong, "An experimental study of a bulan-fed open sleeve dipole in front of a metallic reflector," IEEE Trans. Antennas and Propagat., AP-20, pp. 201-204, Mar. 1972.

[28] Y. Ebine and K.Kagoshima, "Multi-frequency dipole antenna with closed-spaced parasitic elements," Trans. IEICE Japan, J-71-B, pp. 1252-1258, Nov. 1988.

[29] T. Maruyama and K. Kagoshima, "Dual-frequency corner-reflector antennas fed by elements connected to parallel feed lines," Trans. IEICE Japan, J77-B-II, pp. 459-466, Sept. 1994.

[30] K. Hirasawa and K. Fujimoto, "On wire-grid method for analysis of wire antennas near/on a rectangular conducting body," Trans. IEICE Japan, J65-B, pp. 382-389, Apr. 1982.

[31] K. Ogawa and T. Uwano, "A diversity antenna for very small 800-MHz band portable telephones," IEEE Trans. Antennas and Propagat., AP-42, pp. 1342-1345, Sept. 1994.

[32] K. Ito, and Y. Okano, "Preliminary study on two-point-feed dual-frequency antenna for portable phone systems," 1992 Spring National Convention Rec. of IEICE, B-102, p2-102, March 1992.

[33] P. Erätuuli, P. Haapala and P. Vainikainen, "Dual frequency wire antennas," Electron. Lett, 32, 12, pp. 1051-1052, June 1996.

[34] T. Morioka, K. Hirasawa and S. Shibasaki, "Analysis of a bent slot antenna with a parasitic element for dual band operation," Int. Symp. on Antennas and Propagat., Japan, pp.497-500, Sep. 1996.

[35] T. Morioka, S. Araki and K. Hirasawa, "Slot antenna with parasitic element for dual band operation," Electron. Lett., 33, 25, pp. 2093-2094, Dec. 1997.

[36] K. Hirasawa, "Bounds of uncertain interference between closely located antennas," IEEE Trans. Electromagn. Compat., EMC-26, pp. 129-133, Aug. 1984.

[37] T. Morioka and K. Hirasawa, "Reduction of coupling between two wire antennas using a slot," IEICE Trans. on Commun., E80-B, pp.699-705, May 1997.

[38] T. Morioka, K. Hirasawa and A. Henderson, "Reduction of coupling between two wire antennas using a slot," Int. Wireless and Telecommun. Symp., Malaysia, pp.46-51, May 1997.

[39] R. Satterwhite, "Diffraction by a quarter plane, the exact solution, and some numerical results," IEEE Trans. Antennas and Propagat., AP-22, pp. 500-502, May 1974.

[40] W. D. Burnside, N. Wang and E. L. Pelton, "Near-field pattern analysis of airborn antennas," IEEE Trans. Antennas and Propagat., AP-28, pp. 318-327, May 1980.

[41] D. A. Pozer and E. H. Newman, " Analysis of a monopole mounted near an edge or a vertex," IEEE Trans. Antennas and Propagat., AP-30, pp. 401-408, May 1982.

Appendix A

Hybrid method of moment method and geometrical theory of diffraction

The hybrid method of MM and GTD is a method for solving electromagnetic problems in which antennas are located on or near a conducting body, such as antennas on ships or airplane, or wire and slot antennas on a finite ground plane. This method can solve these kinds of problems by properly analyzing the interaction between the antenna and the conducting body or between antenna and a discontinuity in the conducting body[1]-[5].

To simplify the discussion, consider two half-wave dipoles oriented near a conducting half-plane as shown in fig. A1. The direct electric field radiated from dipole #1 illuminates antenna #2. The diffracted field by the edge and the reflected field reach to antenna #2. Thus the total electric field at a point of the dipole #2 can be written as

$$\overline{E}_2 = \overline{E}_{12} + \overline{E}_{12}^R + \overline{E}_{12}^d \qquad \text{(A.1)}$$

where $\overline{E}_{12}$, $\overline{E}_{12}^R$ and $\overline{E}_{12}^d$ are the direct, reflected and the diffracted electric fields, respectively. The diffracted field is shown in equation (2.69) and the reflected field can be treated as the field due to the image of antenna #1. Then $\overline{E}_2$ satisfies the boundary condition on the surface of antenna #2 shown in (2.51).

$$\overline{E}_2 \times \overline{e}_n = \left(\overline{E}_{12} + \overline{E}_{12}^R + \overline{E}_{12}^d\right) \times \overline{e}_n = -\overline{e}_\varphi \delta(l_0) \qquad \text{(A.2)}$$

The moment method is applied same as Section 2.3, the boundary condition (A.2) can be expressed as follows.

$$Z'_{mn} I_n = [Z_{mn} + \Delta Z_{mn}] I_n = V_m \qquad \text{(A.3)}$$

Finally the matrix equation (2.59), where both the electric and the magnetic currents exist is rewritten as

$$\left[\begin{bmatrix} Y_S & C_{SW} \\ C_{WS} & Z_{WW} \end{bmatrix}+\begin{bmatrix} \Delta Y_S & \Delta C_{SW} \\ \Delta C_{WS} & \Delta Z_{WW} \end{bmatrix}\right]\begin{bmatrix} V_S \\ I_W \end{bmatrix}=\begin{bmatrix} I_S \\ V_W \end{bmatrix} \qquad \text{(A.4)}$$

where all the elements of the delta matrix can be obtained in the same forms where the electromagnetic fields in equations (2.60)-(2.63) are replaced by the diffracted electromagnetic fields calculated by GTD.

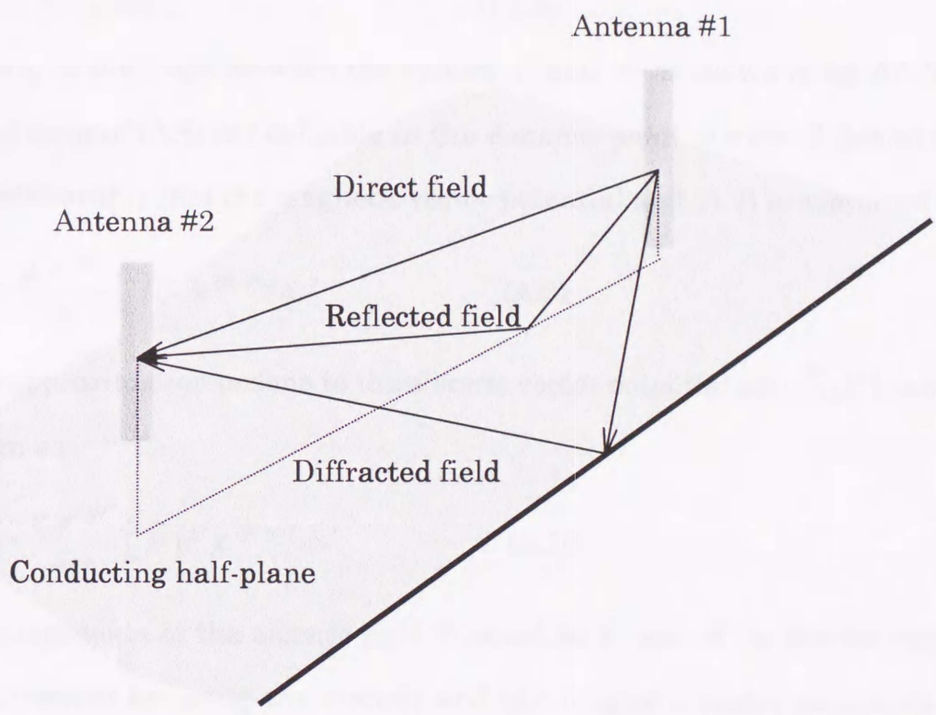

fig. A1 Radiated field paths to antenna #2.

Far field calculation

Electromagnetic fields $\overline{E}$ and $\overline{H}$ due to the electric current in free space are expressed with the magnetic vector potential $\overline{A}(\overline{r})$ as

$$\overline{H} = \frac{1}{\mu_0} \nabla \times \overline{A} \qquad \text{(A.5)}$$

$$\overline{E} = -j\omega\overline{A} + \frac{\nabla(\nabla \cdot \overline{A})}{j\omega\varepsilon_0\mu_0} \qquad \text{(A.6)}$$

$$\overline{A}(\overline{r}) = \frac{\mu_0}{4\pi} \int_V \frac{\overline{J}(\overline{r}')e^{-j\beta|\overline{r}-\overline{r}'|}}{|\overline{r}-\overline{r}'|} dv' \qquad \text{(A.7)}$$

In the far region, the distance between the source point and the observation point $|\overline{r}-\overline{r}'|$ is nearly equals $r - r'\cos\xi$ as

$$|\overline{r}-\overline{r}'| \approx r - r'\cos\xi \qquad \text{(A.8)}$$

where ξ is the angle between the vectors $\overline{r}$ and $\overline{r}'$ as shown in fig. A2. The second term of (A.8) is negligible in the distance point of view. Substituting this relationship into the magnetic vector potential and (A.7) is expressed as.

$$\overline{A}(\overline{r}) = \frac{\mu_0 e^{-j\beta r}}{4\pi r} \int_V \overline{J}(\overline{r}')e^{j\beta r'\cos\xi} dv' \qquad \text{(A.9)}$$

Same approximation is done to the electric vector potential and $\overline{A}_m(\overline{r})$ can be written as

$$\overline{A}_m(\overline{r}) = \frac{\varepsilon_0 e^{-j\beta r}}{4\pi r} \int_V \overline{M}(\overline{r}')e^{j\beta r'\cos\xi} dv' \qquad \text{(A.10).}$$

The components of the electric field directed to $\overline{\theta}$ and $\overline{\phi}$ in the far region are expressed by using the electric and the magnetic vector potentials as follows.

$$E_\theta = -j\omega A_\theta - \frac{j\beta A_{m\phi}}{\varepsilon_0} \qquad \text{(A.11)}$$

$$E_\phi = -j\omega A_\phi + \frac{j\beta A_{m\vartheta}}{\varepsilon_0} \qquad \text{(A.12)}$$

Electric fields diffracted by the edge are expressed in the ray fixed

coordinate system as

$$E^d_{\substack{// \\ \perp}}(s) = -D_{\substack{// \\ \perp \ \perp}} E^i_{// \perp}(Q) A(s) e^{-j\beta s} \qquad \text{(A.13)}$$

where $s \approx \left|\bar{r} - \bar{d}\right| = r - d\cos\xi'$. ξ' is the angle between the vectors $\bar{d}$ and $\bar{r}$. $\bar{d}$ is the position vector from the origin to the diffraction point. By using the relationship between $\bar{s}$ and $\bar{r}$, equation (A.13) can be rewritten as

$$E^d_{\substack{// \\ \perp}}(s) = -D_{\substack{// \\ \perp \ \perp}} E^i_{// \perp}(Q) A(s) e^{-j\beta r} e^{j\beta d\cos\xi'} \qquad \text{(A.14).}$$

The diffracted fields in (A.13) are going to be rewritten with the expression in the spherical coordinate system centered at O. Let's consider only the electric current is the source. The diffracted electric field is written as

$${}^J\bar{E}_d = {}^J E^d_{//}(s)\hat{\gamma} + {}^J E^d_{\perp}(s)\hat{\phi} \qquad \text{(A.15).}$$

J indicates that the electric field is due to the electric current. $\hat{\gamma}$ and $\hat{\phi}$ are the unit vectors in the ray fixed coordinate system as shown in fig. 2.4.

θ and ϕ components in the spherical coordinate system can be written as

$${}^J E^d_\theta = {}^J\bar{E}_d \cdot \bar{\theta} = -\left(D_{//}\, {}^J E^i_{//}(Q)\hat{\gamma}\cdot\bar{\theta} + D_\perp\, {}^J E^i_\perp(Q)\hat{\phi}\cdot\bar{\theta}\right) A(s) e^{-j\beta r} e^{j\beta d\cos\xi'} \qquad \text{(A.16)}$$

$${}^J E^d_\phi = {}^J\bar{E}_d \cdot \bar{\phi} = -\left(D_{//}\, {}^J E^i_{//}(Q)\hat{\gamma}\cdot\bar{\phi} + D_\perp\, {}^J E^i_\perp(Q)\hat{\phi}\cdot\bar{\phi}\right) A(s) e^{-j\beta r} e^{j\beta d\cos\xi'} \qquad \text{(A.17).}$$

- and ^ represent the vectors in the spherical coordinate system centered at o and the ray fixed coordinate systems, respectively.

In the far region $s' << s$, the spatial attenuation factor $A(s)$ can be reduced into the simple form as

$$A(s) = \sqrt{\frac{s'}{s(s'+s)}} \approx \frac{\sqrt{s'}}{s} \approx \frac{\sqrt{s'}}{r} \qquad \text{(A.18).}$$

Finally the diffracted field components ${}^J E^d_\theta$ and ${}^J E^d_\phi$ are written into following forms.

$$ {}^{J}E_{\theta}^{d} = -\left(D_{//}\,{}^{J}E_{//}^{i}(Q)\hat{\gamma}\cdot\bar{\theta} + D_{\perp}\,{}^{J}E_{\perp}^{i}(Q)\hat{\phi}\cdot\bar{\theta}\right)\frac{\sqrt{s'}}{r}e^{-j\beta r}e^{j\beta d\cos\xi'} \qquad \text{(A.19)} $$

$$ {}^{J}E_{\theta}^{d} = -\left(D_{//}\,{}^{J}E_{//}^{i}(Q)\hat{\gamma}\cdot\bar{\phi} + D_{\perp}\,{}^{J}E_{\perp}^{i}(Q)\hat{\phi}\cdot\bar{\phi}\right)\frac{\sqrt{s'}}{r}e^{-j\beta r}e^{j\beta d\cos\xi'} \qquad \text{(A.20)} $$

The total electric fields are the sum of the direct and diffracted field as

$$ {}^{Total}E_{\theta} = E_{\theta} + E_{\theta}^{d} \qquad \text{(A.21)} $$

where E_{θ}^{d} can be expressed as $E_{\theta}^{d} = {}^{J}E_{\theta}^{d} + {}^{M}E_{\theta}^{d}$, by using electric fields ${}^{J}E_{\theta}^{d}$ and ${}^{M}E_{\theta}^{d}$ are the diffracted fields by the edge and incident fields are due to the electric and the magnetic current, respectively. E_{θ} is already shown in (A.11).

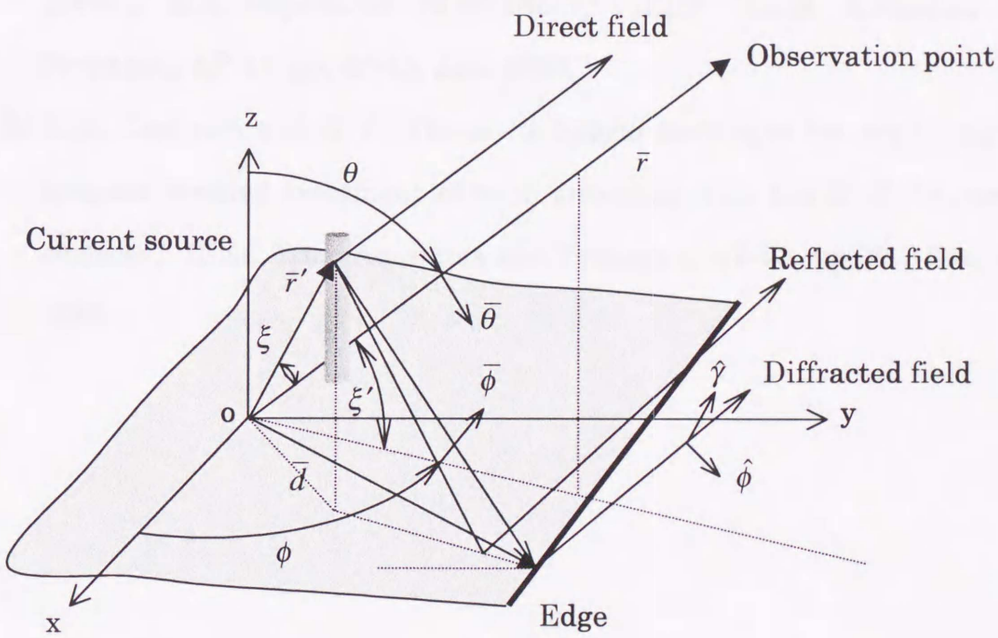

fig. A2 Radiated field paths.

References

[1] R. G. Kouyoujian and P. Pathak, "A uniform geometrical theory of diffraction for an edge of a perfectly conducting surface," Proc. IEEE, 62, pp.1448-1461, Nov. 1974.

[2] G. A. Thiele and T. M. Newhouse, "A hybrid technique for combining moment methods with the geometrical theory of diffraction," IEEE Trans. Antennas and Propagat., AP-23, pp. 62-69, Jan. 1975.

[3] D. A. Pozer and E. H. Newman, " Analysis of a monopole mounted near an edge or a vertex," IEEE Trans. Antennas and Propagat., AP-30, pp. 401-408, May 1982.

[4] A. R. Lopez, "The geometrical theory of diffraction applied to an antenna pattern and impedance calculations," IEEE Trans. Antennas and Propagat., AP-14, pp. 40-45, Jan. 1966.

[5] E. P. Ekelman and G. A. Thiele, "A hybrid technique for combining the moment method treatment of wire antennas with the GTD for curved surfaces," IEEE Trns. Antennas and Propagat., AP-28, pp. 831-839, Nov. 1980.

Acknowledgement

I wish to have this opportunity to express my heartfelt thanks to everyone that has contributed to and supported me to complete this work. First and foremost I must thank Professor Kazuhiro Hirasawa in the Institute of Information Sciences and Electronics at the University of Tsukuba. It would not have been possible to complete this dissertation without his supervision and a great deal of valuable advice. I am also grateful to Professor Yukio Ishibashi, Professor Shojiro Nemoto, Associate Professor DongSheng Cai in the Institute of Information Sciences and Electronics and Professor Keinosuke Nagai in the Institute of Applied Physics at the University of Tsukuba for their constructive and valuable advice and comments on the revision of this dissertation. I express my thanks to all of my friends who have supported me in many ways and who have worked together with me to fulfill this study.

Finally I thank my parents and sisters for their understanding, patience, dedication and encouragement throughout the years of this dissertation.

List of papers

Journal

[1] T. Morioka and K. Hirasawa, "Reduction of coupling between two wire antennas using a slot," IEICE Trans. on Commun., E80-B, pp. 699-705, May 1997.

[2] T. Morioka, S. Araki and K. Hirasawa, "Slot antenna with parasitic element for dual band operation," Electron. Lett., 33, 25, pp. 2093-2094, Dec. 1997.

International Symposium

[1] T. Morioka, K. Hirasawa and S. Shibasaki, "Analysis of a bent slot antenna with a parasitic element for dual band operation," Int. Symp. on Antennas and Propagat., Japan, pp. 497-500, Sep. 1996.

[2] T. Morioka, K. Hirasawa and A. Henderson, "Reduction of coupling between two wire antennas using a slot," Int. Wireless and Telecommun. Symp., Malaysia, pp. 46-51, May 1997.

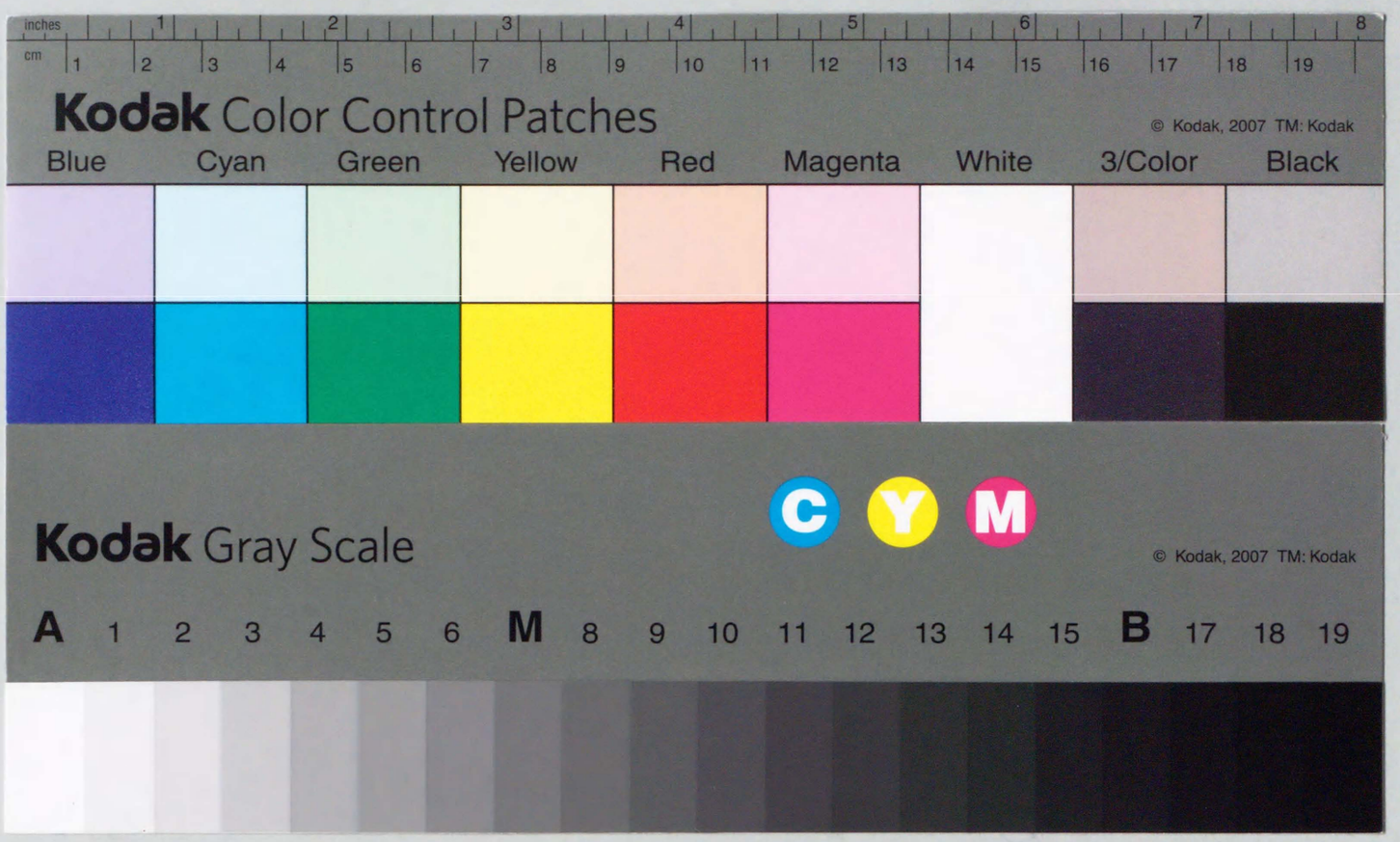
inches
cm
Kodak Color Control Patches
© Kodak, 2007 TM: Kodak
Blue
Cyan
Green
Yellow
Red
Magenta
White
3/Color
Black
Kodak Gray Scale
C
Y
M
© Kodak, 2007 TM: Kodak
A 1 2 3 4 5 6 M 8 9 10 11 12 13 14 15 B 17 18 19